DATA COLLECTION ENERGY EFFICIENT ROUTING PROTOCOL FOR ENERGY HARVESTED BASED WIRELESS SENSOR NETWORK

BY

TARIQ ABU AMRIA

A Thesis Presented to the

DEANSHIP OF GRADUATE STUDIES

KING FAHD UNIVERSITY OF PETROLEUM & MINERALS

DHAHRAN, SAUDI ARABIA

In Partial Fulfillment of the

Requirements for the Degree of

MASTER OF SCIENCE

In

COMPUTER NETWORKS

DECEMBER 2015

IN THE NAME OF ALLAH, THE MOST GRACIOUS AND THE MOST MERCIFUL

KING FAHD UNIVERSITY OF PETROLEUM & MINERALS

DHAHRAN- 31261, SAUDI ARABIA

DEANSHIP OF GRADUATE STUDIES

This thesis, written by Tariq Abu Amria under the direction of his thesis advisor and approved by his thesis committee, has been presented and accepted by the Dean of Graduate Studies, in partial fulfillment of the requirements for the degree of **MASTER OF SCIENCE IN COMPUTER NETWORKS.**

Dr. Uthman Baroudi
(Advisor)

Dr. Ahmed Al-Mulhem
Department Chairman

Dr. Shokri Selim
(Member)

Dr. Salam A. Zummo
Dean of Graduate Studies

Dr. Marwan Abu-Amara
(Member)

28/1/16
Date

To my parents, my sisters and brothers

For their endless love, support and encouragement

To my lovely son and daughter, Owais and Shatha

To my dear wife for her endless love and support.

ACKNOWLEDGMENTS

All the praise and thanks to Allah. There is no strength or power except Allah.

I would like to express my gratitude to my advisor, Dr. Uthman Baroudi, for his guidance, expertise, patience, motivation, enthusiasm, and immense knowledge. I would like to thank the members of the thesis committee, Dr. Shokri Selim and Dr. Marwan Abu-Amara. I would like to thank King Fahd University of Petroleum and Minerals (KFUPM) for granting me this opportunity of pursuing graduate studies.

TABLE OF CONTENTS

LIST OF TABLES

LIST OF FIGURES

LIST OF ABBREVIATIONS

AODV	:	Ad hoc On-Demand Distance Vector
ACK	:	Acknowledgement packet
APR	:	Application Packet Rate
C	:	Constant
DEECP	:	Data Energy Efficient Collector Protocol
DSSS	:	Direct Sequence Spread Spectrum
DSSC	:	Dye Sensitized Solar Cells
EHR	:	Energy Harvesting Rate
$\boldsymbol{E_t}$	:	Energy at time t
PRE	:	Packet Receive Energy
PTE	:	Packet Transmission Energy
PTT	**:**	**P**acket Transmission Time
HAN	:	Home Area Network
IP	:	Internet Protocol
IGRP	:	Interior Gateway Routing Protocol
TCP	:	Transmission Control Protocol

T_w	:	Time Window
UDP	:	User Datagram Protocol
IS-IS	:	Intermediate System to Intermediate System
JREQ	:	Joint Request Packet
JREP	:	Joint Replay Packet
L	:	Level
MANET	:	Mobile Ad-hoc Network
MAC	:	Medium Access Control
PR	:	Packet Rate
RSSI	:	Radio Signal Strength Indicator
RREQ	:	Route Request
RERR	:	Route Error
RREP	:	Route Reply
TTL	:	Time to Live
MPPT	:	Maximum Power Point Tracker
MINHP	:	Minimum Harvestable Power
MAXHP	:	Maximum Harvestable Power

Mbps	:	Mega bit per second
OFDM	:	Orthogonal Frequency-Division Multiplexing
OSPF	:	Open Shortest Path First
Kbps	:	Kilo bit per second
QoS	:	Quality of Service
SG	:	Smart Grid
WMN	**:**	Wireless Mesh Network
WSN	:	Wireless Sensor Network
WSN-HEAP	:	WSN Powered by Ambient Energy Harvesting

ABSTRACT

Full Name : Tariq Mahmoud Ahmad Abu Amria

Thesis Title : Data Collection Energy Efficient Routing Protocol for Energy Harvested Based Wireless Sensor Network (DEECP)

Major Field : Computer Networks

Date of Degree : 2015

Wireless sensor networks have become the preferred solution in many applications. The main restriction in using wireless sensor nodes is that the power source of the sensor nodes is limited, as these sensors usually rely on a battery. Typically, a wireless sensor network (WSN) deploys a large number of sensors. When the sensors' batteries run out, they need to be replaced. The replacement process is a costly process which necessarily increases as the WSN increases in size. Using an ambient source to power a wireless sensor network is a promising solution. There are a variety of renewable ambient energy sources available, such as vibration, temperature, solar power, and pressure, etc. An ambient resource is an intermittent energy source. Usually, a sensor uses a super capacitor to store harvested energy from ambient sources. In this thesis, a Data Collection Energy-Efficient Routing Protocol with Harvested Energy is proposed. The node's energy, energy harvesting rate, packet data rate and node capability are considered in the DEECP protocol to choose the best path. Moreover, a handover local route repair mechanism is integrated in the DEECP protocol. Extensive simulation experiments were conducted using NS-3 to study the behavior of DEECP. We have compared DEECP with AODV and IEEE 802.11s at proactive mode using different performance metrics. The DEECP protocol has shown an outstanding perform in term of increasing the flow application throughput by 1148%,

decreasing the packet loss ratio by 80%, and decreasing the packet end-to-end delay by 65% with respect to AODV. In addition, DEECP outperform IEEE 802.11s at proactive mode in term of increasing the flow application throughput by 284%, decreasing the packet loss ratio by 16%, and decreasing the packet end-to-end delay by 75%.

ملخص الرسالة

الاسم الكامل: طارق محمود احمد ابوعامرية

عنوان الرسالة: بروتوكول جامع للمعلومات بستخدام الطاقة بشكل فعال بلاعتماد على حصاد الطاقة في مسشعرات الشبكة اللاسلكية.

التخصص: شبكات حاسوب

تاريخ الدرجة العلمية:2015

شبكات الاستشعار اللاسلكية أصبحت الحل المفضل للاستخدام في العديد من التطبيقات.إلا أنه من أهم القيود التي تحد من الشبكات الاستشعارية هو محدودية مصدر الطاقة ألازمه لتشغيل العقد الإستشعارية في الشبكة اللاسلكية. شبكات الاستشعار اللاسلكية تتكون عادةً من عدد كبيرا من أجهزة الاستشعار، وعادةً تعمل المجسات بواسطة طاقة البطارية. وفي حالة نفاذ طاقة البطاريات، فهناك حاجة إلى عملية استبدال هذه البطاريات في شبكة الاستشعار اللاسلكية وهي عملية مكلفة وتزداد طرديا مع إتساع الشبكة. ومن الحلول الواعدة لهذه المشكلة هو استخدام مصادر الطاقة المتجددة من البيئة المحيطة .إلا ان هذه المصادر من الطاقة المتجددة تتوفر بشكل متقطع، ومن مصادر الطاقة المتجددة المحيطة مثل الاهتزاز، ودرجة الحرارة، والطاقة الشمسية، والضغط، إلخ .حيث يتم تخزين الطاقة المحصودة من هذه المصادر في مكثف عالي القدرة . وفي هذه الرسالة تم إقترح ودراسة بروتوكول جامع للمعلومات بستخدام الطاقة بشكل فعال بلإعتماد على حصاد الطاقة في مستشعرات الشبكة اللاسلكية. وقد أخذ في الاعتبار الطاقة المتبقية في العقدة، ومعدل حصاد الطاقة، ومعدل حزم البيانات و قدرة العقدة الاستشعارية في عملية اختيار المسار في البروتوكول المقترح (DEECP) . وعلاوة على ذلك، تم دمج آلية إصلاح المسار بحيث يتم الانتقال الى المسار الافضل بطريقة سلسة لا تؤدي إلى إنقطاع أو فقد للمعلومات المرسلة. وقد أجريت تجارب محاكاة واسعة باستخدام NS-3 لدراسة

سلوك هذا البروتوكول. م تمت مقارنتة مع بروتوكول AODV و IEEE 802.11s في حالته استباقية اختيار المسار باستخدام مقاييس أداء مختلفة.و تمكن DEECP من زيادة سرعة تدفق البيانات بنسبة 1148% وتقليل نسبة فقدان البيانات بنسبة 80% وكذلك فقد قلل الوقت اللازم لوصول البيانات بنسبة 65% بالمقارنة مع AODV. اما بالمقارنة مع IEEE 802.11s فقد حقق بروتوكول DEECP زيادة في سرعة تدفق البينات بنسبة 284% وقلل نسبة فقدان البيانات بنسبة 16% وكذلك فقد قلل الوقت اللازم لوصول البيانات بنسبة 75%.

CHAPTER 1

INTRODUCTION

In this chapter, wireless sensor network is discussed. The types of routing algorithms are mentioned briefly. Finally, the problem statement is presented.

1.1 Wireless Sensor Networks

Wireless sensor network consists of a number of small self-powered sensing nodes. These nodes are able to detect specific events, gather information, and communicate wirelessly. The main goal for the sensing nodes is to process data and hand them to the base station. When one small device has the capabilities of sensing, processing and communication, it can promise a vast number of applications [1] . The data flow in this type of networks converge in the base station that uses this information or at a data sink node. In case of the data sink node, it takes the responsibility to transfer this data to control center. The power consumption in sink node is not reason for concern as the sensor nodes. Traditionally, the power source of the sensor nodes is a battery. The sensor nodes batteries need to be recharged or replaced with new one from time to time. Replacing the batteries of sensor nodes after deployment is not an easy task especially in a hazardous area. The solution to avoid replacing the battery for sensor nodes is to use energy harvesting from ambient resources. Usually, the ambient resources are intermittent sources, likewise sun it is unavailable at night time. Hence, sensor nodes use a super capacitor to store the harvested energy. The stored

energy will be used at the time when the harvesting energy is low or unavailable. Figure 1.1 shows wireless sensor network example.

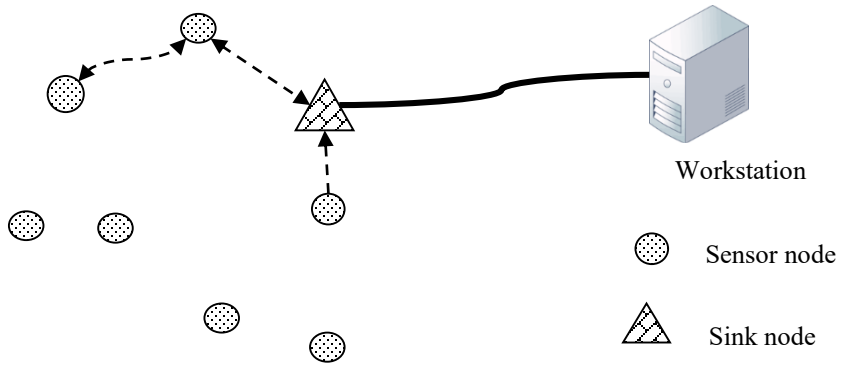

Figure 1.1: example of wireless sensor network

1.2 Routing Protocols

Routing protocol is one of the significant factors that affect the computer network's functionality. In specific, it is the factor that steering a packet from hop to hop until the packet reaches to its destination. The next sub sections will go briefly on the basic techniques used in routing.

1.2.1 Ad-Hoc Networks

If there is no infrastructure and no special router in an area, the collection of nodes in an area will form an ad-hoc network. In this type of network there is no central controller and every node plays the role of router and host [2] . These nodes send, receive, and forward packet to other nodes. In other words this network is a self-configured network. Usually the media used is the wireless like MANET Mobile Ad-hoc Network [3] .

1.2.2 Proactive Routing Protocol

This type of routing protocol stores routing table for all destination on the network [4] . When the packet reaches a router, the router searches on its table to send the packet to next hop. As the

network becomes large the amount of data needed to store becomes large, and also the computation power becomes large, which may become not suitable for network with limited power. These protocols are faster than reactive in forwarding a packet but become slower in a dynamically changed network, i.e. MANET. But, if an application sends the data periodically this type of protocol will be preferred more than reactive routing protocol, and become more reliable, if a routing protocol decreases the amount of data needed to store overhead. On consequence, the computation power will be decreases.

1.2.3 Reactive Routing Protocol

If no one sends to the destination its route path will not be available. As soon as one node needs to send to unknown destination a route discovery will start. When the route path found, a route entry will be added on the nodes routing table for a finite time. This is suitable to decrease the overhead for discovering unused route, but it is employees a significant delay at first packet to destination or rarely used route [4] .

1.2.4 Ad-hoc On-Demand Distance Vector

It is a reactive routing protocol. It inherits all the disadvantage of reactive protocols, i.e. delay. The route to destination formed when it requested by the node. This route is valid for a period of time. This protocol is suitable for dynamic networks that change with time[5] . In addition, this type of network can be used in stationary nodes that powered by harvested energy, the nodes are turned on and off which is similar to dynamic networks.

1.2.5 IEEE 802.11s Protocol

IEEE 802.11s draft define two protocol Hybrid Wireless Mesh Protocol (HWMP) and Airtime Link Metric (ALM). HWMP has the new routing capabilities proposed using the MAC layer.[6] IEEE 802.11s has a proactive mode [6], in this mode the protocol build a tree in order to collect

the data to a sink node. IEEE 802.11s mandatory profile defines the HWMP as the path discovery mechanism and the ALM as the path selection metric.

1.2.5.1 Airtime Link Metric

The ALM send a test frame and accounts for its transmit time, the bit rate at which the frame can be transmitted, physical implementation overhead, and the probability of retransmission, which relates to the link error rate. According to the standard the airtime cost, *Ca*, is calculated as:

$$Ca = \left[Oca * Op + \frac{Bt}{r}\right]\frac{1}{1-ef} \quad (1.1)$$

Where *Oca* is the channel access overhead and *Op* the protocol overhead which varies according to the PHY layer implementation. *Bt* is the test frame size, *r* is the data rate in Mbps at which the Node would transmit a test frame and *ef* is the measured test frame error rate. i. e the value of *Oca* and *Op* is 75µs and 110µs for 802.11a, respectively.

1.2.5.2 Hybrid Wireless Mesh Protocol

Hybrid Wireless Mesh Protocol (HWMP), HWMP adopt; on-demand routing protocol and proactive tree-based routing protocol. Both of these routing can run simultaneously. HWMP is specified 4 information elements Path request (PREQ), Path reply (PREP), Path error (PERR), and Root announcement (RANN).

In the proactive tree-based routing mode there are two mechanism. One is based on proactive Path request (PREQ) and the other is based on proactive Root announcement (RANN).

In the proactive PREQ mechanism, the root node periodically broadcasts a PREQ element. A node in the network receiving the PREQ creates/updates the path to the root, records the hop count and metric to the root, updates the PREQ with such information, and then forwards PREQ. Thus, the presence of the root and the distance vector to the root can be disseminated to all nodes in the

mesh. If the proactive PREP bit in the proactive PREQ element is set to 1, then the receiving node sends a gratuitous PREP to the root so that a route from the root to this node is established.

In the proactive RANN mechanism, the root node periodically floods a RANN element into the network. When a node receives the RANN and also needs to create/refresh a route to the root node, it sends a unicast PREQ to the root. When the root node receives this unicast PREQ, it replies with a PREP to the node. Thus, the unicast PREQ forms the reverse route from the root to the originating node, while the unicast PREP creates the forward route from the originating Mesh STA to the root.

1.3 Problem Statement and Contribution

The routing protocols have a significant impact on the wireless sensor networks. The routing protocols are steering the radio transceiver module operation. The literature has many proposed energy aware protocols [7] , these routing protocols are not considering energy harvesting with Quality of Service. This thesis addresses the harvesting energy in routing protocol decision. Energy harvesting techniques gather the energy from the ambient energy sources that present in the environment like solar, thermal, vibration energy, etc. and convert that energy into a form that can be stored and used to power the devices.

Smart Grid is a data communications network integrated with the electrical grid that collects and analyzes data captured in near-real-time about power transmission, distribution, and consumption [8] . WSNs are used in Smart Grid networks to provide a cost-effective sensing and communication platforms for monitoring and diagnostic systems. Smart Grid network consisting of three networks: Home Area Network (HAN) is communication network in a home for devices. Neighborhood Area Network (NAN) is a network that consist a multiple HANs, used to deliver control date to HANs and to deliver the metering data to data centers, Wide Area Network (WAN) is a data communication network among data centers, and The SG-HAN network with harvesting

energy have its properties, first the location of sensor nodes are stationary, second, the energy source is infinite but intermittent as it not continuously available. The sensor nodes that depend on harvesting energy, subject to temporarily die when its energy exhausted. The sensor nodes can return back to operations when it harvests enough amount of energy. In consequence, these the network topology changes continuously that makes it similar to a mobile network where the network topology changes as the nodes moves. By building a special routing protocol that takes care of these properties, such as reliability, latency, and network throughput, the network can support specific quality of service requirements suitable to Smart Grid. In this thesis work, this protocol is proposed, evaluated, and compared under different performance criteria such as energy consumption, delay, and outage.

Chapter 2 discusses the related work of energy-aware routing protocols, and provides an overview of energy harvesting techniques, energy harvesting model, and energy consumption device models of NS-3 simulation package. Chapter 3 discusses in detail our proposed data collector protocol which we called DEECP. Chapter 4 describes simulation setup and the comparison study of DEECP, IEEE 802.11s, and the AODV protocol using ns-3. The thesis is concluded in Chapter 5.

CHAPTER 2

LITERATURE REVIEW

2.1 Related Work

This section surveys the existing related works in energy aware and energy-harvesting aware routing protocols in WSNs.

T. Voight [9] Proposed one of the first routing algorithms that integrated the harvesting energy from solar into the route decision. Simply, the protocol classifies sensor nodes into nonharvesting and harvesting nodes. The protocol tries to avoid nonharverting nodes as possible. In [10] the authors proposed a routing protocol for energy harvesting wireless sensor network based clustering algorithm EHGUC-OAPR (energy harvesting genetic-based unequal clustering algorithm and optimal adaptive performance routing algorithm). It uses unequal clustering and multi-hop routing to manage energy-harvested wireless sensor network. The EHGUC choose an optimal group of sensor nodes which have high weighted sum of (distance between nodes, energy harvesting rate, etc.) as a cluster-heads and the other sensor nodes in the network form the cluster with different size. The EHGUC-OAPR algorithm maximize the outcome gained by successfully routing packets, and also optimize the management of energy of the EH-WSN, the clusters have smaller size as it become closer to base-station . And also the burden of computation did by the base-station.

In [11] the authors introduce and utilize Energy Potential Function to extend the LEACH [12] [1] protocol and to measure the node's capability of energy harvesting. The extended protocol is Energy Potential LEACH (EP-LEACH), which is suitable protocol for energy harvesting wireless sensor networks. This protocol improves the network throughput in energy harvesting wireless sensor networks. The authors prove the performance of this protocol numerically and analytically.

The evaluation shows that this protocol performs better than other previous work in term of throughput and lifetimes. The energy potential function introduce in [11] is a basic version where to determine the exact formula of EP-Function is not a simple task. The EP-Function of a node is a function of hardware characteristics (battery capacity, transmission power) and ambient conditions around the node (humidity, temperature, illumination intensity). The computation done for time slots to determine if the node can works as cluster- head for next time slot or not.

In [14] the authors proposed a routing scheme that considers energy wastage in network. The energy wastage produced from overcharging of batteries that have a finite capacity, the [14] is the first one considers the energy wastage in routing decision, this is done by minimizing the cost associated with the packet transmission energy consumption, and the energy wastage comes from battery overcharge. The simulation results show that can be achieved higher residual energy levels by using this wastage awareness protocol. In [15] , calculate the energy budget for a time slot. When the node have enough energy budget it involve in packet relaying during the exploratory phase of direct diffusion. An adaptive opportunistic routing protocol is proposed in [16] , the data packets are broadcasted towards the data sink. But this will cause many data duplication specially when using an application with high data rate.

In [11] the authors proposed a routing algorithm that takes into account three factors, wasted energy, energy consumption and transmission quality, such that quality is affected by bit error rate (BER). Where these factors were given different weights to represent their significant effect to the performance of the wireless sensor network, this algorithm divided the path between source and destination node into different layer, so that the evaluation of the results become easy. So the network can be treated as direct graph.

In [17] , [19] , and [20] the authors represent an algorithms that take cost metrics represents a node's available energy with the links. Then they found the route using Directed Diffusion,

Bellman Ford, or any other applicable least cost or shortest path algorithms that can be applied to these metrics

LEACH (Low-energy adaptive clustering hierarchy) proposed in [12] [1] which is an adaptive clustering protocol for distributing energy consumption among the sensor nodes in the network. LEACH elect a cluster-heads randomly among the cluster nodes and the corresponding clusters and is able to distribute energy consumption evenly throughout the sensors, because the cluster-head nodes consumed there energy more quicker than other child nodes, as The clusters are used for transmitting data to the base station because all sensor nodes located in the transmission range, so LEACH will doubling the lifetime. LEACH requires only a few nodes for transmitting the data far distances to the base-station. It increases the performance of classical clustering algorithms by using adaptive clusters and rotating cluster-heads, allowing the energy to be used in efficient way. In addition, LEACH is able to perform local computation in each cluster-head to reduce the amount of data that need to transmit to the base station. This achieves a large reduction in the energy consumption. Many improvements were proposed for LEACH in literature like in [22] , [23] , and [24] .

HEEP (Powered by ambient energy harvesting) protocol proposed in [25] and by using this routing algorithm the network performance improved, and also it improves the placement scheme for relay nodes for WSNs. This protocol use a super capacitors as energy storage device instead of batteries, the recharge cycles is nearly unlimited for endless deployment, so it is a very suitable protocol for the applications where it is sensor nodes are so costly for replacement or accessing. The HEAP comprises 3 types of nodes: sink, relay, and source nodes. These nodes are different from each other. The relay nodes are used to forward data packets to sink nodes that are come from source node. These nodes are needed when the source nodes located out of range from sink node for communication. The source nodes same as relay nodes except that if it in the reception

time and does not receive any packet, it will send its data in that transmission period of time. The sink node is not a power concern, and it receives any packet come from the sensor nodes if it in range of sensor.

2.2 Energy Sources

There are two types of energy sources: battery or combination of chargeable battery or/with supper capacitor and ambient energy harvester. In this section, we present briefly the common energy harvesting techniques in WSNs.

2.2.1 Energy Harvesting Techniques

The renewable energy technology is not new, while using it with small devices as sensor nodes is a new challenge. The common renewable energy techniques include but not limited to hydroelectric power generation using water, wind turbines, solar panels, piezoelectric, and thermal sources. The renewable energy technology has to be comparable in size with the sensors. The most appropriate energy harvesting technologies for WSNs are solar, mechanical, and thermal.

2.2.2 Solar Energy (Photovoltaic Cells)

It's the best known and most available source of energy around the earth. The use of solar energy harvester is affected by the seasons of the year, and the availability of light. Sometime it's difficult to reach some places to replace the sensor battery. Using solar harvester is a solution for many networks [9] . Solar radiation yields around 0.001W/mm^2 (1 Joule/day/mm^2) in direct sunlight or around one micro watt per mm^2 in indoor. The efficiency of the solar energy source is up to 30% which makes it a productive energy source. High efficiency solar cell designed for indoor light is presented in [26] . This photovoltaic system called GaAs, Its power density was found to be over 300% greater than Dye sensitized solar cells (DSSC) modules under indoor light levels.

2.2.3 Thermal Energy

The temperature difference between p type and n- type ends of a semiconductors results in a heat flow which results in diffusion of charge carriers' [27] . The flow of charge carriers between the hot and cold regions in turn creates a voltage difference. An energy harvesting circuit uses hybrid of indoor light and thermal was proposed in [28] to extend the lifetime of sensor nodes. The circuit harvested an average of 620 μW at an average indoor solar irradiance of 1010 lux and a thermal gradient of 10 degrees. The area of the solar panel used is about 16cm^2. In [29] , a thermoelectric energy harvester was integrated into a shirt and tested on people in real life. It generates a power in 0.5–5 mW range at ambient temperatures of 15 °C–27 °C, respectively.

2.2.4 Mechanical and Vibration Energy

The energy of vibration, movement, mechanical, and other forms of kinetic energy can be harvested and converted to electrical energy. Vibrations exist around us like bridges and roads because of the vehicles movement. Vibration, pressure, or force energy is commonly converted by piezoelectric capacitor material into electrical energy [30] . Spring-loaded mechanism can be used to harvest kinetic energy.

2.3 Energy Storage Technology

One of the disadvantages of use of built-in sensors in structures such as bridges and buildings is that they are hard to replace their batteries. In addition, the recharge cycles for the batteries is limited. The batteries cannot be more recharged outside the threshold. For that reason, an alternative energy storage form is necessary such as supercapacitors. The energy storage density of supercapacitors is higher than the normal capacitors. The supercapacitor can be manufactured in smaller form factors which is more suitable for sensor nodes. The sensor nodes powered by ambient resources with supercapacitor will be a sustainable solution. The batteries can be replaced

by supercapacitors, which are recharged by ambient energy harvester. The operational lifetime of a supercapacitor is ten-years, before its energy capacity become 20% less. In addition, supercapacitor can have more than half a million recharge cycle [31] .

CHAPTER 3

PROPOSED ALGORITHM (DEECP)

In this chapter the DEECP protocol proposed. The next sections describe DEECP protocol, and introduce the techniques that this protocol equipped with it; this techniques includes weighted RSSI, soft handover and relative On-Off thresholds. In addition, an analytical comparison between DEECP and AODV is conducted in terms of memory requirement. Last section discuss a case study for a better understanding of this protocol. Following sections explains the details of this protocol.

3.1 Description

The main motivation in our proposal are to minimize energy consumption, minimize end-to-end delay, and maximize throughput. In order to achieve these objectives, our design depends on two main factors: avoiding a single hop from the sensor node to the sink, and the node capacity. The node capacity is defined as the ability of the sensor node to transmit a certain number of packets within a predefined energy budget during a defined period of time. Implementing these two factors will lead to an evenly distributed load and a longer lifetime for a data path. Our protocol is composed of two phases: the tree building phase and data transfer phase.

In our protocol, the RSSI is the basis for computing several parameters. RSSI (Received Signal Strength Indicator) indicates the strength of a signal arriving at a receiver. A typical RSSI measurement includes the energy from the intended transmission, external noise, and the energy from concurrent interfering transmissions. In order to avoid temporary peaks in the RSSI value of received signals, most Wi-Fi cards maintain an exponential weighted average as shown in equation 3.1.

$$RSSI_{new\ ave} = RSSI_{old\ ave} * X + RSSI_{last\ measured} * Y \qquad (3.1)$$

where X and Y represent weights for the old average RSSI and the newly measured RSSI respectively. For example, Intel-2915 cards use X=0.9 and Y=0.1, and Y=1-X. The RSSI is used by a node in order to indicate the quality of the channel.

On other hand, we need a parameter to control the load associated with the served node (child node). This parameter must represent the capability of the node to handle the load. Simply, this parameter can be a packet rate. The definition of the packet rate is the number of packets that can be handled by a wireless sensor node in a given period of time, which we will later term as a time window(T_w). The packet rate (PR) presented by a node depends on the following parameters: the current energy of the node (E_t), the energy harvesting rate (EHR during a time window(T_w)., the energy needed to transmit one packet (PTE), and the energy needed to receive one packet (PRE). The calculation of PR is shown by equation 3.2.

$$PR = \frac{(E_t + EHR * T_w)}{(PRE + PTE) * T_w} \quad (3.2)$$

In view of performance, the time window T_w has a significant impact on the network stability as well as network topology. If T_w is very short this will increase the consumed computation power because the sensor nodes need to check its routing table at the end of each T_w as it looks for updated information. Consequently, more protocol control messages overhead comes from the broadcasting beacon's messages (see section 3.4). If T_w is too long, the adaptation of the network nodes will be slow in responding to the power change. T_w must be long enough to accommodate a suitable number of data packets and control packets of the protocol. For example, if the network consists of just two nodes, the minimum T_w is equal to one packet transmission time; so the node can send one data packet, one beacon message, and receive one beacon message from its neighbor.

Hence, the efficiency will be 1/3, or 33.3% (assume the packets have same length), where the efficiency can be defined as the percentage of data packets with respect to total packets (e.g. beacon messages) in a time period. To increase the efficiency, the time used sending data packets must be increased and the time used receiving beacon messages must be decreased. Determining the best T_w is an optimization NP-hard problem. Alternatively, the best T_w can be determined either practically or by simulation by varying the value of T_w and measuring the performance as in scenario 5.1.2. Additionally, the beacon message's overhead can be decreased by decreasing the rate of beacon messages. Consequently, when a node anticipates that the PR will not change in a number of xT_w , the node delays its broadcasting beacons after that xT_w. This decision depends on the calculated number of packets that can be handled by the node and the budget that it receives from its parent node; this point will be clarified after section 3.7. As a result, the total number of beacon messages is decreased

3.2 Computation of Transmission Power and Packet Rate

By using the transmission power model [35] , as in equation 3.3:

$$P(d) = \gamma + \alpha d^{\beta} \qquad (3.3)$$

where ϒ and α are system dependent parameters and 2 ≤ β ≤ 4. In general, ϒ is a small constant. Let ϒ =0, let $\propto = 6.73 \times 10^{-8}\, w/m^2$, and let β =2; this depends on the value calculated from [36] . For example, the maximum transmission rate with Zigbee technology is 250 kbps. The PTT (packet transmission time) is 0.5 ms when the

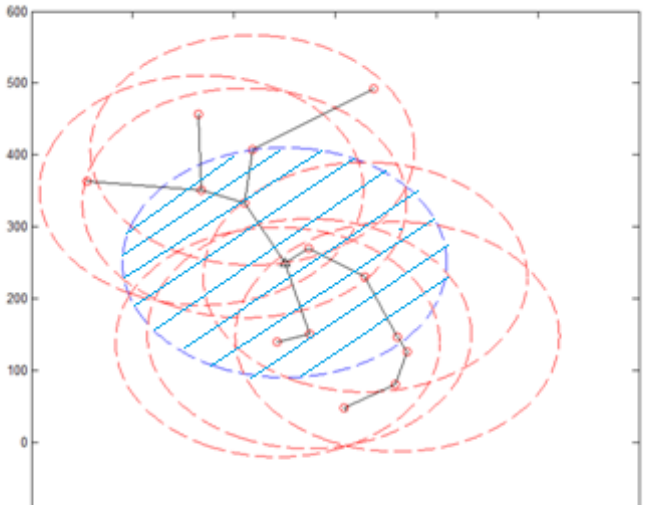

Figure 3.1: The hashed circle area represents the coverage area of the sink node. In consequence, all nodes in this area are at level 1, the dashed circle represents the beacon messages' range of the second level; all nodes located in this level belong to level 2.

packet length is 128 bit, which is the case in most modern packetized radio models [36] . Under these conditions, at 140 meters, the transmission power will be$P_{Tx} \approx \alpha\ (140m)^2 = 1.3mW$, and so the packet transmission energy $= 1.3mW * 5ms/packet = 0.65\mu J/packet$. If the energy available in a node is 0.5 Joules, then the total number of the packets that can be handled in a T_w is given by the available node energy E_t at time t and the energy harvesting rate (EHR), divided by the PTE (Packet Transmission Energy) and PRE (Packet Received Energy). We assume that the power consumed by other parts of the sensor hardware can be neglected. The PR is given by equation 3.2:

$$Energy = Voltage * Current * Time \qquad (3.4)$$

$$\text{Packet Transmission } Time = Packet\ size\ /\ Bandwidth \qquad (3.5)$$

Assume T_w =100ms, and PRE = 0. Therefore, according to equation 3.2 the PR= (0.5J+ (0.7uJ/s * 100ms)) / ($0.65\mu J/packet$ x 100ms) =7.69×10^5packets. The wireless sensor nodes are assumed to have the capability to adjust their transmission power; every node has its own PTE.

The physical limitation of the PR is determined by the technology used. For example, if the technology used is Zigbee, then the maximum bit rate is 250 Kbit/s [19], so the maximum PR will give by

$$PR_{max} = \frac{250K \times T_w}{Packet\ lenght\ in\ bits} \qquad (3.6)$$

3.3 Tree Building Phase

By using a top-down approach, the network will be divided into multiple levels. Each level contains a number of nodes; the first level which is level 0, is the sink itself. For every node that hears the beacon message from $level_i$, it will set its level value to $level_{i+1}$. All the nodes at same $level_i$ will try to connect to the nodes in $level_{i-1}$. If the node is not successfully connected before a predefined timeout, it must connect to a node at same level that has the maximum measured RSSI, and it is already connected, and has enough PR. Figure 3.1 shows a network's tree and the levels concept.

Initially, the sensor node tries to collect information from its neighbors to form its routing table. Every node sends a beacon message that informs its neighbors about its connection. The neighbor nodes measure the RSSI for the received signals that were generated from the node. After that, the node searches its routing table It chooses the expected parent node with the maximum RSSI, and if the following conditions are achieved:

- The Hop count does not exceed the Max-Hop-Count
- The expected parent node has more available PRs than the node needs
- The expected parent node has a connection to another node as a destination

These conditions guarantee the direction of the flow toward the sink or base station, where the node will be connected to other nodes that have same level or less. If the routing table entry for a hop violates any of these conditions, then the node takes one or both of the following actions to overcome isolating itself: first, the node searches and chooses from its routing table the next expected parent node with the next maximum RSSI. This process is repeated until all options are exhausted. If the node fails to connect then it will first refine its search by relaxing the conditions, by increasing the maximum allowed hop count. This relaxing is allowed if the application is less

sensitive to delay QoS; if it not then the node will go to a sleep state. Of course, this feature is enabled by the applications that use the information collected by the sensor node. Second, the node decreases its required packet rate by decreasing the PTR (packet transmission rate) in an interval of time (observation time windowT_w). Figure 3.2 shows the flow chart for establishing a connection, in order to fully understand this figure go through it after complete this section.

```
1:Start
2:Label1: Set State = Listening
3:          DelayTimer
4:        If Beacon_Msg is Received Then
5:          Set: NodeLevel= 1+ Select min(level) From Info_Table
6:          Schedule Sending of Beacon_Msg event every T_W
7:          Set State = Route Building.
8:          Set Delay_Timer
9:          If Delay_Timer is Expire  Then
10:LabelS:      NodeX = Select node from Info_Table Where nodePR > APR && nodeRSSI
11:                =max(RSSI)
12:      If ([RSS to NodeX >  weighted( RSS to node at less level  ]&& [ RSS for NodeX to less level  >
13:      weighted ( RSS to less level )]  Then
14:Label3:          Send Join_Request_Msg
15:          Set JoinExpireTimer = 40ms
16:       End If
17:       If JoinExpireTimer is Expire Then
18:          Neglect: nodeX
19:          Go To: LabelS.
20:      End If
21:               If JoinReplay Received.Accept Then
22:                 Set ParentNode = NodeX
23:               End If
24:               If JoinReplay.NewProposal Then
25:                   Go To: Label3
26:               End If
27:               Else Go To: Label1
28:       End If
```

Figure 3.2: Pesudo code to establish a connection

Let us assume that there is two nodes (A and B) located at same level, and the computed RSSI by these two nodes from lower level nodes has small different at each one of them. In addition the RSSI between these two nodes is higher than the RSSI from nodes that have lower level. Assume one of these two nodes (B) is connected to other node at lower level, so if the node A depend on computed RSSI it will decide to connect to node B. hence, the node B will consume energy for receiving and sending the packets come from node A. in addition, the forwarding delay will be added to packets come from node A. in this case, if node A take a decision to connect to nodes at lower level will be better than connect to node B in terms of delay and saving more network energy. Even, the node A will consume more of its energy when it send to node at lower level. In order to overcome this situation, we propose a weighted RSSI that takes into consideration the computed RSSI, the correction factor, and the level of the node. This weighted RSSI is applied to the computed RSSI for nodes of lower levels. The RSSIs are weighted before the routing table is processed; the RSSI comes directly from a lower level, it will have more weight as in (3.7). The proposed weighted RSSI aimed to shorten the path. This done by encouraging a node to take the path with a smaller hop-count, when the difference between the RSSI from a node with a lower level and a node with the same level is not significant in terms of total network energy saving.

$$RSSI_{weighted} = RSSI_{computed} * C_f + L \times L_w \quad (3.7)$$

Where C_f is a correction factor for RSSI, L is the level of the node, and L_w is a weight assigned to the level. The $RSSI_{weighted}$ value will be computed for all entries in the routing table that come from lower levels. If L_w is set to a value larger than zero this will encourage the node to take the direct connection to nodes that have a lower level value. The C_f value will be depend on RSSI and hardware characteristic which including and not limiting to forwarding delay, energy consumptions by the hardware. Hence, the exact value of C_f need a complex function, so we delayed this as a future work. In this work, we fix C_f to 0.94. This approach in weighting the RSSI

will result in decreasing the number of hops. When the node is located away from the sink node it will be attracted to connect to nodes with lower levels. This behavior is intuitive; the farther the node is from the sink, it is expected to serve a fewer number of nodes. Consequently, its remaining energy is higher than other nodes which are closer to the sink. In order to balance the energy consumption among all networks nodes, we will exploit this fact and we will allow such nodes to transmit with higher transmission power. Hence, the number of hops will be reduced.

3.4 Protocol Control Messages

In order to facilitate the execution of the above process, we use the following messages:

1. Beacon message: this message contains the available PR (if the node not connected, let the PR field remains empty), the maximum RSSI to the next hop that has a PR, and a node ID. Figure 3.3 shows the beacon message.
2. Join Proposal Request: it is sent from a node that wants to join another parent node with the requested PR.
3. Join Proposal Response: this message informs the requester whether his join request was accepted, not accepted, or not accepted with another proposed PR.

3.4.1 Beacon Message

Figure 3.3 shows the data fields of the beacon message. Table 3.1 shows these fields in detail. The length of the message is 176 bits which includes the length of all fields. The length of fields select to be held the data beyond current network needs. For example, the length of Node ID field is 16 bit that can held a 65535 node id, the node level can have 255 levels same as the hop count in AODV [38] and so on for other fields in this message and following messages. This can be easily added to any existing standardized beacon message.

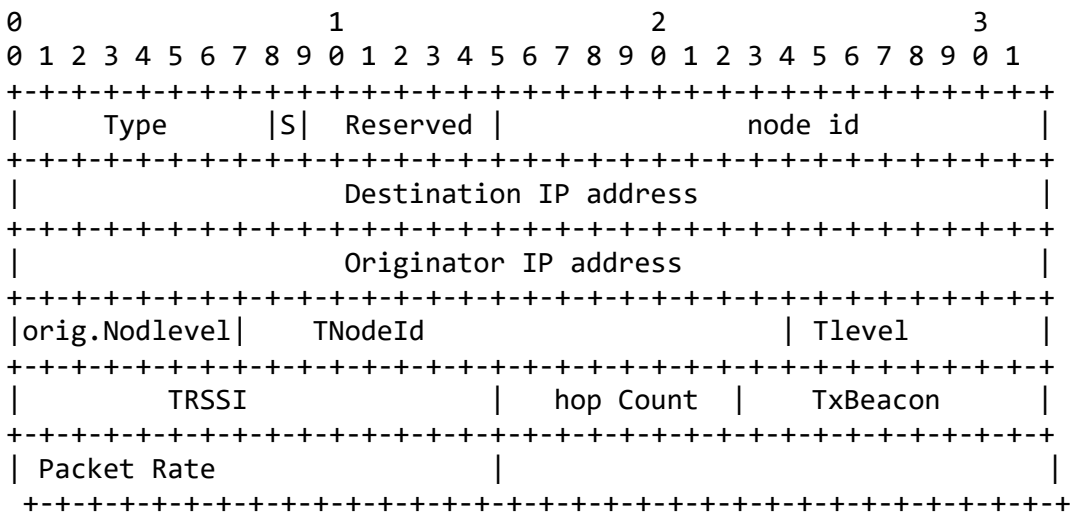

Figure 3.3: Beacon Message format

Table 3.1 : The data fields of the Beacon Message

Data Field	Length in bit	Description
Type	**8**	To determine the message type (Beacon, Request, Reply)
Flag	**2**	Flag = 0; the next (TNodeId, Tlevel, TRSSI) for the expected parent node. Flag = 1; next (TNodeId, Tlevel, TRSSI) for the parent node.(the node has valid connection)
Reserved	**6**	Not used
NodeId	**16**	Node identification number
Destination IP address	**32**	IP address of target node, nodes
Originator IP address	**32**	IP address of source Node.
Node level	**8**	Determine the level of the node (1-255)
TNodeId	**16**	Node identification number determine by Flag
Tlevel	**8**	Determine the level of the node (1-255)
TRSSI	**16**	Received signal strength indicator
hop Count	**8**	Number of hops to the node
Available packet Rate	**16**	Available Packet Rate in the Node
TxBeacon	**8**	Expected next Beacon after X beacon interval

3.4.2 Join Request Message

Figure 3.4 shows the format of a Join Reply message. Table 3.2 shows the details of this message fields. The length of this message is 136 bits.

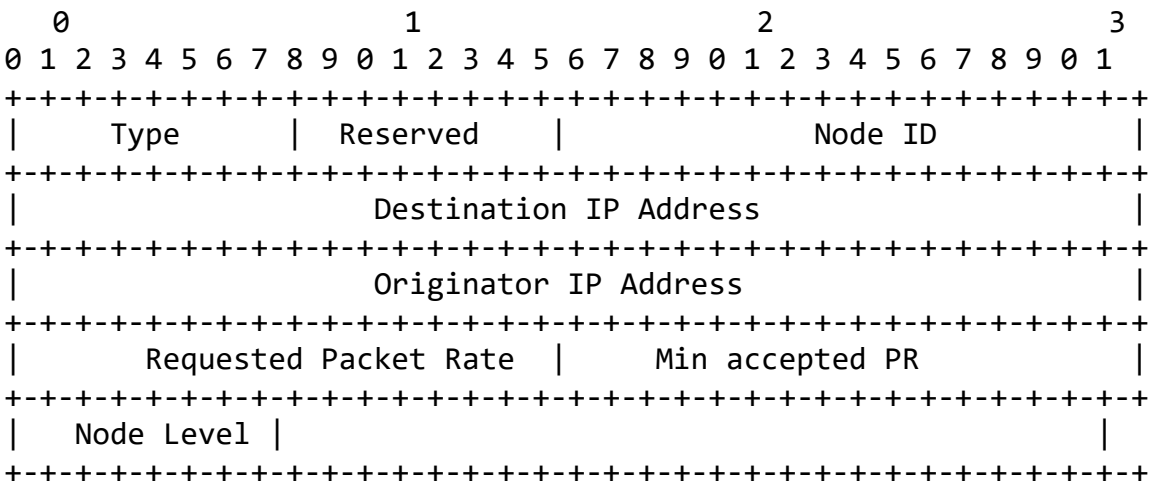

Figure 3.4: Join Request Message format

Table 3.2 : The data field of the Join Request Message.

Data Field	Length in bit	Description
Type	**8**	To determine the message type (Beacon, Request, Reply)
Reserved	**8**	Not used
NodeId	**16**	Node identification number
Destination IP address	**32**	IP address of target node, nodes
Originator IP address	**32**	IP address of source Node.
Node level	**8**	Determine the level of the node (1-255)
Requested packet Rate	**16**	Requested Packet Rate by Node
Minimum accepted PR	**16**	Minimum Packet Rate that can by accepted

3.4.3 Join Reply Message

Figure 3.5 shows the format of Join Reply message. Table 3.3 shows the Join Reply message field's length and descriptions. The overall length of the message is 128 bits.

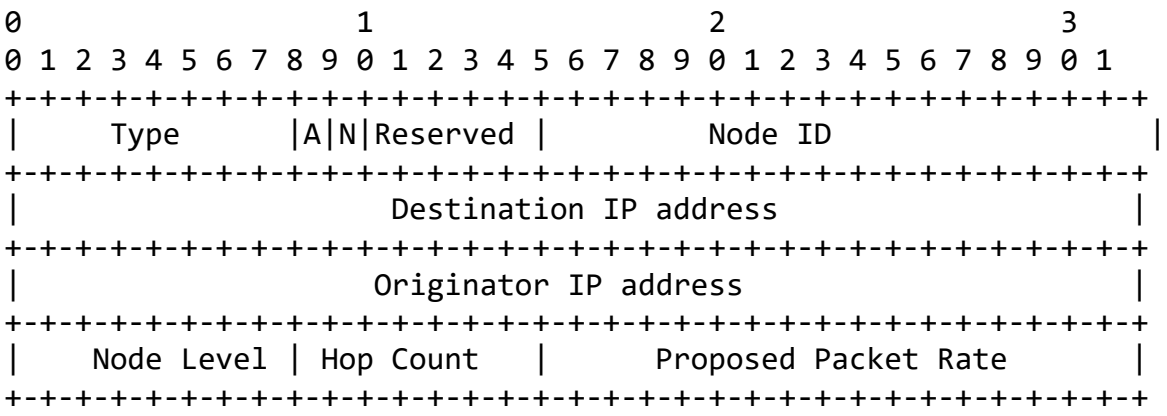

Figure 3.5 : Join Replay format

Table 3.3: The data field of Join Reply Message.

Data Field	Length in bit	Description
Type	**8**	To determine the message type (Beacon, Request, Reply)
Flag	**2**	Flag = 2; request accepted Flag = 1; retry with proposed packet rate
Reserved	**6**	Not used
NodeId	**16**	Node identification number
Destination IP address	**32**	IP address of target node, nodes
Originator IP address	**32**	IP address of source Node.
Node level	**8**	Determine the level of the node (1-255)
Requested packet Rate	**16**	Requested Packet Rate by Node
Proposed accepted PR	**8**	New Proposed Packet Rate that can by accepted

3.5 Soft Handover Process

The idea here is to decrease the number of power outages (see section 4.5.7) and the packet loss. The node monitors its remaining energy and as a result it reassign the packet rate parameter. If the value of the PR decreases below the value of the packet rate that grant to its children (leased-to-PR parameter) by a certain value, the node will start retrieving unused PR from its children as follows. First, the parent node will request its children's nodes to return all unused PR. Second, if the retrieved unused PR is not enough to extend the life of the node, the parent node requests its children to choose another parent. Then the children nodes elect a new node to play the role of parent. Children node start exchanging messages to join to a new parent node. It is important to note that the nodes will connect to a new parent before disconnecting from the old one. The process of parent replacement is called soft handover, where the packet delivered from the child node is not interrupted. Figure 3.9 illustrates an example of soft handover process. Figure 3.6 shows the flow chart for the soft handover process.

```
1:Start
2: Label1: Set DelayTimer = 250 ms.
3:        If ! Request_Un_used_PR Msg Sent Then
4:            Send Request_Un_used_PR Msg
5:        Else If PR > APR Then
6:                Go To: Label1
7:            End If
8:        Else If ! Abandon_Msg Sent Then
9:                Send Abandon_Msg.
10:           End If
11:       Else Go To: Label1.
12:       End If
```

Figure 3.6: The handover pesudo code

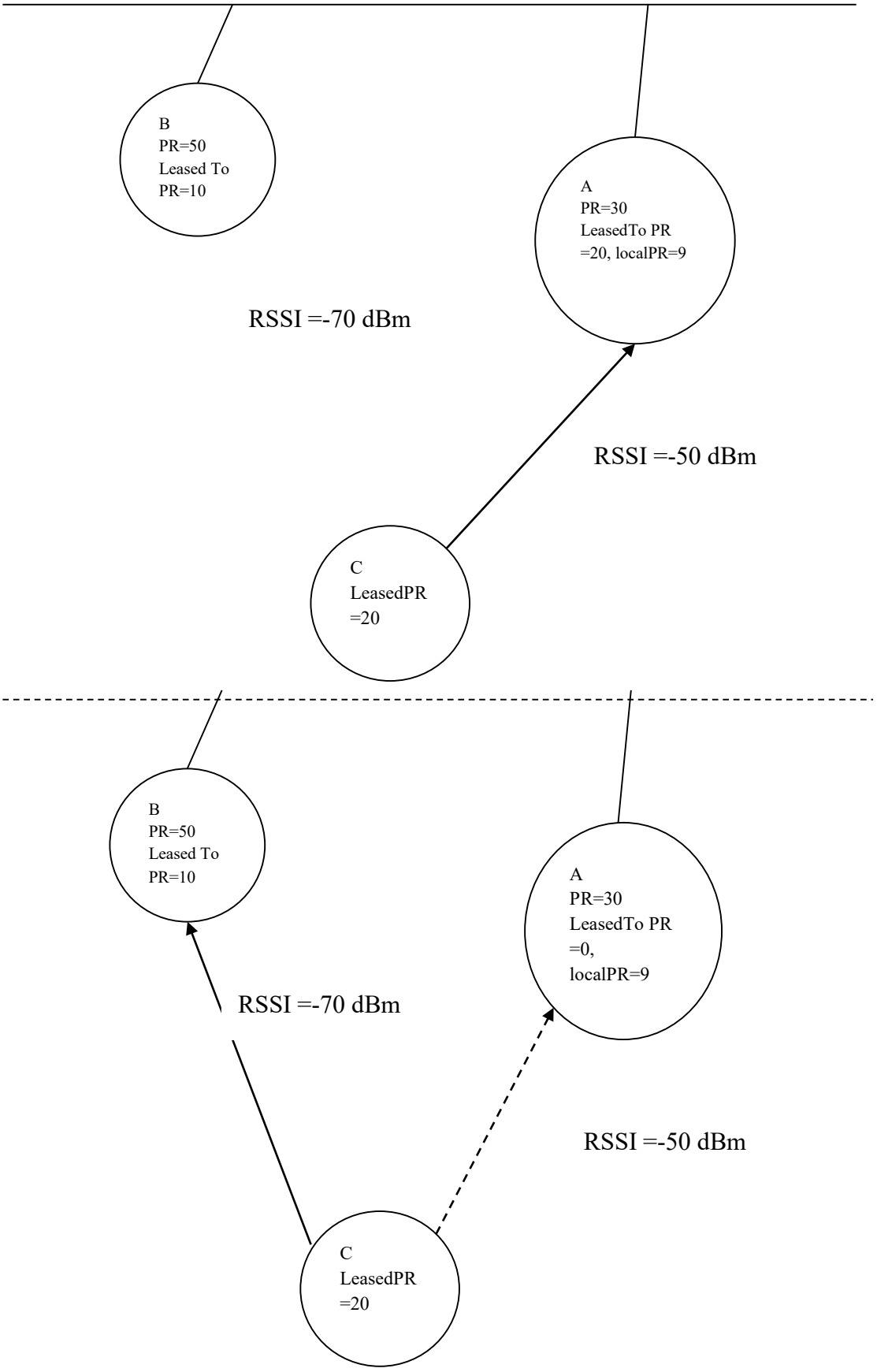

Figure 3.7: The soft handover process. Node C connects to node B before disconnecting from node A.

3.6 Relative On-Off thresholds

When the density of the network becomes high, the probability that are far away nodes from the sink node to initialize a connection with a parent becomes low. The on-off thresholds is defined as the parameter that determines when the node power on or off. In case of a low harvesting rate, the closer nodes to sink become weak and they cannot serve distant nodes. In addition, the misconfiguration of the on-off threshold of the nodes, and an increase in the application data rate, will weaken the closer nodes. As a result, the coverage area of the network will shrink, and the number of power outages will increase. To address this problem, we propose a relative on-off threshold of the network, where every parent must sleep for a time to store enough energy until it can support its children. The relative on-off threshold must be related to the node capability and the application data rate. In section 3.2 we represent the node energy capability of the PR (packet rate) on the observation window (T_w). The node sends an amount of data during T_w depending on the application data rate. Therefore, we can compute the application packet rate to compare with the PR in T_w as in equation 3.8

$$APR_j = \frac{(Application\ data\ rate(bps))}{paket\ length} \qquad (3.8)$$

APR stands for application packet rate. Figure 3.8 shows the relative on-off process, where B is a constant and A represents the expected number of children nodes. The relationship is shown by equation 3.9, which is derived from the previous total number of joined nodes. In other words, the effect of A will offer to a perent node the minimum PR needed to serve its children for at least one T_w after the parent node power on. The value of B is configured by the predefined value of the stored energy level, but represented by PR value. so that the node does not completely deplete its energy.

$$\mathrm{PR}_i \geq \sum_{j=i+1}^{A} APR_j \qquad (3.9)$$

PR_i represent the parent packet rate at the *i*th level, APR_j represent the APR of *j*th child, and A represent the nummber of children nodes. It is important to note that when the parent grant a PR budget to its children it keep track to the total of this value by storing it in Reserved-PR variable.

```
1:Start
2:Label1: Set Delay_Timer =250 ms
3:        If (PR_i ≥ ∑_{j=i+1}^{A} APR_j ) && State == OFF Then
4:            Set State = ON.
5:        Else If (PR < APR*T_w*B) && State == ON  Then
6:                Set State = OFF
7:                End If
8:        Go To: Label1
9:        End If
```

Figure 3.8: The relative on-off thresholds pesudo code, A and B are constants. A determines how many children for this node. B is configred at a low energy level, so the node does not completely deplete its energy.

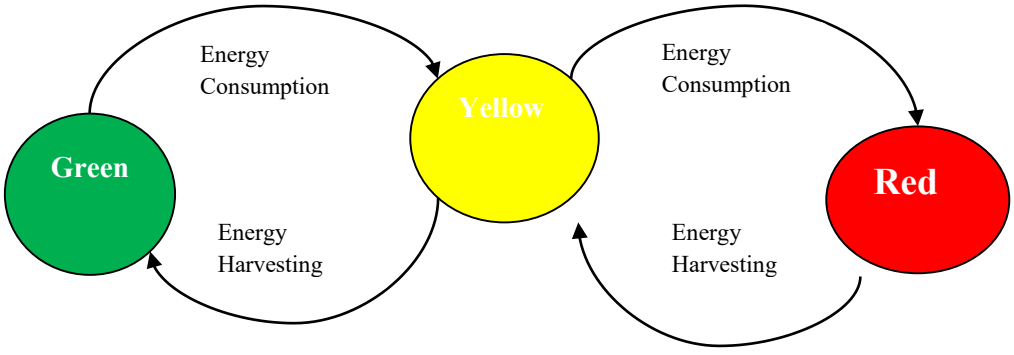

Figure 3.9: The power level state. At green state there is enough energy. At yellow state the node try to go back to green state by request some of its children to leve. At red state a node serve it self just.

Figure 3.10 illustrates the effect of the relative On threshold. First, at t_1 node A is connected to the sink, and node B is connected to node A with the PR values shown in the figure. At time t_2, node A energy's drops to the point where the PR value decreases to a level, at which node A can only support itself. At t_3, node A enters the sleep state, because the PR value is lower than this node needs to support its application demand. It remains in the sleep state until its PR's become 120 packets according to equation 3.9, so it can support itself and two children with assumption that the minimum needed PR equals to APR which is in this example is 40. Following this node (A) can support all its children, as shown at t_5.

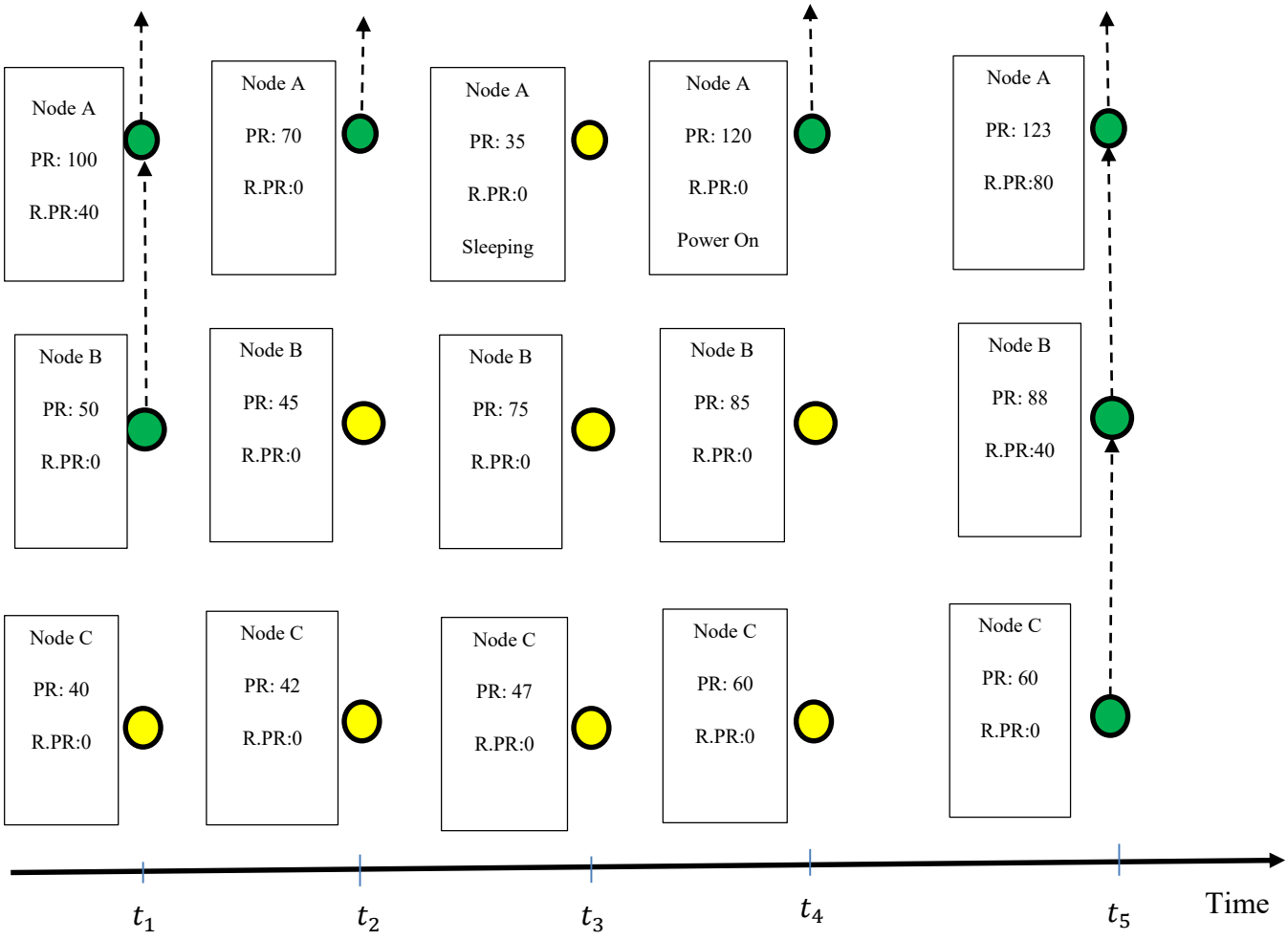

Figure 3.10: Three nodes A, B, and C in line topology. Node A is closer to the sink and node C is the farthest one. The figure shows the varying On connection using the Relative On-Off threshold. * R.PR stands for Reserved-PR. The minimum supported PR = APR by the node.

3.7 Protocol FSM

The sensor node in this proposed protocol can be at any of the following states are shown in Figure 3.11.

1. Listening state: when the node turns on it has no data about the surrounding area. The node starts collecting the beacon messages to build the routing table; after a few seconds the node goes to State 2. If the node does not receive any beacon message or

fails to receive any updated beacon message after returning from State 2, it goes to State 5.

2. Routing building state: this state is triggered by the end of State 1, when it has updates. If the node is successfully connected, it goes to State 3; otherwise it returns to State 1.
3. Data sending (operation) state: if the node is connected it proceeds to this state. If the reserved PR to this node from its parent node does not changed or does not receive any abandon order from the parent node it will stay at this state; otherwise it goes to State 4. Abandon order is a message send from parent to children in order to inform them to choose another parent.
4. Routing maintenance: in this state the node tries to join to another parent while it is still joined to the old parent node. The node enters this state when it receive an abandon order from the current parent or the connection to current parent node is lost.
5. Sleep state: when the node at State 1 times out, it goes to this state. The node stays at this node for a period of time and then goes to State 1.

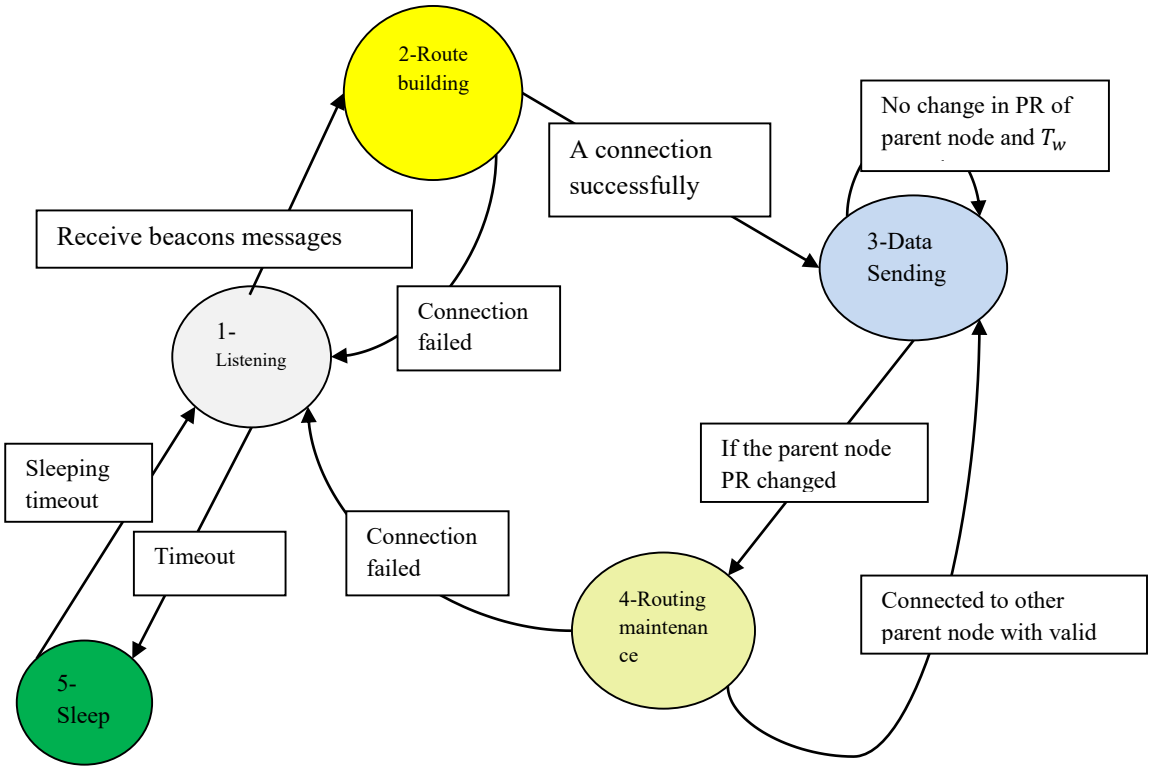

Figure 3.11: State transition diagram: the circle represents states, the rectangle represents conditions, and the arrows represent action

3.8 Comparison between DEECP and AODV in Term of Required Memory and Read/Write Energy Consumptions

After routing search phase the AODV node will have a full routing table of the other nodes. For example, if the network has 11 nodes, a node may have a 10- routing table entry that has a total of 2250 bits [38] . In addition, each node will have kept data for its neighbors with 112 bits. On the other hand, a DEECP node will have only one route entry with 64 bit length for its parent, and a 176 bit entry for each of its neighbors. Table 3.4: shows the comparison between DEECP and AODV protocols in terms of required memory. Table 3.5 shows the flash memory energy consumption for different brands. The writing process consumes more energy than reading. From the previous example of 11 nodes, we take a node with three neighbors and assume the memory

used is the Atmel NOR. It will consume 60.2uJ*Number of its neighbors, which equals to 180.6uJ in the case of the AODV protocol, and it consumes 283.8uJ in the case of the DEECP. For the routing table the AODV node needs 1376uJ for all entries, while the DEECP node needs 34.4uJ to store the route entries. In total, the AODV node consumes 1436.2uJ for writing its neighbor's table and the routing table; the DEECP node need 318.2uJ, which is 77% less than the AODV. It is important to note that AODV routing table entry timeout timer fields (32 bit) updated when the node receive any data packet. Hence, the read/write operation will directly related to application data rate, same as the read/write energy consumption. While DEECP update timeout for the routing table entry at the end of T_w.

AODV have four control messages Route Request (RREQ), Route Reply (RREP), Route Error (RERR), Route Reply Acknowledgment (RREP_ACK), and a periodic HELLO message broadcast every second (1 second default configuration). The DEECP has three main control messages discussed in section 3.4, with the T_w configured to be one seconds. Figure 3.12 shows five nodes, node A represent a sink node. Let use trace what happen when the node E want to send a packets at constant bit rate to node A for 100 seconds with AODV and DEECP protocols. In case of DEECP, first the tree will be built, this need to exchange 5 beacon messages in order to assign levels value. In order to connect B to A need 3 message (one join request message, one join reply message, and one beacon message), and so on, we need 3 messages for each connection (D to B, C to B, and E to D). In total, to build the tree we need 20 control messages. As this network stable for next 100 seconds, it need in total 520 (20+100*5) control messages (100 beacon messages for each nodes). In case of AODV, the node E broadcast RREQ messages which will forwarder by nodes D, C, and B. node A unicast RREP message to node E through nodes B and D. In addition of three RREP_ACK messages (or 4 messages via path A, B, C, D, and E). In total AODV exchange 10 control messages to initialize the routing. As this network stable for next 100 seconds, it need in total 510 (10+100*5) control messages (100 HELLO messages for each node). But if

the node E sends at low rate in which the jitter will be larger than the route record timeout (AODV configuration which is 3 seconds (default)), the ten control messages will be repeated when node E wants to send. In contrast, DEECP preserves on the tree even the data rate is low. It is important to note that nearly the number of beacon messages at DEECP is equivalent to the number of HELLO messages used in AODV to check if the neighbors node alive.

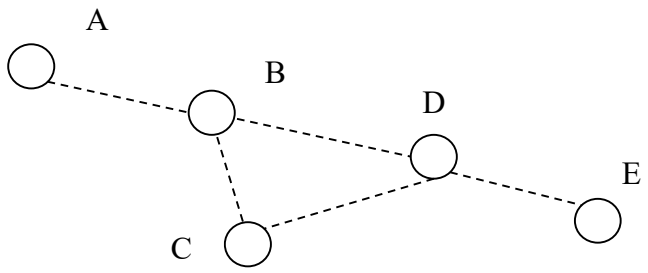

Figure 3.12: Five nodes, node A represent sink node. dashed line represent probability of connection

Table 3.4: shows the comparison between DEECP and AODV protocols in terms of required memory

Parameter	AODV	DEECP
Periodic Advertisement Packet	HELLO Messages send every seconds	Beacon Messages sends every T_w
Store Neighbors Data	Store in `neighbor table (IP, MAC, with Timer)`	Store in info table (IP, RSSI, PR, Next Node IP, with timer)
Neighbor Data For each record length	112 bits	176 bit
Queue Entry	Packet length + 32bit Timer	None
Route table at each node	`(dev, dst ,vSeqNoFage, m_seqNo, iface, hops, nextHopAddress, lifetime );`	(parent address, lifetime);
Routing table record length	`225 bit for each records * (number of nodes -1)`	64 bit

Table 3.5: Flash Energy Consumption - Read, Write,[55]

	Energy per byte (µJ)				
	Read	Write	Erase	Bulk Erase (Page count)	Total
Atmel NOR	0.26	4.3	2.36	n/a	6.92
Telos NOR	0.056	0.127	n/a	0.185 (256)	0.368
Hitachi MMC	0.06	0.575	0.47	0.0033 (16)	1.108
Toshiba 16MB NAND	0.004	0.009	n/a	0.004 (32)	0.017
Micron 512MB NAND	0.027	0.034	n/a	0.001 (64)	0.062

3.9 Case Studies

In this section we will show the tree building process cases, which illustrated in case 1, case 2, and case 3.

Case 1: Figure 3.14 shows four nodes: A, B, C, and D. Let node A belong to Level 0 (sink).

Initially, the other nods will be in the listening state. DEECP protocol uses a top-down approach.

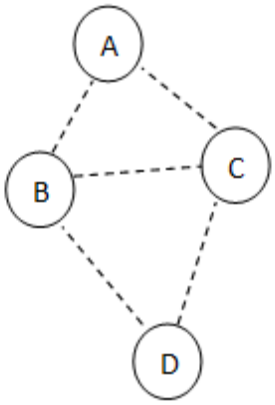

Figure 3.14 Tress building phase. The dashed lines represent the possible connections. The nodes B, C, and D are in the transmission range of node A.

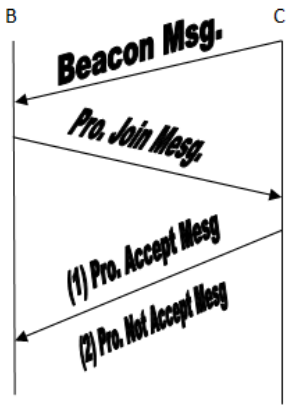

Figure 3.13: Shows the communication messages to join child to parent node.

The first beacon message will be sent from the sink node, which is node A in our case; all other nodes (B, C, and D) will receive the beacon message. These nodes will set their level to level 0 + 1 =Level 1. The nodes now go into an active routing building state (see Figure 3.11). From the perspective of node B, after node B goes into the active routing building state, it exchanges beacon messages with other nodes. If node B sends first, nodes C and D will know the RSSI at node B, and the best RSSI estimated by node B from level i-1, which is in this case level 0 (RSSI A-B). Table 3.6 shows the information after exchanging beacon messages among nodes B, C, and D. Now, apply equation 3.7 and let the parameter C_f= 0.93 and L_w = 1. The entry A-B will give a modified RSSI from -43 dBm to -38.99 dBm. Therefore the best choice, according to Table 3.6 to connect to node C by comparing weighted RSSI for direct connection to A with the RSSI from node C, and with RSSI between node A to C, This comparison as the *[RSS(C-B) > weighted(RSS(A-B))]&& [RSS(A-C) > weighted(RSS(A-B))*] condition is satisfied. But if node C is not yet connected, the packet rate will not yet be available in node C. Thus, node B will go back for a random time (normal distributed random variable 0 to 40 ms) as set by its timer, and it listens to beacon messages. If node C connects to A then it receives its packet rate. The other nodes will be announced in the next beacon message broadcast. Node B will send a Request Join proposal message. Then node C will respond with a Response Join proposal message, as Figure 3.5 shows. The response message from node C may indicate that the join request is accepted, so node C reserves the PR to node B. or may indicate that the join request is not accepted, and proposes a new PR value to node B. Hence, node B sends a new join request message with proposed PR's to node B. Table 3.6 shows the data collected by node C. Figure 3.15 shows the connection timeline to connect node C to B, as in this case.

Table 3.6: RSSI Stored in the Neighbor's Data Table, Case 1. Note: Nodes arranged as Sources-Destination of beacon message.

Nodes	RSSI (dBm)	RSSIweighted (dBm)
A-B	-43	-38.99
C-B	-38	-34.34
A-C	-35	-31.55
D-B	-70	-64.1
A-D	-85	-78.05

Table 3.7: RSSI and RSSI weighted as in case 1. Note: Nodes arranged as Sources-Destination of beacon message.

At node C		
Nodes	RSSI (dBm)	RSSIweighted (dBm)
A-C	-35	-31.55
A-B	-43	-38.99
B-C	-38	-34.34
D-C	-70	-64.1
A-D	-85	-78.05

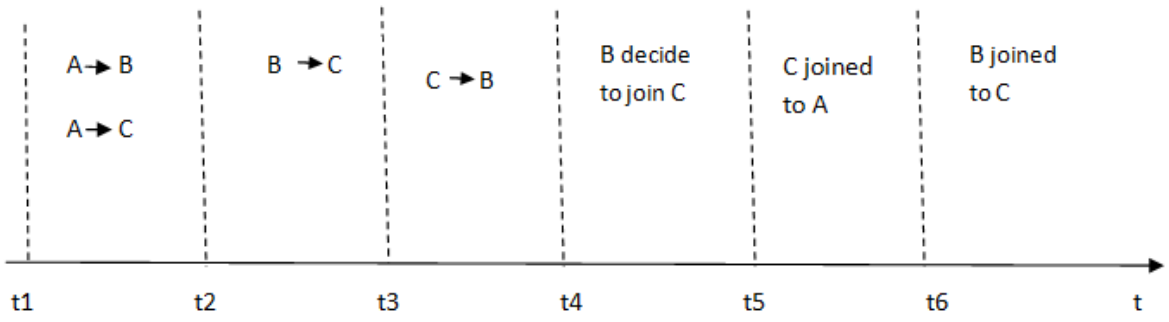

Figure 3.15: Timeline for nodes A, B and C connection.

Case 2: Assume the RSSI value is as in Table.3.8, and other assumption as in case 1; by using equation 3.7, the modified (RSS (B-A)) will become -34.34 dBm. By applying the condition *[RSS(C-B) > weighted(RSS(A-B))]&& [RSS(A-C) > weighted(RSS(A-B))*] the best connection here is to connect node B to node A. Figure 3.13 shows the sequence of steps in the connection.

Table.3.8: RSSI and RSSI weighted as in case 2

Nodes	RSSI (dBm)	RSSIweighted (dBm)
B-A	-38	-34.34
B-C	-33	-29.69
C-A	-36	-32.48
B-D	-70	-64.1
D-A	-85	-78.05

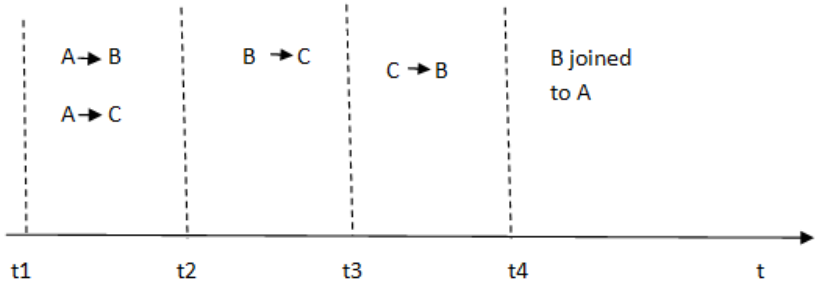

Figure 3.16: The sequence of steps to connect Node B to node A

Case 3 This case shows the handover process triggered by a node, where its power is decreasing below the operational level. The operational level is defined as the minimum power needed by a node to send its sensed data. Figure 3.6 illustrate this process.

This chapter introduced DEECP protocol in details, this protocol is a proactive protocol, so that we equipped it by techniques to mitigate the disadvantage of proactive protocols. The traditional proactive protocols will have high computational overhead when the network becomes dense, DEECP treats this drawback by restricting the node to deal with its direct neighbors' information at lower level and at the same level. In addition, on-off threshold guarantee that all nodes involved in a flow will cooperate together in order to deliver data packet to sink node. Hence, the delay and packet loss will decrease, goodput (see section 4.5) and total delivered bytes will increase. In the next chapter, we will discuss the simulation tool and setup.

CHAPTER 4
SIMULATION SETUP

In this chapter simulation setup will discussed. But, first the simulation tools and needed background will be described. Also, the DEECP parameter configuration will be shown. The last section will illustrate a simple example to show the behavior of network when the number of nodes increases

4.1 Network Simulator V3 Energy Harvesting Model

Network Simulator version 3 is the discrete event simulator that can be used for real time simulation. It has a well-documented models for easy to use and debug. In order to simulate a network that considers the nodes energy consumption, an energy model is needed. Network Simulator 3 (NS-3) has an energy model described in [39] which was added to NS-3 version 3.9. The energy framework of NS-3 consists of two basic models. The first one is the energy source model which represents the node energy supply source. Examples of this is linear, Li-ion battery models, and RV battery model which implements an analytical non-linear battery model. The other one is the device energy model, which represents the energy consumption of the node such as Wi-Fi radio model. An energy-harvesting model was recently implemented in NS3 version 3.22. This model allows the energy source remaining energy to increase based on predefined configurations. A harvester model which is add uniformly distributed random amount of energy to the remaining energy of the energy source every period of time (configured, default value 1 seconds). There are two attributes affect the harvesting rate, they are minimum harvestable power (*minhp*) and maximum harvestable power (*maxhp*). The actual harvested energy every second is a uniformly distributed value lies between *minhp* and maxhp:

$$EH(t) = Uniform\,[minhp, maxhp] \quad (1)$$

The available energy in a node in idle time (when the node is sleeping) i.e. no energy consumption, can be represented as a function of time as following:

$$AE(t) = \sum_{0}^{t} EH_t + IE\,; \qquad t = 0, 1, 2\ \ldots \quad (2)$$

Where AE (t) is the available energy at time t, and IE is the initial energy.

4.2 Network Simulator V3 Propagation Loss Model

The NS3 has eleven diverse propagation loss models. The Loss Models used to characterize wireless channels. In order for the simulator to compute the signal strength of a transmitted signal at the receiving stations, a propagation loss models are needed, which in turn is required to determine whether or not each of the receivers can in fact receive the information without bit errors. There are a variety of such models, varying from a models accounting for fast fading, to models accounting for ground reflections, to abstract fixed models, to a simple exponential decay related to the distance between a receiver and transmitter. We can classify those loss models into three groups [40] :

A. Abstract propagation loss models: do not represent real propagation loss, but need to be formed to fit the given scenario.
    1. Fixed Received Signal Strength: Unrelatedly to the distance, the receive power is fixed to a preconfigured value.
    2. Matrix Loss Model: The propagation loss is static between each pair of nodes. Maximal Range*:* it determines the distance where the signal is regained. Within that range the signal is regained at the transmit power level.

3. Random Propagation Loss: *it uses* a random distribution.

B. Deterministic path loss models, it is deterministic over the distance from sender to receiver.
    1. COST-Hata Model: It use to predict path loss in urban areas, A model based on various experiments [41] .
    2. Friis Propagation Model: it calculates quadratic path loss as it occurs in free space [42] .
    3. Log Distance Path Loss Model: It is designed for suburban scenarios, it assumes an exponential path loss over the distance from sender to receiver [43] .
    4. Three Log Distance Model: this model applies altered factors to the logarithmic path loss for different intervals of distance, it is a variant of the log distance model.
    5. Two Ray Ground Model: Two Ray Ground Model assumes a radio propagation via two paths: One reflects on the ground, the other one ray is received directly. This model was initially developed by Rappaport [44] .

C. The third class includes fading models: In order to account for the non-deterministic effects caused by moving objects, A stochastic fading process is applied on top of a path loss model
    1. Jakes Model: it[45] modeling a set of transmitted rays from the sender to the receiver through different paths to calculate the propagation loss [45] .
    2. Nakagami Model: it is similar to the Rayleigh model, but it describes different fading equations for long-distance and short-distance transmissions [46] .

In the next section (simulation setup) we will use the Friis Propagation Model, because the propagation loss models at class one and three not suitable as the node is stationary. In addition, the two other loss modes in class two is heavy in terms of computation power and time [40] .

4.3 Tmote Sky Sensore Device

This sensor uses the chipset CC2420 which provide reliable wireless communication. This chip is an IEEE 802.15.4 compliant radio providing the PHY and some MAC functions. The main feature of this chipset is that it has a programmable output power. Common CC2420 register values and their corresponding current consumption and output power are shown in Table 4.1. A device model was implemented in ns3 and tested to test the sending power variation. The Table 4.2 shows the computed distance with respect to input power [47] depending on [48] .

Table 4.1: Output power configuration for the CC2420 [48]

PA_LEVEL	TXCTRL register	Output Power [dBm]	Current Consumption [mA]
31	0xA0FF	0	17.4
27	0xA0FB	-1	16.5
23	0xA0f7	-3	15.2
19	0xA0F3	-5	13.9
15	0xA 0EF	-7	12.5
11	0xA 0EB	-10	11.2
7	0xA 0E7	-15	9.9
3	0xA 0E3	-25	8.5

Table 4.2: Transmission Power and Range for Tmote sky sensor [47]

Level	1	2	3	4	5	6
$R_i\,(meters)$	5.49	15.85	39.0	60.96	71.0	87.5
$P_i(mW)$	33.1	39.6	45.0	51.1	57.2	61.9

4.4 Simulation Setup

A Random topology with Wi-Fi nodes was created. In order to compare DEECP protocol with different protocols such as AODV, the topologies were stored and loaded at simulation time. Each protocol runs on the same set of topologies. One sample of these topologies is shown in Figure 4.1.

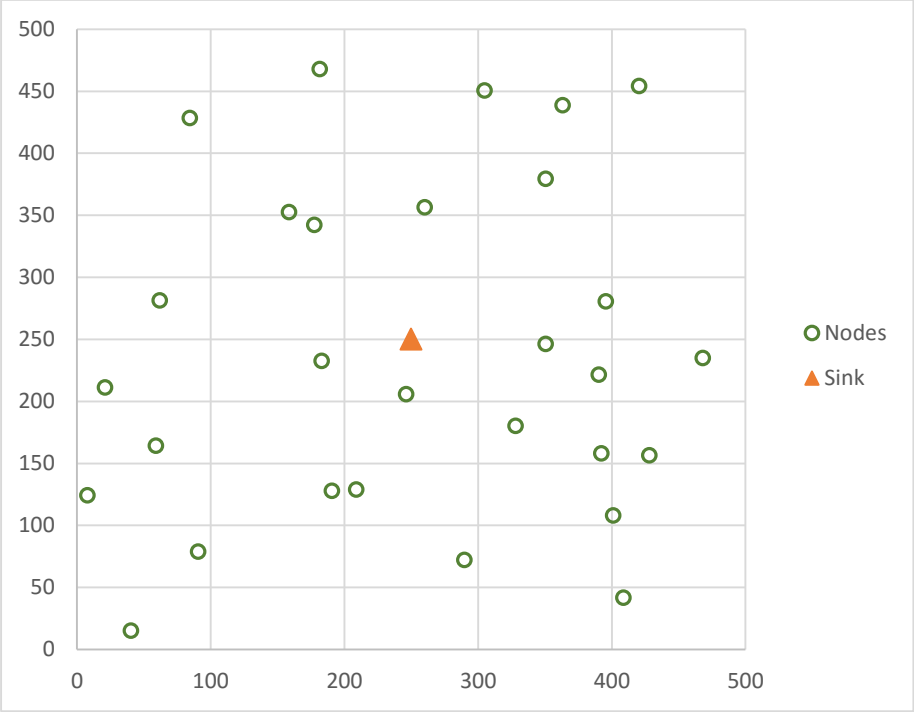

Figure 4.1: Nodes placement.

The MICAz mote sensor has outdoor transmission distance between 75 m to 100 m and 20 m to 30 m Indoor [49] . In subsequent scenarios, the configured transmission distance is considered to be 100 meters. The node located at the center functions as a sink node. It can communicate directly with the surrounding nodes. The topology is random but it is fixed for every simulation run. The nodes do not move from their initial location (stationary). In other words, the DEECP protocol and AODV protocol are simulated based on the same random topology. One sink application is installed in the center node. All other nodes are the source of traffic. Each one of the source nodes

has a data to be sent to the sink node at constant bit rate. The source nodes start sending their data to the sink at the beginning of the simulation and stop at the end of simulation. For example the Figure 4.1 shows 30 nodes (one sink and twenty nine of traffic sources). The simulation was replicated at least to achieve 90% level of confidence. The replication was performed by changing the random variable seeds.

The DEECP protocol has many parameters that affect the routing process. These parameters, include Packet Rate budget, received signals strength indicator etc... are shown in Table 4.3

Table 4.3:DEECP protocol parameters.

Parameter	**Description**	**Value**
BeaconInterval	Beacon messages emission interval	1sec = T_w
JreqRetries	Maximum number of retransmissions of JREQ to a node	3
JreqRateLimit	Maximum number of JREQ per second	10
NodeJoinTimeExpire	The time to consider a negative replay if we do not receive a reply	30 millisecond
ActiveRouteTimeout	Period of time during which the route is considered to be valid (connection to parent node).	3 * T_w
NodeLevel	Estimate the lowest hop count can be taken.	0 to N-1
AppDataRate Budget	Lowest Application Data Rate needed to operate an application per Interval	Up to physical limitation

In the next sub sections the energy and energy harvesting models will be discussed. These models are used in scenarios with DEECP, IEEE 802.11s, and AODV. In addition, the propagation path loss will be configured with Friis Propagation Loss Model

4.4.1 Energy Model

The NS-3 energy models were discussed in section 4.1 and Tmote sky sensor specifications were discussed in section 4.3. An energy model and energy harvesting model were installed on the nodes. The nodes in the simulation start with initial amount of energy to initiate the

communication. The nodes consume energy during transmission, receiving data, and data processing. The consumption amount depends on the radio energy device model parameters. The parameters that affect the amount of energy consumption are listed below. The values are compatible with CC2420 radio chip [48] .

- The Tx transmitter current: The default current in NS-3 is 17.4 mA.
- The Rx receiver current: The default current in NS-3 is 18.8mA.
- Voltage: The default voltage value in NS-3 is 2.5V. The default value was used in the simulation.
- The transmission time: this depends on the channel bandwidth. The channel type that used is 11Mbps DSSS.
- Idle consumption current: default value is 426 uA.
- Switching and sleeping current: default value is 20 uA.

In the simulation, Tx and Rx currents were considered while other currents were set to zero, because we assume that the node will not consumes any energy when it is sleeping. The amount of energy consumption is calculated using Eq. 3.4. and the time is measured using Eq. 3.5

The sink node was assumed to be powerful enough such that it never turns off. This is achieved by assigning high initial energy value to it.

4.4.2 Energy Harvesting Model

The energy harvesting model of NS-3 was described in section 4.1. The energy harvesting model was installed on all the nodes in the network. The minimum power harvesting rate and maximum power harvesting rate parameters control the amount of the harvested energy. The minimum harvesting power rate was set to zero for all nodes, while the maximum harvesting power rate was set randomly between 0.2mW to 0.8mW. As a result, the maximum harvesting power rate differs

from node to node. The minimum harvesting power rate and the maximum harvesting power rate are uniformly distributed. Nodes with higher maximum harvesting power rate harvest more energy than the nodes with lower harvesting power rate. The amount of harvested energy for a node in the entire simulation is computed using Eq. 4.1:

$$Totl\ Harvisting\ Energy = Sim.Time * Avg(minhp, maxhp) \qquad (4.1)$$

Figure 4.2 shows the total harvested energy and the consumed energy of nodes in a test run. The simulation time of the test was 300 seconds. The *minhp* is set 0 and the *maxhp* of the nodes was chosen randomly between 2 mW to 8 mW. The initial energy is 0.02 joules. The average harvesting energy of all nodes is 0.025J.

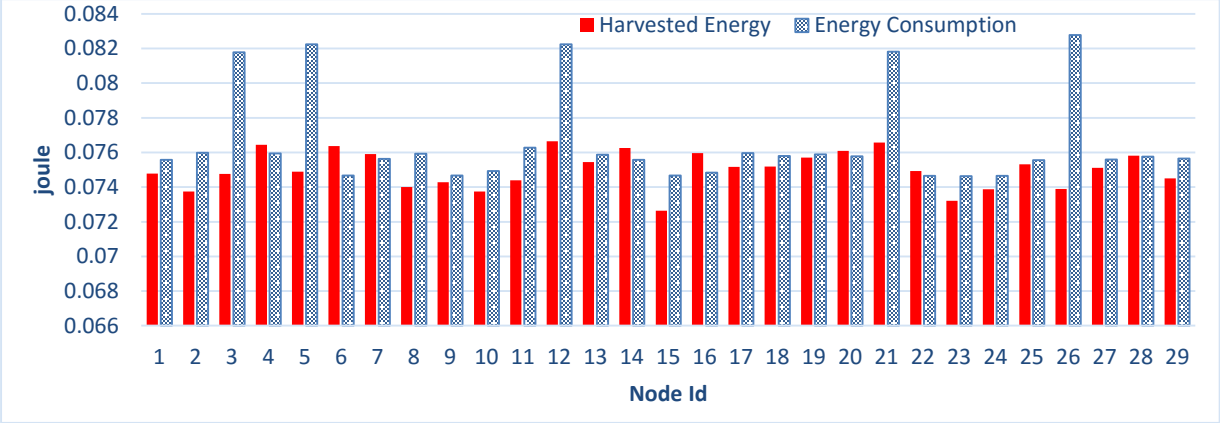

Figure 4.2: Nodes total harvested energy and and consumed energy.

The nodes with higher harvesting rate have higher amount of harvested energy. We can observe that there are some nodes have higher energy consumption than other nodes. It is clear from Figure 4.2 that the harvesting power rate of the nodes is uniformly distributed.

4.5 Performance Metric

The energy consumption increases when the amount of traffic increases. More sensor nodes in the network produce more traffic that is carried in the network. In this study, a power outage is defined as a node goes from on state to off state when the node exhaust its energy. In other words, the sum of alive nodes is the sum of nodes on active state. With low number of traffic sources, the nodes power outages dramatically decreases. NS3 software package consists of a flow monitor module that provides a flexible system to measure the performance of the network. Flow Monitor can only capture packets at network level (level 3). The module uses probes installed in nodes to track the packets exchanged by nodes. Packets are divided according to their flow, where each flow is defined according to the probe's characteristics. Flow monitor can provide the following measures: (1) the number of transmitted packets (2) the sum of transmitted bytes (3) the number of received packets (4) the sum of received bytes (5) the sum of delay for these packets in each flows. The flow is defined based on protocol, source IP, source port, destination IP, and destination port tuple. The probes measure the packet bytes and IP headers while layer-2 headers are not included [50] . In order to evaluate these scenarios; we may use all or some of the following performance metrics. This metrics can be extracted directly from the flow monitor output or it can be calculated from the flow monitor outputs:

1. Packet End-to-End Delay

It is the time needed by a packet to travel between source and destination. This time includes propagation time and forwarding time. The propagation time is the time needed to transfer a packet from node to node. However, the forwarding time is the time needed by intermediate node to receive and retransmit a packet. The flow monitor model provides the sum of end to end delay for all transmitted packets per flow. The average of end to end delay can be calculated by dividing the sum of end to end delay for all flow by total number of received packets.

2. Packet Loss Ratio

The flow monitor traces the number of sent and lost packets for each flow. The packet loss ratio equals the number of lost packets divided by the number of sent packets. The network loss ratio is defined as the average packet loss of all flows.

3. The Sum of Received Bytes

This metric counts all bytes received by the sink at L4protocol (transport layer).

4. The Sum of Consumed Energy

It is the sum of consumed energy by all nodes during the simulation. The sum of consumed energy is in correspondence with the sum of node active time (mainly sent/received) packets time.

5. The Sum of Active Nodes

This metric traces the state of all nodes in the network whether they are in off\on state.

6. Average Goodput per Flow

Goodput is defined as the application layer quantity of error-free data packet that is received per unit of time. On other hand, Throughput is defined as the quantity of error-free data packet that is transmitted per unit of time (bps) [51] . This metric equals the average of flows goodput, where the flow goodput is calculated by take the sum of received bytes per flow divided over the flow time. If the flows' times are equal, we can calculate the goodput as the sum of received bytes per flow divided over the sum of flows times.

7. Total Number of Power Outages

Outages is defined as the node goes to sleep or shutdown due to lack of power. This metric traces the total number of power outages in the network across the entire simulation.

4.6 Study the Effect of Increasing Number of Nodes

In this section a simple scenario was conducted to investigate effect of increasing the node number on goodput and packet loss ratio. It is important to note that every node is a traffic source. Table 4.4 shows the simulation parameters

Table 4.4: Simulation parameters

Parameter	**Value**
Test Area	500m X 500m
Number of nodes	2, 3, 4, and 10
Placement	Uniformly random placement
Radio range	100 m
Transmission bandwidth	11 Mbps
Application traffic	ON/OFF with 50% duty cycle, Data Rate: 20 Kbps, Transport Protocol: UDP
Initial Energy	8J
Number of sources	Number of nodes -1
Packet size	64 Bytes
Number of packets per source	unlimited
Energy harvesting	None
Routing protocol	AODV
Simulation time	450 sec

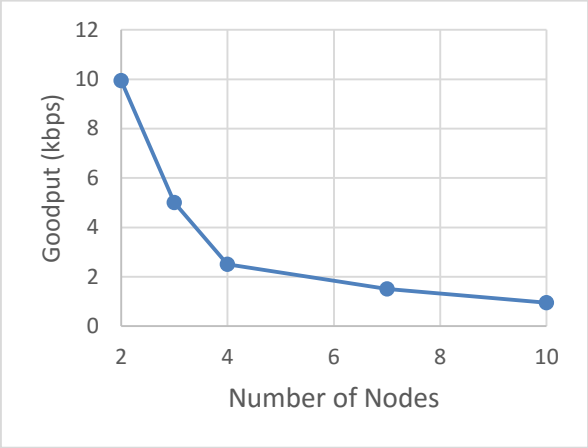

Figure 4.3: Average Goodput. Application data rate 20 kbps, duty cycle 50%

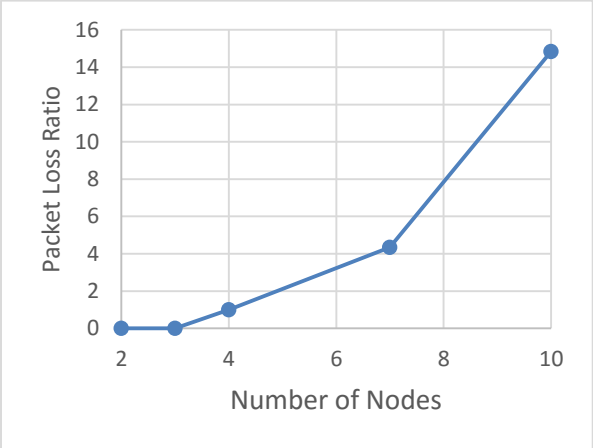

Figure 4.4: Packet loss ratio. Application data rate 20 kbps, duty cycle 50%

Figure 4.3 shows the goodput versus the number of nodes. The goodput is equal to 10 kbps when the number of nodes is two (sink node and one traffic source), when the number of nodes increases to three the goodput drops more than a half, at 10 node the goodput decreases to nearly by 90% to become 0.99 kbps. The reason for this drops in goodput when the number of nodes increases is the increases of contention among the nodes. Which will result in increasing the packet loss ratio at shown in Figure 4.4.

After we discuss simulation tool and setup the next chapter will discuss simulation results that test the DEECP versus AODV and IEEE 802.11s protocols

CHAPTER 5
SIMULATION RESULTS

The DEECP protocol is designed especially for applications that require data collection from sensor nodes. DEECP protocol was implemented using NS-3 simulator. In this chapter, we introduce different simulation scenarios that show the performance of DEECP versus the other protocols like AODV and IEEE 802.11s. Performance metrics used in the evaluation are discussed in previous chapter.

5.1 Simulation Scenarios

The following sections present the different simulation scenarios that were conducted to test the performance of DEECP against AODV algorithm and IEEE 802.11s at proactive mode. For each scenario the simulation parameters, results, and discussion are shown.

5.1.1 Study the Effect of Changing Number of Nodes without Energy Harvesting

The goal of this scenario is to show the performance of DEECP and AODV in terms of end-end delay, goodput, and packet loss ratio. In this experiment the number of nodes was varied around the sink node with a battery as energy source. The performance metrics were discussed in section 4.5. The simulation parameters are shown in Table 5.1.

Table 5.1: Simulation Parameters.

Parameter	**Value**
Test Area	500m X 500m
Number of nodes	7, 10 ,15, 20, and 30
Placement	Uniformly random placement
Radio range	100 m
Transmission bandwidth	11 Mbps
Application traffic	ON/OFF with 50% duty cycle, Data Rate: 8 Kbps, Transport Protocol: UDP
Initial Energy	0.5 J
Number of sources	Number of nodes -1
Packet size	64 Bytes
Number of packets per source	unlimited
Energy harvesting	None
Routing protocol	AODV, DEECP.
Simulation time	300 sec
T_w	1 second
DEECP A parameter	10

An example of the network topology, nodes, and sink are shown in Figure 4.1. An on-off application is installed on the source nodes, which sends data packets to the sink in on/off manner. As soon as, the source has packets to be sent, the application sends data for maximum 1 second at rate of 8 Kbps then stops for maximum of 1 second. This process continues until the end of the simulation.

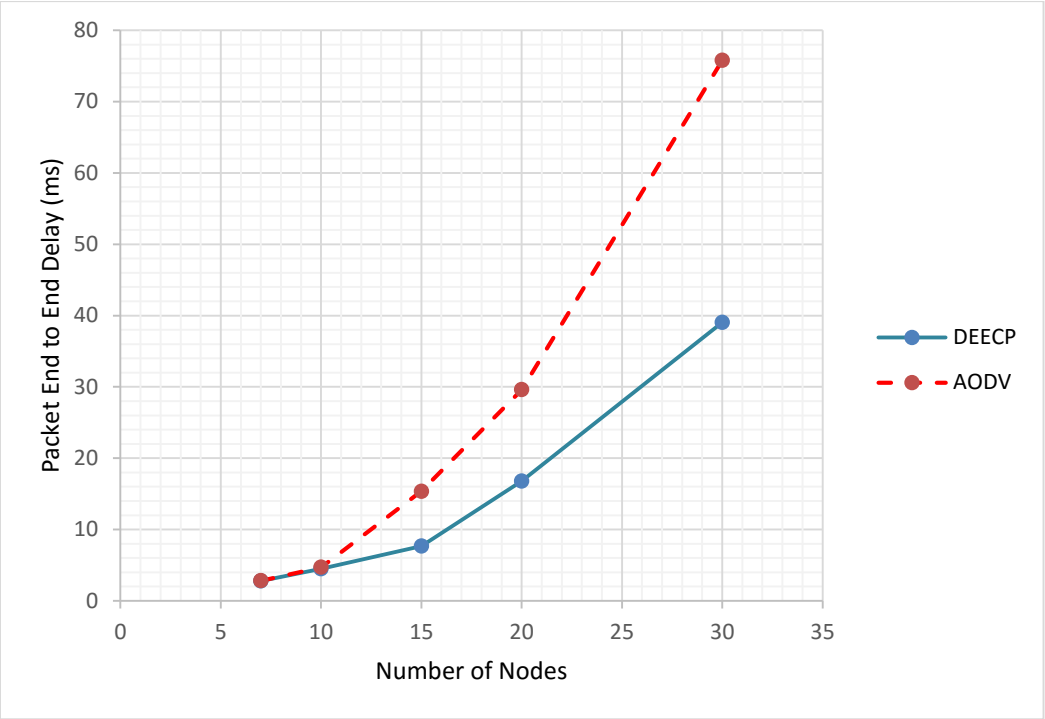

Figure 5.1: Average packet end-end delay per flow. UDP flows at average rate of 8Kbps per flow.

Figure 5.1 shows the average packet end-to-end delay versus the number of nodes. It is expected that the value of end-to-end delay increases when the number of nodes increases. The end-to-end delay is affected by the number of nodes. Higher number of nodes extends the coverage area, but it increases the propagation delay and the number of nodes in path. DEECP has the lowest end-to-end delay. This is can be explained by two reasons; first reason is the type of selection criteria of each protocol. DEECP protocol is a proactive protocol so no need to wait until route discovery like in AODV. AODV prefers paths with lowest number of hops, second reason is the queuing delay, where AODV queue a packets until the route is initiated, and DEECP does not have a queue. In order to quantify the performance of the protocols, a two-factor full factorial experimental design analysis is performed to determine the effects of the factors on the delay [52] . Table 5.2 shows the two factors full factorial effects for the routing protocol and number of nodes on the delay.

Table 5.2: Computation of effects of the protocols on end-end delay.

# of nodes	DEECP	AODV	Row Sum	Row Mean	Row Effect
7	2.793775	2.810129	5.603903873	2.8019519	-17.0992399
10	4.468271	4.704125	9.172396154	4.5861981	-15.3149938
15	7.661427	15.36517	23.0265971	11.513299	-8.38789333
20	16.77695	29.6119	46.38884588	23.194423	3.293231066
30	39.02523	75.79495	114.8201758	57.410088	37.508896
Column Sum	70.72565	128.2863			
Column Mean	14.14513	25.65725		19.901192	
Column Effect	-5.75606	5.756062			

The mean of delay is calculated for each row and column. The overall mean are also computed. The effect for each row and column is computed by measuring the difference between its mean and overall mean. The results of the analysis are interpreted as follows; the packet end-to-end delay is 19.9 milliseconds with an average protocol and average number of nodes.

The delay with DEECP is 5.75 milliseconds lower than that with an overall average protocol. The delay with AODV is 5.75 milliseconds higher than that with an overall average protocol. This also means that the mean difference between DEECP and AODV is 11.51 milliseconds. Or in other words, at 7 nodes the DEECP is less packet end to end delay than AODV about 0.5% to 48.5% at 30 nodes. Considering the average number of nodes, the DEECP achieves packet end to end delay less than AODV by 44.86% with 90% of confidence level.

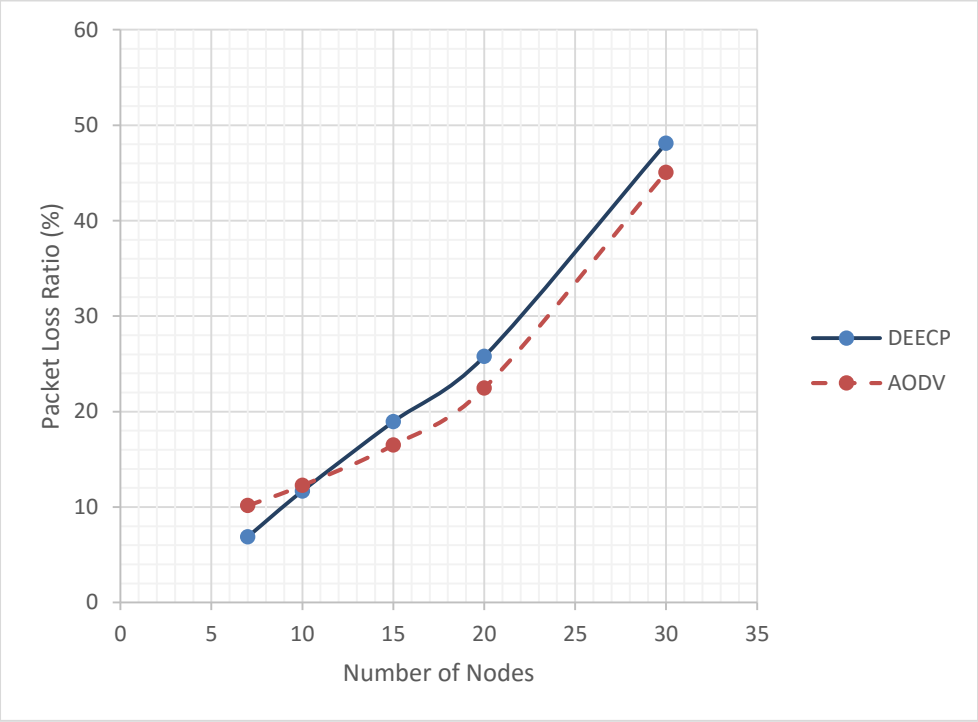

Figure 5.2: Average packet loss ratio per flow. UDP flows at average rate of 8Kbps per flow. Number of data sources are equal the number of nodes -1.

Figure 5.2 shows the average packet loss ratio versus the number of nodes. Packet losses are caused by the communication interference, which is anything alters, modifies, or disrupts a message when it travels along the channel [53] . Table 5.3 shows that the DEECP is 32% less than AODV at 7 nodes. As the number of nodes increased, the packet loss of DEECP protocol increases more than AODV protocol. At 30 nodes the DEECP has 6.7% more packet losses than AODV. In average, the AODV has less packet loss ratio than DEECP by 4.6% without energy harvesting. This because that with AODV the node send at any available path even it is not the shortest one, but the DEECP children nodes compete to get the sending opportunity to parent node this will increase the collision, and in result, the packet loss will increase.

Table 5.3: Computation of effects of the protocols on Packet Loss Ratio

# of nodes	DEECP	AODV	Row Sum	Row Mean	Row Effect
7	6.889544	10.1624	17.05194	8.525972	-13.2686
10	11.68907	12.27775	23.96683	11.98341	-9.81119
15	18.95562	16.50164	35.45726	17.72863	-4.06597
20	25.78049	22.47909	48.25958	24.12979	2.335188
30	48.12835	45.08206	93.21041	46.6052	24.8106
Column Sum	111.4431	106.5029			
Column Mean	22.28861	21.30059		21.7946	
Column Effect	0.494013	-0.49401			

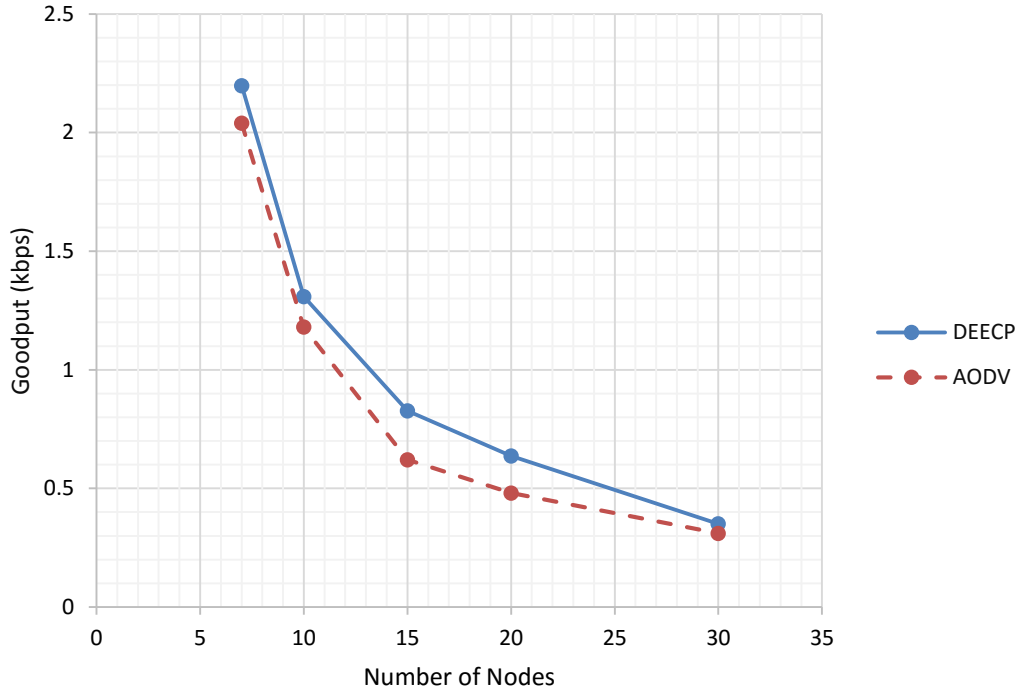

Figure 5.3: Average goodput per flow. From six to twenty nine UDP flows at average rate of 8Kbps per flow.

Figure 5.3 shows the average of flow goodput versus the number of nodes. The goodput decreases when the number of nodes increases, because the competence among the nodes increase, as a result, the collision increases. Hence, the node chance to send its data decreases. DEECP achieved a higher goodput than AODV. Table 5.4 shows that DEECP at 7 nodes is better than AODV by 7.7% to 12.87% at 30 nodes in terms of goodput. In average of all number of nodes, the DEECP has more goodput than AODV by 14.84%.

Table 5.4: Computation of effects of the protocols on Goodput.

# of nodes	DEECP	AODV	Row Sum	Row Mean	Row Effect
7	2.197418	2.040102	**4.23752**	**2.11876**	**1.123583**
10	1.308057	1.180174	**2.488231**	**1.244116**	**0.248939**
15	0.827049	0.620732	**1.447781**	**0.723891**	**-0.27129**
20	0.636928	0.48059	**1.117518**	**0.558759**	**-0.43642**
30	0.350335	0.310386	**0.660721**	**0.330361**	**-0.66482**
Column Sum	**5.319787**	**4.631984**			
Column Mean	**1.063957**	**0.926397**		**0.995177**	
Column Effect	**0.06878**	**-0.06878**			

Table 5.5 shows the average effects of the DEECP on the different performance metrics. The percentage of the enhancement or degradation with respect to AODV is shown

Table 5.5: Computed percentage of effects of DEECP protocol on the performance with respect to AODV. (-) and (+) mean the percentage decrease or increase in the performance metric.

Performance metric	**DEECP Protocol**
End to end delay	-44.8 **%**
Packet loss ratio	4.6%
Goodput	14.84 **%**

5.1.2 Study the Effect of Varying the Time Window Parameter (T_w)

In this scenario, simulation experiments are conducted where the variable is the time window T_w parameter. The time window parameter has a significant effect on the DEECP protocol. Table 5.6 shows the simulation parameters.

Table 5.6: Simulation Parameters.

Parameter	**Value**
Test Area	500m X 500m
Number of nodes	10
Placement	Uniformly random placement
Radio range	100 m
Transmission bandwidth	11 Mbps
Application traffic	On time 1 second and Off time is 1 second Data Rate: 30 Kbps, Transport Protocol: UDP
Initial Energy	0.02 J
Number of sources	Number of nodes -1
Packet size	64 Bytes
Number of packets per source	unlimited
Energy harvesting	minhp: 0, maxhp: [2 mW – 8 mW]
Node Down time	Depending on Application Data rate at DEECP, and on AODV depending on harvesting rate to charge from 0.02J to 0.04J
Routing protocol	DEECP
Simulation time	900 sec
T_w	0.5,1,2,3,4,5,6 seconds

Figure 5.4 shows the end to end delay when the T_w changed from 0.5 second to 6.0 seconds. The lowest delay value was achieved when the time window T_w is equal to 1 second. When the T_w is decreased to 0.5 second the delay increased by 18%. When the T_w increased to 6 seconds the delay increased by 96 %.

Figure 5.5 shows the packet loss ratio versus T_w changed from 0.5 second to 6.0 seconds. The lowest loss ratio was achieved at 1 second. The packet loss has direct relationship with T_w.

Figure 5.6 shows the goodput when the T_w changed from 0.5 second to 6.0 seconds. The figure shows that the best value of T_w is one seconds under these conditions. The goodput at 0.5 seconds is less than at T_w equal one seconds by 1.6%. The goodput was decreased by 51% at T_w equal six seconds. In average, the goodput at one seconds better than other values by 41%.

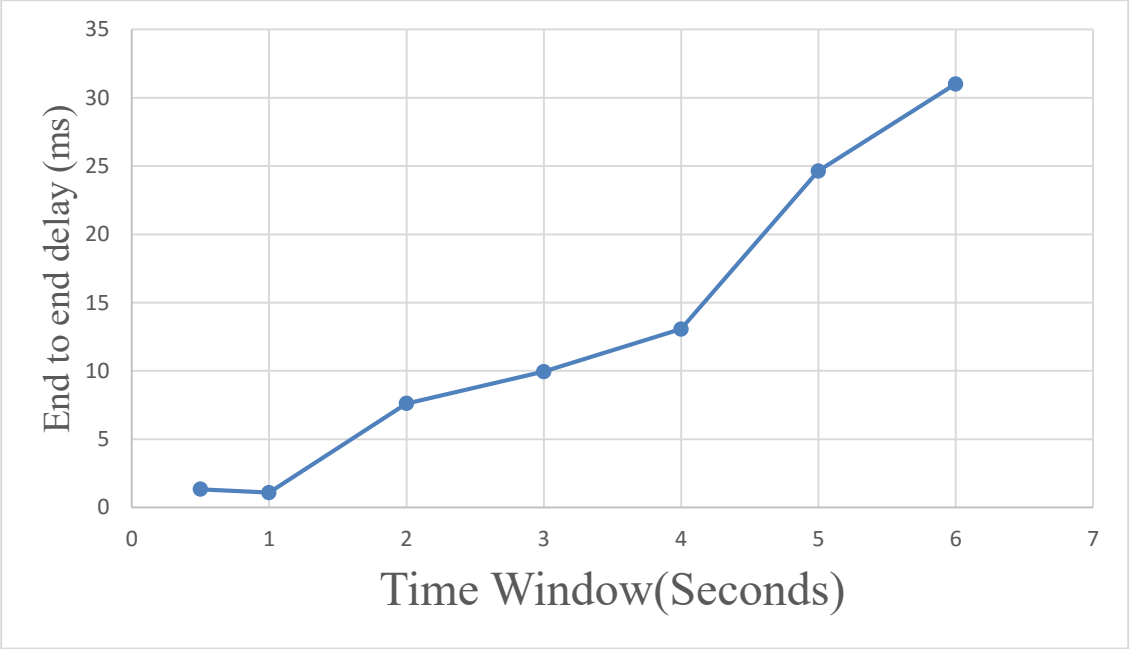

Figure 5.4: End to End delay, 10 nodes, and application data rate is 30 kbps.Tw varying from 0.5 seconds to 6 seconds.

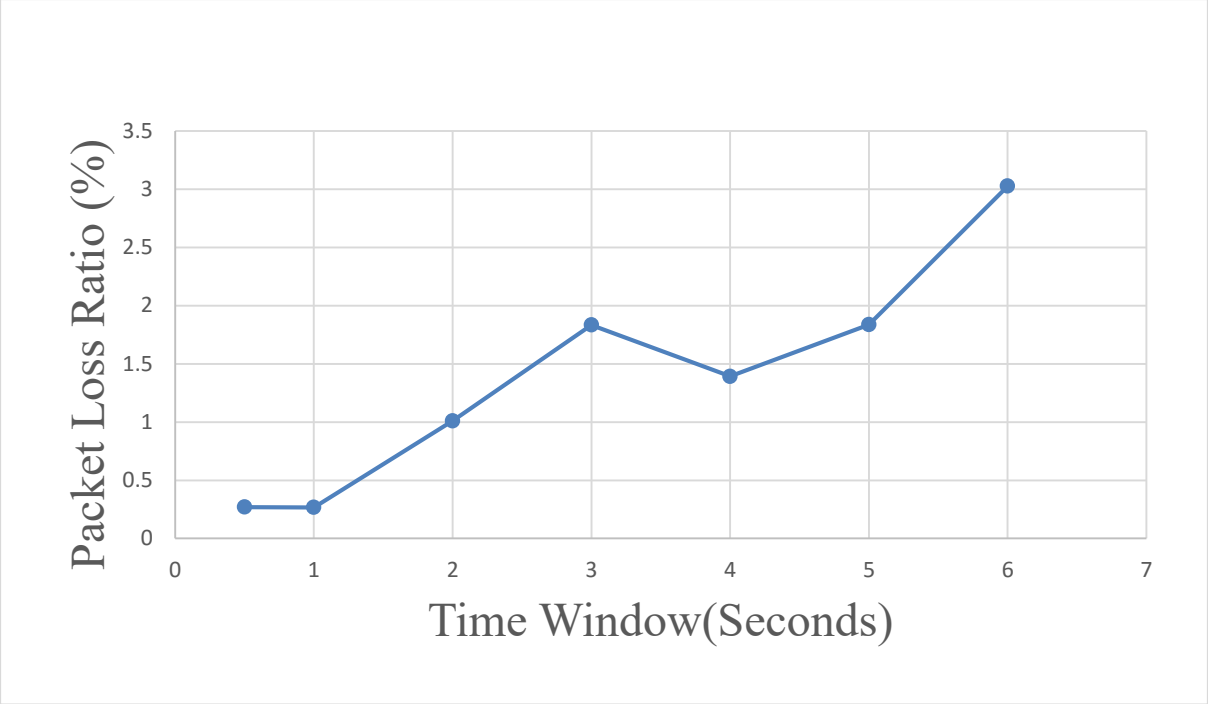

Figure 5.5: Packet Loss ratio, 10 nodes, and application data rate is 30 kbps.Tw varying from 0.5 seconds to 6 seconds.

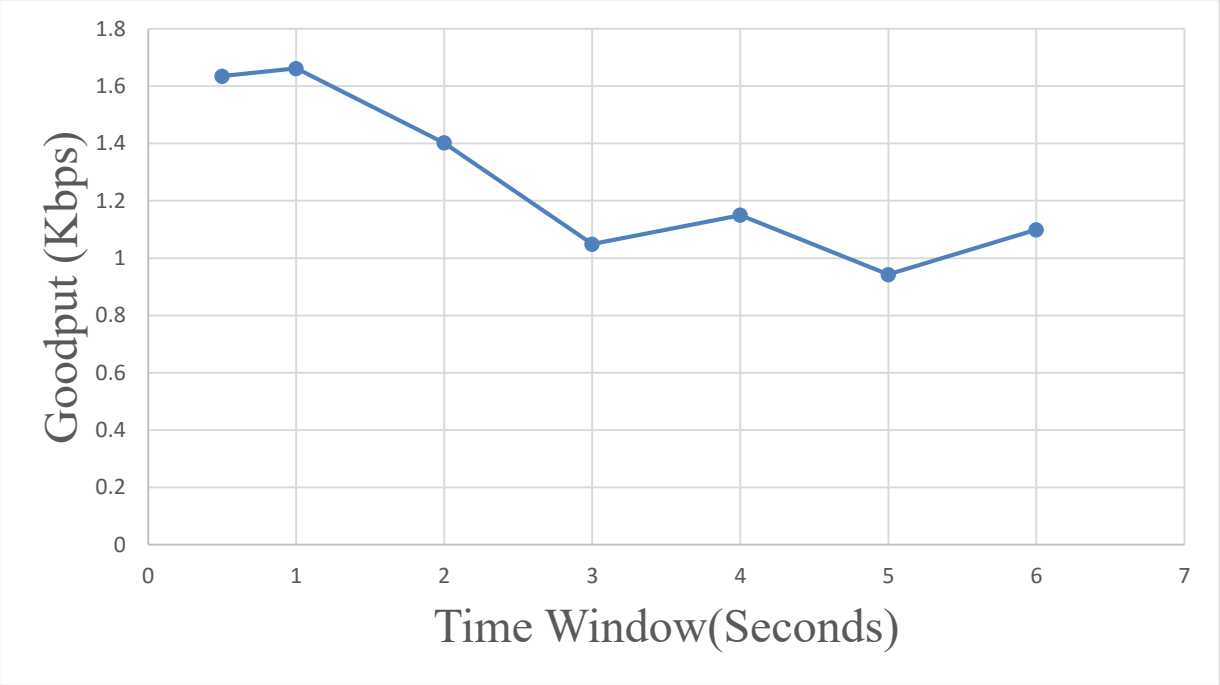

Figure 5.6: Goodput (kbps), at 10 Nodes and application data rate is 30 kbps. Tw varying from 0.5 seconds to 6 seconds.

5.1.3 Study the Effect of Varying the Application Data Transmission Rate with Energy Harvesting on DEECP vs AODV

This scenario evaluates the effect of varying application data rate on the following metrics: goodput, end-to-end delay, packet loss ratio, total energy consumption, and power outages. The goal of this scenario is to study the effect of the application data rate on the network performance. Secondly, the scenario is used to compare DEECP protocol versus AODV protocol with energy harvesting at different application data rate. The energy source for this scenario is the solar power, let us assume it at shadow place. The routing protocols that used in this scenario are DEECP and AODV. The simulation parameters are listed in Table 5.7.

Table 5.7: Simulation parameter.

Parameter	**Value**
Application traffic	ON/OFF with 50% duty cycle. Data Rate: 20 Kbps, 50 kbps, and 80 kbps. Transport Protocol: UDP
Initial Energy	0.02 J
Routing protocol	DEECP, AODV with Energy Harvesting.
Node Down time	Depending on Application Data rate at DEECP. On AODV depending on harvesting rate to charge from 0.002J to 0.02J
Energy harvesting	Minhp: 0- maxhp: [0.2 mW – 0.8 mW]
T_w	1000 milliseconds.
Simulation time	900 sec

The other parameters are as in Table 5.1.

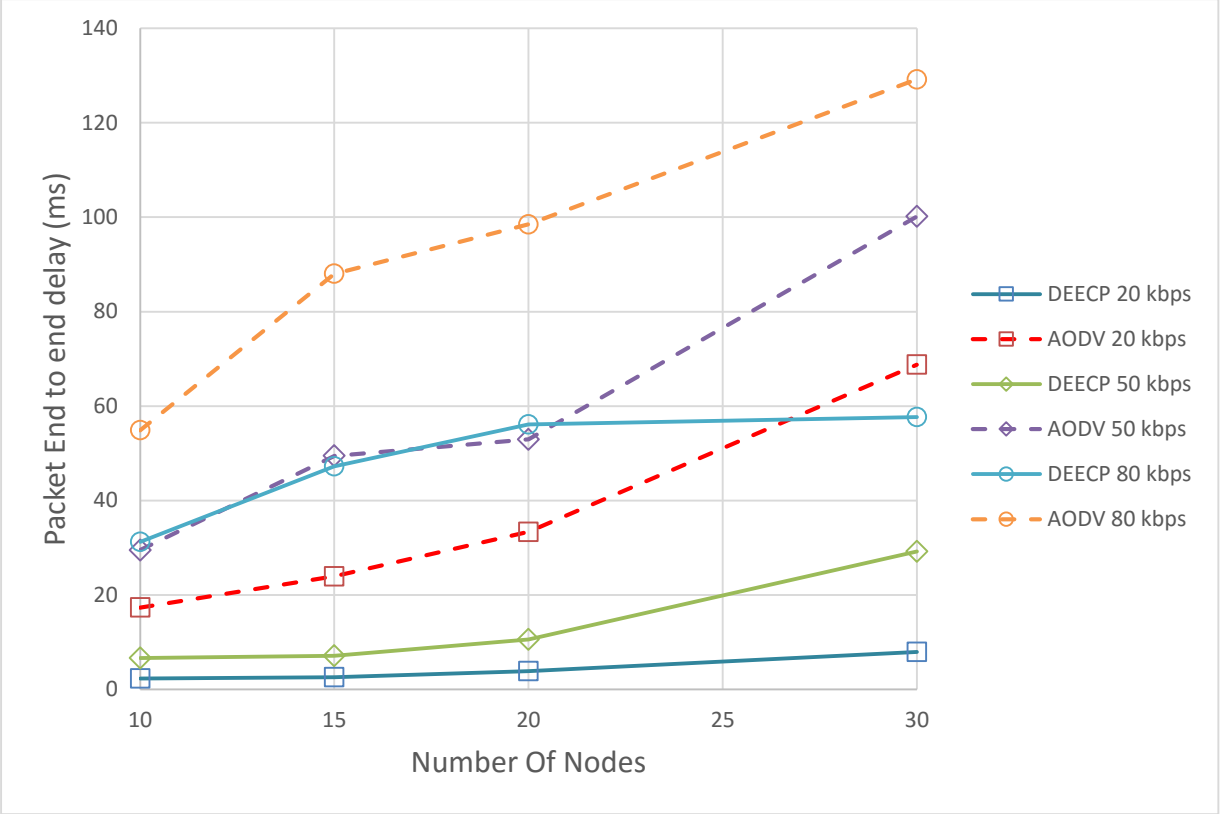

Figure 5.7: Packet end-to-end delay at data rate 20 kbps, 50 kbps, and 80 kbps for AODV protocol and DEECP protocol.

Figure 5.7 shows the average packet end to end delay of the flows versus the number of nodes for different application data rates. The higher the number of nodes causes the packet end to end delay to increase. Increasing the application data rate causes higher buffering delay, because the number of packets needed to be sent by the node increases. The relation between the data rate and the delay is nonlinear. The difference in delay when the rate is changed from 50 Kbps to 80 Kbps is higher than the difference when the rate is changed from 20 Kbps to 50 Kbps. The percentage of difference on delay is 259% and 221% for DEECP protocol for the two differences of application data rate respectively .i.e. the 221% percentage calculated by take the sum of packet end to end delay for all number of nodes at 50 kbps with respect to the sum of packet end to end delay at 20 kbps . Table 5.8 shows the effected end to end delay for varying application data rate and varying number of nodes for DEECP and AODV protocols at 20 kbps, 50k bps, and 80 kbps. Table 5.15 shows the computed percentage of effect of end to end delay for DEECP with respect to AODV.

In average, the DEECP achieves end to end delay less than AODV by 88.4% and 48% at 20kbps and 80 kbps respectively. In average of application data rate and number of nodes, the DEECP has less packet end to end delay than AODV by 65%.

Table 5.8:End to End Delay of DEECP protocol and AODV protocol. The table shows the effect of varying number of nodes and varying the routing protocols at application data rate (20 kbps, 50 kbps, 80 kbps), on pakets end to end delay.

	# of Nodes	AODV	DEECP	Row Sum	Row Mean	Row Effect
20 kbps	10	17.32624	2.326934	19.65317	9.826585	-10.1775
	15	23.93498	2.571918	26.5069	13.25345	-6.75061
	20	33.34898	3.83774	37.18672	18.59336	-1.4107
	30	68.76049	7.925196	76.68569	38.34284	18.33878
	Column Sum	143.3707	16.66179			
	Column Mean	35.84267	4.165447			
	Column Effect	15.83861	-15.8386		20.00406	
50kbps	# of Nodes	AODV	DEECP	Row Sum	Row Mean	Row Effect
	10	29.50342	6.633417	36.13684	18.06842	-17.6256
	15	49.46363	7.090345	56.55397	28.27699	-7.41701
	20	52.95155	10.59238	63.54393	31.77197	-3.92203
	30	100.1351	29.18211	129.3172	64.6586	28.96461
	Column Sum	232.0537	53.49826			
	Column Mean	58.01342	13.37456			
	Column Effect	22.31943	-22.3194		35.69399	
80 kbps	# of Nodes	AODV	DEECP	Row Sum	Row Mean	Row Effect
	10	54.87188	31.25129	86.12317	43.06158	-27.2918
	15	88.00929	47.2637	135.273	67.6365	-2.71689
	20	98.4793	56.13149	154.6108	77.30539	6.952004
	30	129.1701	57.6501	186.8202	93.41008	23.05669
	Column Sum	370.5305	192.2966			
	Column Mean	92.63263	48.07414			
	Column Effect	22.27924	-22.2792		70.35339	

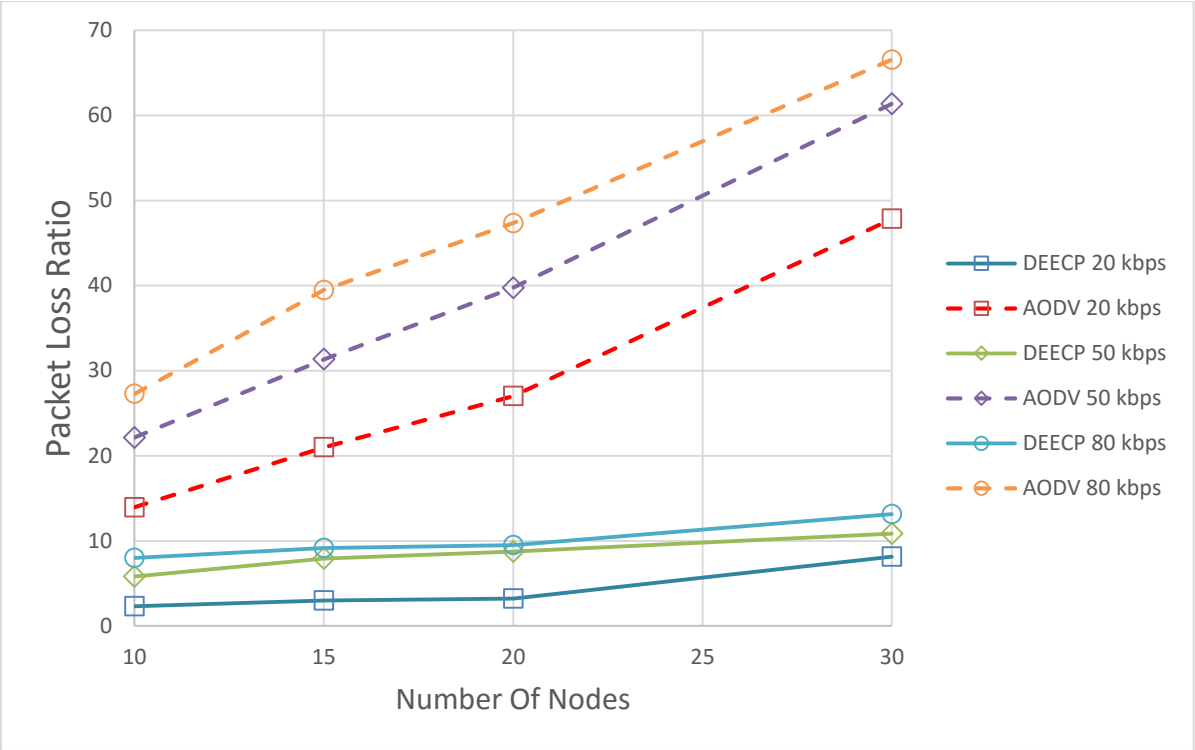

Figure 5.8: Packet Loss Ratio for DEECP and AODV at 20kbps, 50kbps, and 80kbps.the number of node varying from 10 to 30 nodes including the sink node.

Figure 5.8 shows the average packet loss ratio of the flows versus the number of nodes. Packet loss ratio increases as the number of nodes increases. As expected, the configuration with highest application data rate generated the highest packet loss ratio and vice versa, because the contention increase, and in result, the collision increase. In addition, when the number of nodes (number of data sources) increases the packet loss also increases. Table 5.9 shows the effected packet loss ratio for varying application data rate and varying number of nodes for DEECP and AODV protocols at 20 kbps, 50 kbps, and 80 kbps, respectively. Table 5.15 shows the computed percentage of packet loss ratio for DEECP with respect to AODV. On average DEECP achieves packet loss ratio less than AODV by 84.4% and 78% at 20 kbps and 80 kbps, respectively. The Packet loss is caused by two reasons. The first reason is the communication interference [53] . The second reason is the nodes power outage. In AODV protocol, when power outages happens (node dies) it loses all packets stored at its queue. In DEECP protocol, when power outages happens the node loses its buffered packets. In addition, the node will lost the packet that was sent from its

children, if it failed to connect to another parent as described in section 3.5. When the intermediate node dies during participating in an active communication flow, it will lose the packets that were sent but not yet received by the sink. On the other hand, higher number of nodes causes packet loss ratio to increase since the probability of losing a packet is higher as the probability of interfering increases. DEECP on average achieves lower packet loss ratio than AODV.

Table 5.9: Packet loss ratio of DEECP protocol and AODV. The table shows the effect of varying number of nodes and varying the routing protocols at application data rate (20 kbps, 50 kbps, and 80 kbps), on packet loss ratio.

	# of Nodes	AODV	DEECP	Row Sum	Row Mean	Row Effect
20 kbps	10	13.94727	2.309731	16.257	8.128499	-7.68347
	15	21.00058	3.002119	24.0027	12.00135	-3.81062
	20	27.00985	3.220318	30.23017	15.11509	-0.69688
	30	47.84897	8.156885	56.00585	28.00293	12.19096
	Column Sum	109.8067	16.68905			
	Column Mean	27.45167	4.172263			
	Column Effect	11.6397	-11.6397		15.81197	
50kbps	# of Nodes	AODV	DEECP	Row Sum	Row Mean	Row Effect
	10	22.13581	5.790284	27.92609	13.96305	-9.52249
	15	31.32997	7.91174	39.24171	19.62085	-3.86468
	20	39.74936	8.739252	48.48861	24.2443	0.758768
	30	61.36199	10.8659	72.22788	36.11394	12.62841
	Column Sum	154.5771	33.30717			
	Column Mean	38.64428	8.326793			
	Column Effect	15.15874	-15.1587		23.48554	
80 kbps	# of Nodes	AODV	DEECP	Row Sum	Row Mean	Row Effect
	10	27.26864	8.000237	35.26887	17.63444	-9.9164
	15	39.48334	9.142915	48.62625	24.31313	-3.23771
	20	47.33607	9.482908	56.81898	28.40949	0.858653
	30	66.55825	13.13435	79.6926	39.8463	12.29546
	Column Sum	180.6463	39.76041			
	Column Mean	45.16157	9.940102			
	Column Effect	17.61074	-17.6107		27.55084	

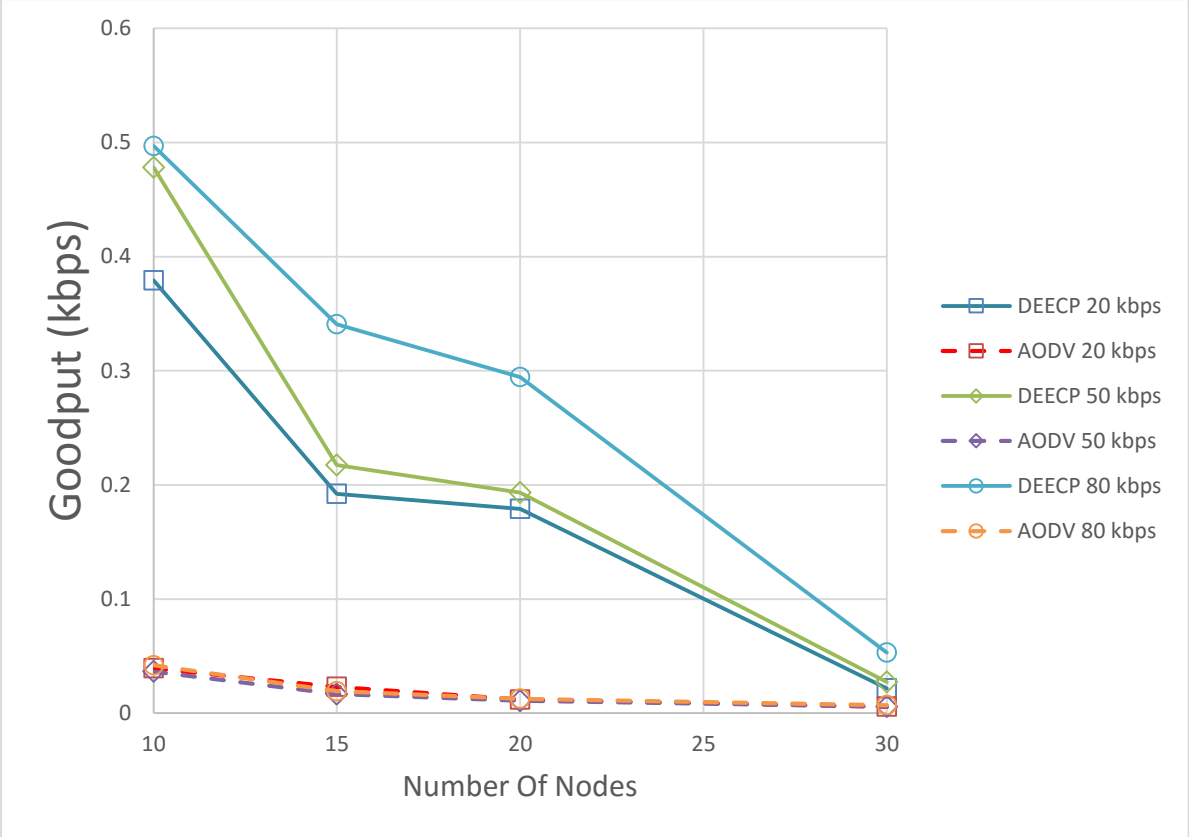

Figure 5.9: Goodput of DEECP and AODV protocols at 20kbps, 50kbps, and 80kbps. The number of nodes (data sources) changed from 10 nodes to 30 nodes.

Figure 5.9 shows the average goodput of the flows versus the number of nodes for different application data rates. The goodput for AODV and DEECP decreases as the number of nodes increases. In addition, it is expected that the goodput increases as the application data rate increases for both AODV and DEECP protocol. Table 5.10 shows the effect for varying application data rate and varying number of nodes on the goodput for DEECP and AODV protocols respectively. Table 5.15 shows the computed percentage of the effect on goodput for DEECP with respect to AODV. In average, the DEECP achieves higher goodput than AODV by 868.5% and 1369% at 20 kbps and 80 kbps, respectively. Figure 5.10 shows the application data rate versus the goodput. When the utilization of the link is low the relation between goodput and application data rate is direct. The network can't achieve higher goodput when the utilization becomes high [54] .

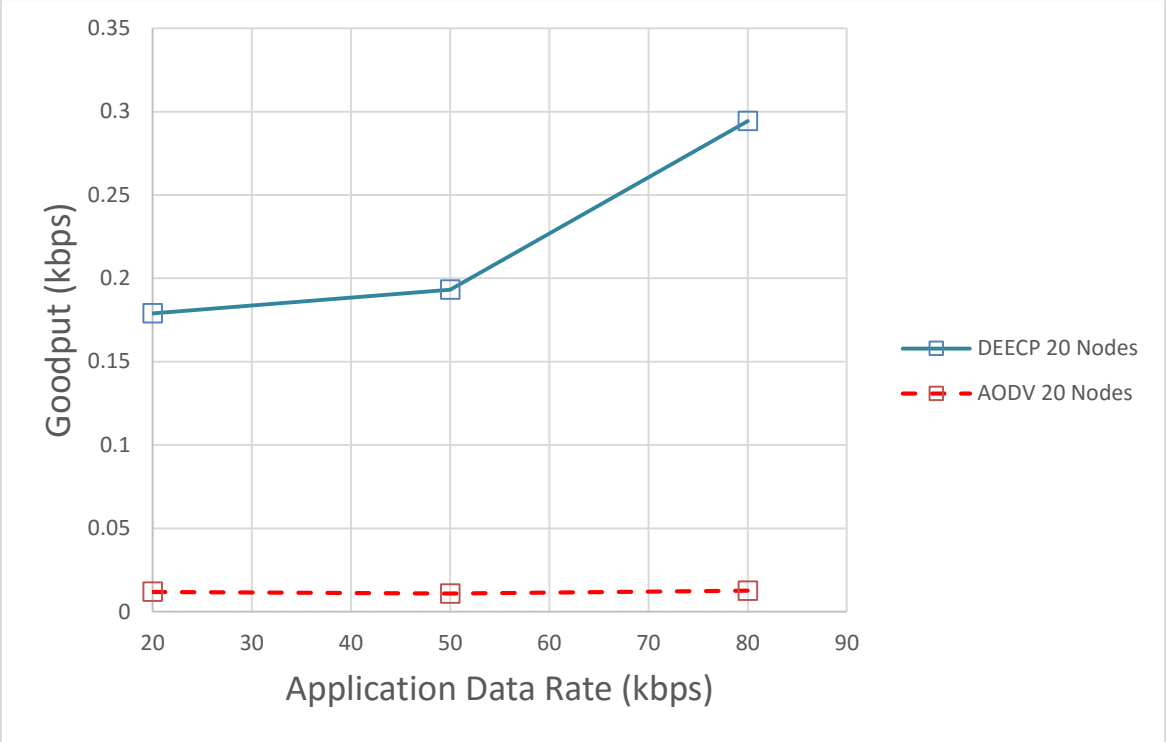

Figure 5.10: Goodput of AODV and DEECP VS the Application Data Rate, Number of nodes = 20.

Table 5.10: Goodput of DEECP protocol and AODV protocol. The table shows the effect of varying number of nodes and varying the routing protocols at application data rate (20 kbps, 50 kbps, 80 kbps), on Goodput.

	# of Nodes	AODV	DEECP	Row Sum	Row Mean	Row Effect
20 kbps	10	0.03929	0.379008	**0.418298**	**0.209149**	**0.102714**
	15	0.022958	0.192155	**0.215113**	**0.107557**	**0.001122**
	20	0.011896	0.178952	**0.190847**	**0.095424**	**-0.01101**
	30	0.005546	0.021673	**0.027219**	**0.013609**	**-0.09283**
	Column Sum	**0.079688**	**0.771789**			
	Column Mean	**0.019922**	**0.192947**			
	Column Effect	**-0.08651**	**0.086513**		**0.106435**	
50kbps	# of Nodes	AODV	DEECP	Row Sum	Row Mean	Row Effect
	10	0.036479	0.478093	**0.514572**	**0.257286**	**0.1341**
	15	0.016697	0.217242	**0.233939**	**0.11697**	**-0.00622**
	20	0.010822	0.193219	**0.204041**	**0.102021**	**-0.02117**
	30	0.005762	0.027178	**0.03294**	**0.01647**	**-0.10672**
	Column Sum	**0.06976**	**0.915732**			
	Column Mean	**0.01744**	**0.228933**			
	Column Effect	**-0.10575**	**0.105746**		**0.123187**	
80 kbps	# of Nodes	AODV	DEECP	Row Sum	Row Mean	Row Effect
	10	0.041947	0.496781	**0.538728**	**0.269364**	**0.111149**
	15	0.019177	0.34081	**0.359987**	**0.179993**	**0.021778**
	20	0.012594	0.294317	**0.306911**	**0.153456**	**-0.00476**
	30	0.006929	0.053167	**0.060096**	**0.030048**	**-0.12817**
	Column Sum	**0.080647**	**1.185075**			
	Column Mean	**0.020162**	**0.296269**			
	Column Effect	**-0.13805**	**0.138054**		**0.158215**	

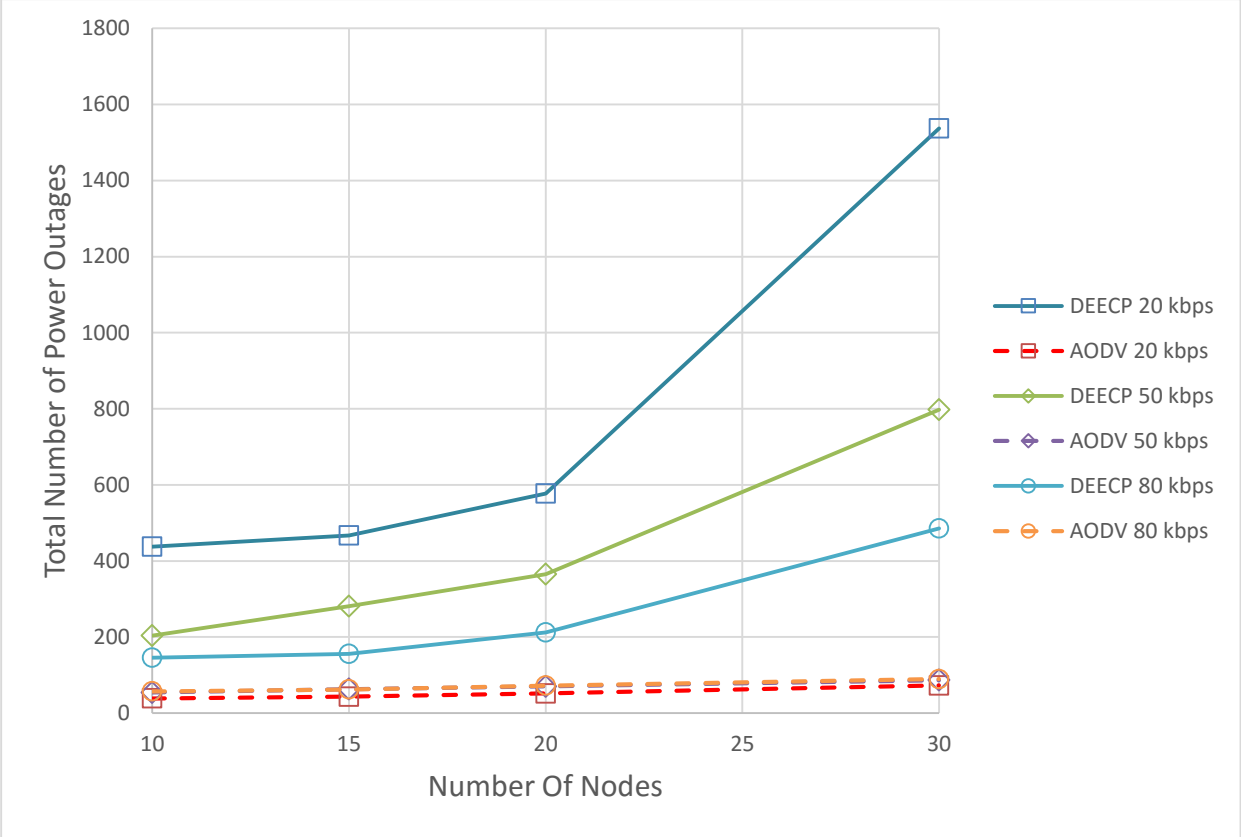

Figure 5.11: Number of outages for DEECP and AODV protocols at 20 kbps, 50 kbps, and 80 kbps.

Figure 5.11 shows the power outage for AODV and DEECP versus the number of nodes. In general, the DEECP protocol has higher power outages than AODV protocol. This happens because the traffic converges at the point of collection (parent node). As it is expected, the power outage increases as the configured application data rate increases for AODV protocols. In contrast, as a result of the use on-off thresholds the power outages of DEECP protocol decreases as the Application data rate increases. These on-off thresholds are related to application data rate. The discussion of these thresholds is provided in more details at section 3.6. On other hand, the number of power outages increases as the number of nodes increases, because there are more traffic in the network for DEECP and AODV Protocols.. Table 5.11 shows the effect of total number of power outages for varying application data rate and varying number of nodes for DEECP and AODV protocols, respectively. Table 5.15 shows the computed percentage of total number of power

outages for DEECP with respect to AODV. In average, the DEECP has higher power outages than AODV by 1362% to 254% at 20 kbps and 80 kbps, respectively. In average of number of nodes and application rate, DEECP has higher power outages than AODV by 644%.

Table 5.11: Power outage of DEECP protocol and AODV protocol. The table shows the effect of varying number of nodes and varying the routing protocols at application data rate (20 kbps, 50 kbps, 80 kbps), on power outage.

	# of Nodes	AODV	DEECP	Row Sum	Row Mean	Row Effect
20 kbps	10	38.83333	437.6923	476.5256	238.2628	-164.942
	15	43.25	467.0339	510.2839	255.1419	-148.063
	20	51.66667	577.4194	629.086	314.543	-88.6618
	30	72.71186	1537.031	1609.743	804.8716	401.6667
	Column Sum	206.4619	3019.177			
	Column Mean	51.61547	754.7942			
	Column Effect	-351.589	351.5894		403.2048	
50kbps	# of Nodes	AODV	DEECP	Row Sum	Row Mean	Row Effect
	10	54	204.086	258.086	129.043	-111.071
	15	62.94643	281.1468	344.0932	172.0466	-68.0671
	20	70	365.0877	435.0877	217.5439	-22.5699
	30	86.5	797.1429	883.6429	441.8214	201.7077
	Column Sum	273.4464	1647.463			
	Column Mean	68.36161	411.8658			
	Column Effect	-171.752	171.7521		240.1137	
80 kbps	# of Nodes	AODV	DEECP	Row Sum	Row Mean	Row Effect
	10	57.33333	145.2941	202.6275	101.3137	-58.7536
	15	62.36842	155.8252	218.1937	109.0968	-50.9705
	20	72.33333	212.1569	284.4902	142.2451	-17.8222
	30	89.5	485.7273	575.2273	287.6136	127.5463
	Column Sum	281.5351	999.0035			
	Column Mean	70.38377	249.7509			
	Column Effect	-89.6836	89.68355		160.0673	

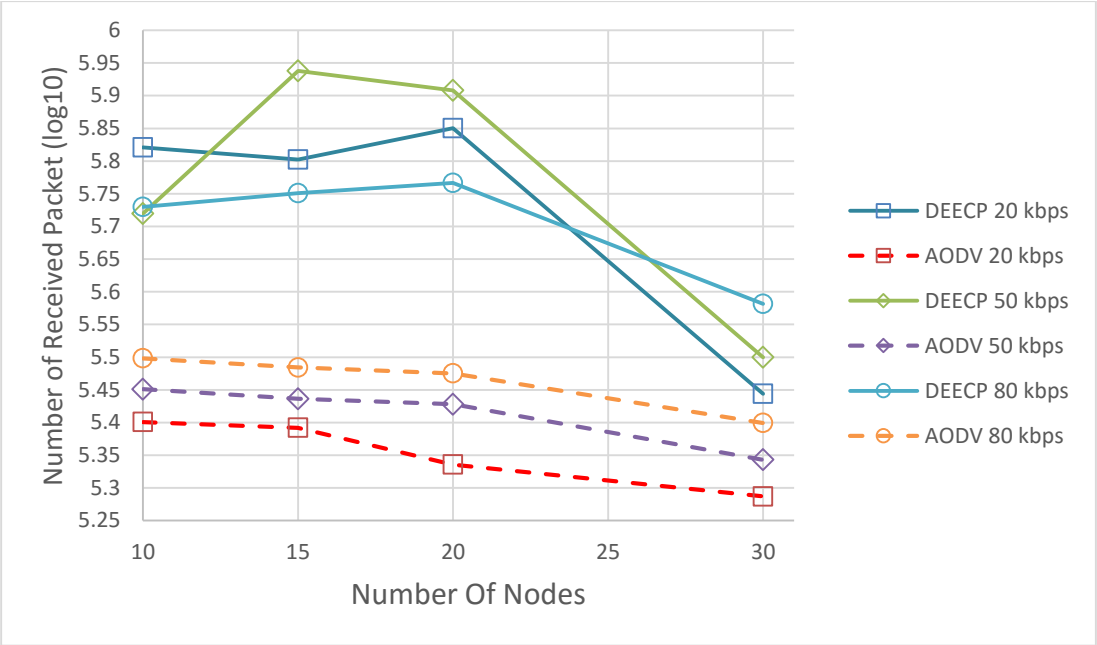

Figure 5.12: Total number of received bytes (log10) for DEECP and AODV protocols at 20 kbps, 50 kbps, and 80 kbps. UDP traffic.

Figure 5.12 shows total number of received bytes for AODV protocol and DEECP protocol versus the number of nodes (data sources). As expected, the total received data increases as the application data rate increases for AODV protocol and DEECP protocol. In addition, the total number of received bytes decreases as the number of nodes increases for AODV protocol. This behavior can be explained as a result of percentage of packets loss increases. In same manner, the total received bytes increase when the number of nodes increases until 20 nodes for DEEP protocol. After the number of nodes reached 20 nodes the total received bytes start decreasing. In general, DEECP protocol has higher received bytes than AODV protocol. Table 5.12 shows the two factors full factorial analysis for three different application data bit rates. This table can be interpreted as previous sections. Table 5.15 shows the computed percentage of the difference between DEECP protocol and AODV protocol. In average, the DEECP has higher received bytes than AODV by 151% and 120% at 20kbps and 80 kbps respectively.

Table 5.12: Total received bytes to sink node of DEECP protocol and AODV protocol. The table shows the effect of varying number of nodes and varying the routing protocols at application data rate (20 kbps, 50 kbps, 80 kbps), on received bytes.

	# of Nodes	AODV	DEECP	Row Sum	Row Mean	Row Effect
20 kbps	10	251587.8	662134.8	**913722.6**	**456861.3**	**57925.2**
	15	246596.1	634550.6	**881146.7**	**440573.4**	**41637.27**
	20	216596.1	708426.2	**925022.4**	**462511.2**	**63575.1**
	30	193650.6	277946.4	**471597**	**235798.5**	**-163138**
	Column Sum	**908430.6**	**2283058**			
	Column Mean	**227107.7**	**570764.5**			
	Column Effect	**-171828**	**171828.4**		**398936.1**	
50 kbps	# of Nodes	AODV	DEECP	Row Sum	Row Mean	Row Effect
	10	282493.2	634056	**916549.2**	**458274.6**	**35180.67**
	15	273017.7	701287.5	**974305.2**	**487152.6**	**64058.7**
	20	267836.5	692853.4	**960689.9**	**480344.9**	**57251.02**
	30	220276.7	312930.3	**533207.1**	**266603.5**	**-156490**
	Column Sum	**1043624**	**2341127**			
	Column Mean	**260906**	**585281.8**			
	Column Effect	**-162188**	**162187.9**		**423093.9**	
80 kbps	# of Nodes	AODV	DEECP	Row Sum	Row Mean	Row Effect
	10	314938.8	677229.5	**992168.3**	**496084.2**	**28355**
	15	305040.5	733308.2	**1038349**	**519174.3**	**51445.18**
	20	298659.5	749844.9	**1048504**	**524252.2**	**56522.99**
	30	250752.5	412059.5	**662812**	**331406**	**-136323**
	Column Sum	**1169391**	**2572442**			
	Column Mean	**292347.8**	**643110.5**			
	Column Effect	**-175381**	**175381.4**		**467729.2**	

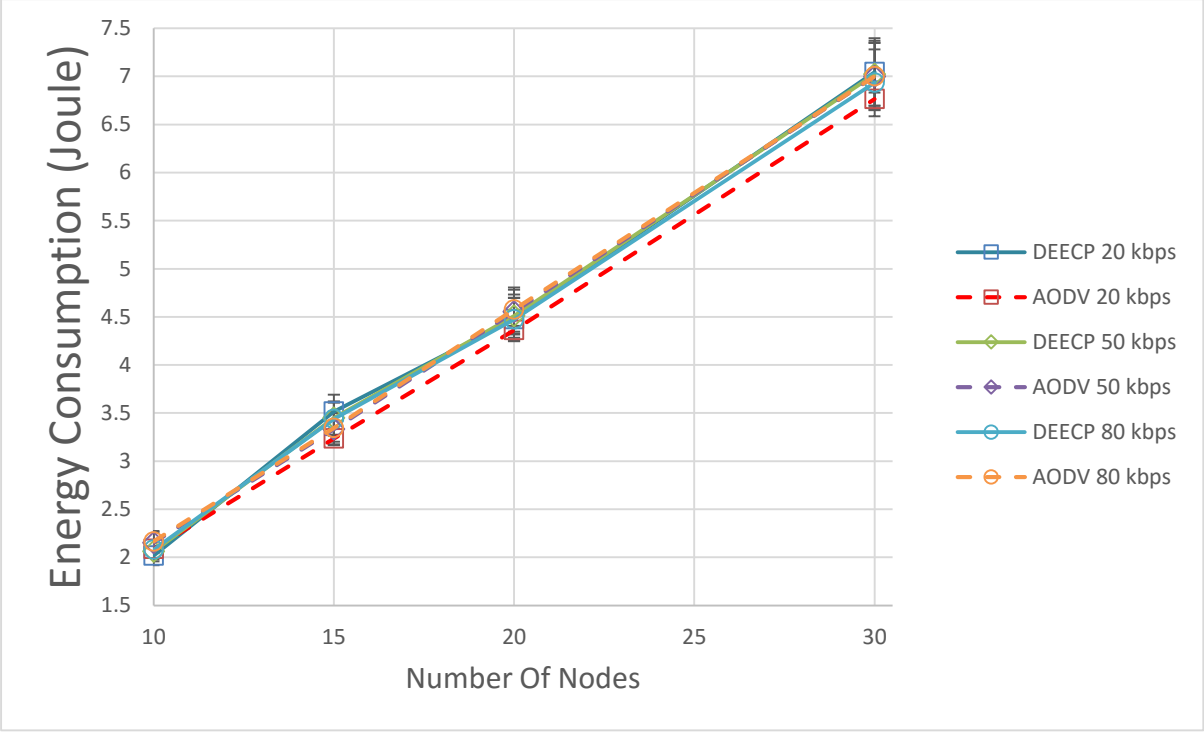

Figure 5.13: Total energy consumption (Joule) for DEECP and AODV protocols at 20 kbps, 50 kbps, and 80 kbps.

Figure 5.13 shows the total energy consumption versus the number of nodes. The energy consumption increases as the number of nodes increase. In general, for all number of nodes, application data rate, and protocols the energy consumption has low variation. Table 5.13 shows the full factorial analysis. Table 5.14 shows that the DEECP protocol consumed energy more than AODV protocol by 4% at 20 kbps. Otherwise, at 80 kbps the DEECP protocol has less energy consumption than AODV protocol by 1%.in average, The DEECP protocol consumes more energy than AODV by 1%.

Table 5.13: Total power consumption by DEECP protocol and AODV protocol. The table shows the effect of varying number of nodes and varying the routing protocols at application data rate (20 kbps, 50 kbps, 80 kbps), on power consumption (joules)

	# of Nodes	AODV	DEECP	Row Sum	Row Mean	Row Effect
20 kbps	10	2.087002	2.018877	4.105879	2.05294	-2.13492
	15	3.234901	3.514413	6.749314	3.374657	-0.8132
	20	4.361748	4.475483	8.837232	4.418616	0.230758
	30	6.764177	7.046263	13.81044	6.90522	2.717362
	Column Sum	16.44783	17.05504			
	Column Mean	4.111957	4.263759			
	Column Effect	-0.0759	0.075901		4.187858	
50 kbps	# of Nodes	AODV	DEECP	Row Sum	Row Mean	Row Effect
	10	2.151629	1.990831	4.14246	2.07123	-2.17497
	15	3.330387	3.513991	6.844377	3.422189	-0.82402
	20	4.553135	4.408986	8.962121	4.481061	0.234856
	30	6.998468	7.02221	14.02068	7.010339	2.764135
	Column Sum	17.03362	16.93602			
	Column Mean	4.258405	4.234004			
	Column Effect	0.0122	-0.0122		4.246205	
80 kbps	# of Nodes	AODV	DEECP	Row Sum	Row Mean	Row Effect
	10	2.164274	2.017206	4.18148	2.09074	-2.15147
	15	3.343489	3.502031	6.84552	3.42276	-0.81945
	20	4.576602	4.414494	8.991096	4.495548	0.25334
	30	7.000779	6.918789	13.91957	6.959784	2.717576
	Column Sum	17.08514	16.85252			
	Column Mean	4.271286	4.21313			
	Column Effect	0.029078	-0.02908		4.242208	

Table 5.14: Computed percentage of effects for DEECP protocol on the performance with respect to AODV. (+) and (-) signs indicate increment or decrement in the performance metric respectively.

	# of Nodes	End to End delay	Goodput	Packet loss Ratio	Power Outages	Received Bytes	Consumed Energy
20 kbps	10	-86.6%	864.7%	-83.4%	1027.1%	163%	-3%
	15	-89.3%	737.0%	-85.7%	979.8%	157%	9%
	20	-88.5%	1404.4%	-88.1%	1017.6%	227%	3%
	30	-88.5%	290.8%	-83.0%	2013.9%	44%	4%
	Percentage of Average Effect	-88.4%	868.5%	-84.8%	1362.3%	151%	4%
50 kbps	# of Nodes	End to End delay	Goodput	Packet loss Ratio	Power Outages	Received Bytes	Consumed Energy
	10	-77.5%	1210.6%	-73.8%	277.9%	86%	-4%
	15	-85.7%	1201.0%	-74.7%	346.6%	217%	4%
	20	-80.0%	1685.5%	-78.0%	421.6%	202%	-1%
	30	-70.9%	371.7%	-82.3%	821.6%	44%	0%
	Percentage of Average Effect	-76.9%	1212.7%	-78.5%	502.5%	141%	0%
80 kbps	# of Nodes	End to End delay	Goodput	Packet loss Ratio	Power Outages	Received Bytes	Consumed Energy
	10	-43.0%	1084.3%	-70.7%	153.4%	71%	-4%
	15	-46.3%	1677.2%	-76.8%	149.8%	85%	3%
	20	-43.0%	2236.9%	-80.0%	193.3%	96%	-2%
	30	-55.4%	667.3%	-80.3%	442.7%	52%	-1%
	Percentage of Average Effect	-48.1%	1369.5%	-78.0%	254.8%	77%	-1%

Table 5.15: Computed average percentage of effects for DEECP and AODV protocol on the performance with respect to application date rate = 20 kbps, respectively. (+) and (-) signs indicate increment or decrement in the performance metric.

	# of Nodes	Endto End delay		Goodput		Packet loss Ratio		Power Outages		Received Bytes		Consumed Energy	
		50 kbps	80 kbps	50 kbps	80 kbps	50 kbps	80 kbps	50 kbps	80 kbps	50 kbps	80 kbps	50 kbps	80 kbps
DEECP	10	185.1%	1243.0%	26.1%	31.1%	151%	246%	-53%	-67%	-21%	-19%	2%	3%
	15	175.7%	1737.7%	13.1%	77.4%	164%	205%	-40%	-67%	37%	-11%	-2%	-2%
	20	176.0%	1362.6%	8.0%	64.5%	171%	194%	-37%	-63%	14%	-18%	1%	0%
	30	268.2%	627.4%	25.4%	145.3%	33%	61%	-48%	-68%	14%	37%	0%	-2%
	Percentage of Average Effect	221.1%	1054.1%	18.7%	53.5%	100%	138%	-45%	-67%	10%	-9%	0%	-1%

	# of Nodes	Endto End delay		Goodput		Packet loss Ratio		Power Outages		Received Bytes		Consumed Energy	
		50 kbps	80 kbps	50 kbps	80 kbps	50 kbps	80 kbps	50 kbps	80 kbps	50 kbps	80 kbps	50 kbps	80 kbps
AODV	10	70.3%	216.7%	-7.2%	6.8%	59%	96%	39%	48%	12%	25%	3%	25%
	15	106.7%	267.7%	-27.3%	-16.5%	49%	88%	46%	44%	11%	24%	3%	24%
	20	58.8%	195.3%	-9.0%	5.9%	47%	75%	35%	40%	24%	38%	4%	38%
	30	45.6%	87.9%	3.9%	24.9%	28%	39%	19%	23%	14%	29%	3%	29%
	Percentage of Avarage Effect	61.9%	158.4%	-12.5%	1.2%	41%	65%	32%	36%	15%	29%	4%	29%

In order to understand the behavior of the node during the simulation and see how the power outage affects the goodput, on flow was tracking

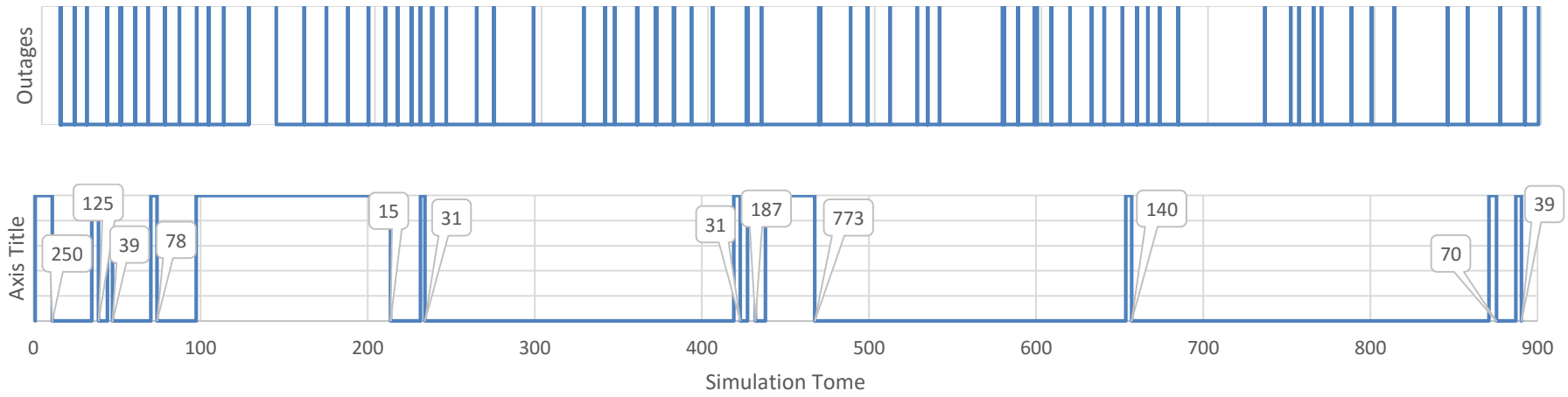

Figure 5.14: Power outages in the network versus time and active data dissemination intervals of a single node

Figure 5.14 shows the power outages occurrences in the network for a single run and also shows the active data dissemination intervals of same node. The node started sending data to the sink around time 1.02s and continued sending until time 11.25s. The first power outage in the network occurred at time 11.25s; it happened on this node. What caused the flow to stop is the twelve outages that occurred during simulation time. At time 34.9s, the node resumed sending data after it joined to a parent until time 39s when the flow was interrupted again because of another power outage in the network. This behavior continues until the end of simulation. We notice that each time the flow is interrupted; it was interrupted because of a power outage.

The number in the labels that indicates to end of on intervals represents the total number of packets that are sending during that interval. The total number of sending packets in all intervals is 1778 packets. Multiplying number of packets by packet size gives the total bytes which is 910.336Kbytes. The flow time in NS-3 is measured by the time the first packet is sending until the time the last packet is sending which equals in this scenario 890.5 seconds. Therefore, the goodput of this scenario is 1.023Kbps where the data generation rate is 20 Kbps.

The sum of active time intervals equals 189.599s. Then the sending rate for the active intervals only equals 4.801Kbps. The node generates data at rate of 20 Kbps, when there is no route to sink node, the node buffers the generated data. Once a route is created, the node sends all its buffered packets. This caused the goodput of the active time intervals increases than the actual data generating rate. The loss ratio for this run is 12% and the overall goodput is 0.88 Kbps.

The fact that the data flow is being interrupted causes the goodput to be less than the configured sending data rate. The number of bytes (N) that is assumed to take T seconds based on the sending data rate is taking more than T seconds because of the interrupts in the flow. The goodput is calculated by dividing the total received bytes over the total flow time. Having periods of idle intervals in the flow causes a drop in the goodput as it is shown in all scenarios. Having higher number of nodes (sources), higher data rate or less energy in the network result in higher number of power outages and hence higher drop in the goodput and the performance in general.

5.1.4 Studying the Effect of Varying Energy Harvesting Rate

In this scenario, a simulation experiment is conducted where the variable is the number of nodes around the sink and the energy harvesting rate (EHR). The goal of this scenario is to study the effect of varying energy harvesting rate on the network performance. DEECP protocol is used in this scenario. The simulation parameters are listed in Table 5.16. The other simulation parameters are the same as in Table 5.7.

Table 5.16: Simulation parameters.

Parameter	Value
Routing protocol	DEECP
Energy harvesting	minhp: 0 maxhp: [1-4], [2-8], [4-10] mW

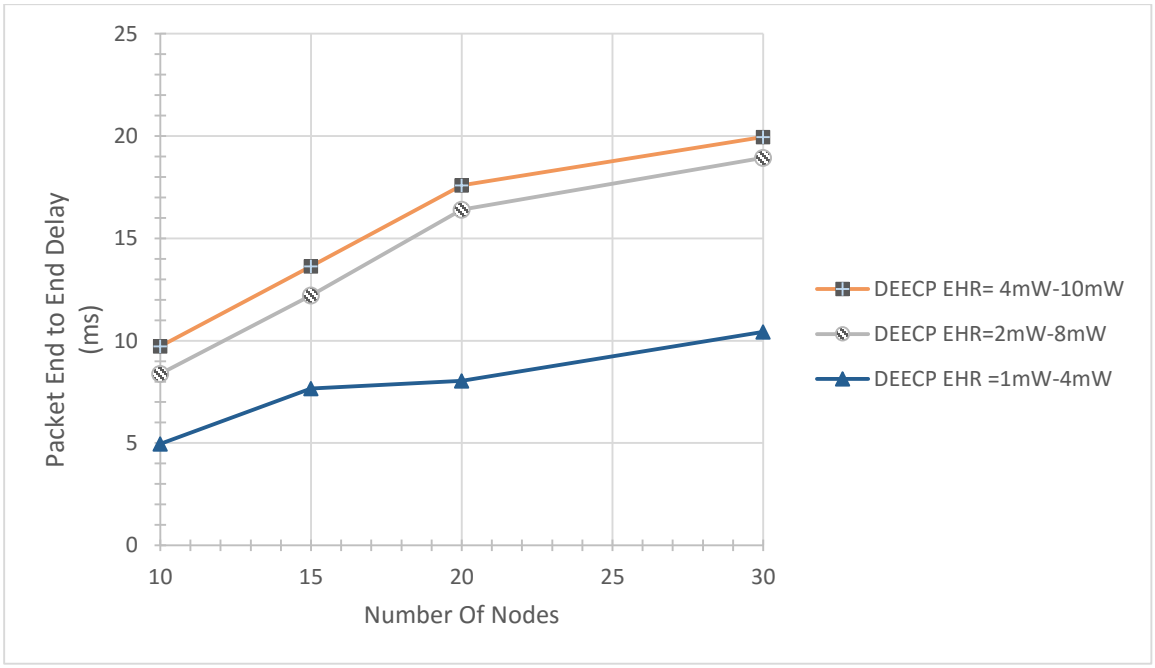

Figure 5.15: End to End Delay at EHR [1-4], [2-8], and [4-10] mW. The routing protocol is DEECP. Application data rate = 80 kbps.

Figure 5.15 shows the packet end to end delay of the flows versus the number of nodes for different energy harvesting configurations. The higher energy harvesting configuration rate achieves higher end-to-end delay. When *maxhp* is configured with higher value the node's power outages is less. The relationship between packet End-to-end delay and the number of nodes is direct. Table 5.17 shows the packet end to end delay effect by energy harvesting rate and number of nodes. Table 5.18 shows the percentage of effect to energy harvesting rate and number of nodes, it shows the percentage of effect of varying number of nodes for all configured energy harvesting rate. In average, Table 5.18 shows that at the higher configured energy harvesting rate increases the end to end delay by 95% with respect to lower configured energy harvesting rate. On other hand, Table 5.20 and Table 5.22 show that the higher configuration of energy harvesting rate increases the goodput and decreases the packet loss ratio by 174% and 46%, respectively.

Table 5.17: End to End Delay of DEECP protocol. The table shows the effect of changing energy harvesting rate and number of data sources on end to end delay.

	Harvesting Rate					
# of Nodes	0 mW to(1-4 mW)	0 mW to(2-8 mW)	0 mW to(4-10 mW)	row Sum	average	row effect
10	4.95947	8.387688	9.735267	**23.08243**	**7.694142**	**-4.63263**
15	7.65743	12.21286	13.63518	**33.50547**	**11.16849**	**-1.15828**
20	8.03596	16.3967	17.5865	**42.01916**	**14.00639**	**1.679612**
30	10.4357	18.93414	19.94444	**49.31424**	**16.43808**	**4.111306**
col. Sum	**31.0885**	**55.9314**	**60.90138**			
col. Ave.	**12.4354**	**22.37256**	**24.36055**		**12.32677**	
col. Efect	**0.10863**	**10.04578**	**12.03378**			

Table 5.18: Computed percentage of effects for DEECP protocol on the end to end delay with respect to lower energy harvesting rate and with respect to lower number of nodes, respectively. (+) and (-) signs indicate increment or decrement in the performance metric(packet end to end delay)

	with respect to 1-4 mW				with respect to 10 nodes				
# of Nodes	0 mW to(1-4 mW)	0 mW to(2-8 mW)	0 mW to(4-10 mW)		0 mW to(1-4 mW)	0 mW to(2-8 mW)	0 mW to(4-10 mW)		Ave. Effect
10	0.00%	69.12%	96.30%		0.00%	0.00%	0.00%		0.00%
15	0.00%	59.49%	78.06%		54.40%	45.60%	40.06%		45.16%
20	0.00%	104.04%	118.85%		62.03%	95.49%	80.65%		82.04%
30	0.00%	81.44%	91.12%		110.42%	125.74%	104.87%		113.64%
col. Sum									
Ave. Effect		79.91%	95.90%						

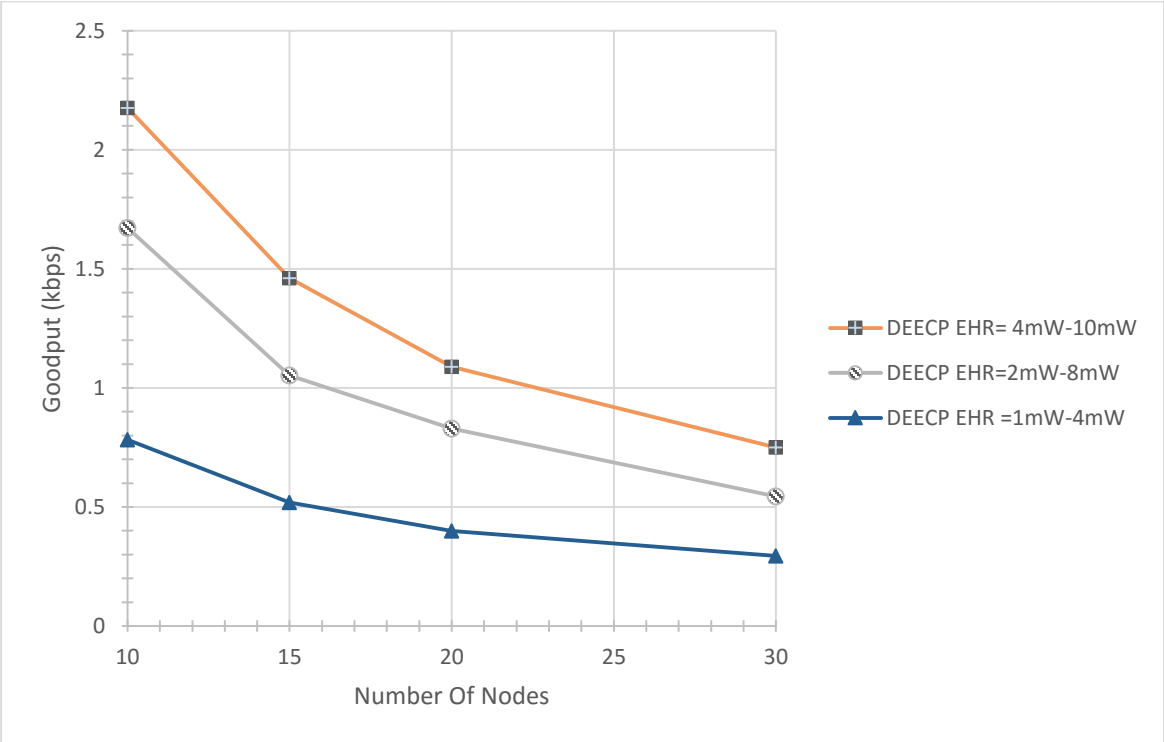

Figure 5.16: Goodput at EHR [1-4], [2-8], and [4-10] mW. The routing protocol is DEECP. application data rate 80 kbps.

Figure 5.16 shows the average goodput of the flows versus the number of nodes. Goodput decreases as the number of nodes increases. As expected, the configuration with highest energy harvesting rate achieves the highest goodput and vice versa. This behaver happens because as the number of nodes increases the data sources increase (every node considered as a source of traffic). Hence, the node delayed sending its packet, because the channel is

busy for longer time when number of nodes increases. In average, Table 5.20 shows that the goodput increases by 174% at higher configured harvesting rate with respect to lower configuration harvesting rate. Table 5.19 shows the two factors full factorial analysis for varying configuration of energy harvesting rate and varying number of nodes effect.

Table 5.19: Goodput of DEECP protocol. The table shows the effect of changing energy harvesting rate and number of data sources on Goodput.

	Harvesting Rate					
# of Nodes	0 mW to(1-4 mW)	0 mW to(2-8 mW)	0 mW to(4-10 mW)	row Sum	average	row effect
10	0.78191	1.672548	2.17521	**4.629665**	**1.543222**	**0.579308**
15	0.51824	1.052607	1.461511	**3.032359**	**1.010786**	**0.046872**
20	0.39923	0.828658	1.088358	**2.31625**	**0.772083**	**-0.19183**
30	0.29426	0.544366	0.750065	**1.588693**	**0.529564**	**-0.43435**
col. Sum	**1.99365**	**4.098178**	**5.475144**			
col. Ave.	**0.79746**	**1.639271**	**2.190058**		**0.963914**	
col. Effect	**-0.16646**	**0.675357**	**1.226144**			

Table 5.20: Computed percentage of effects for DEECP protocol on the Goodput with respect to lower energy harvesting rate and with respect to lower number of nodes, respectively. (+) and (-) signs indicate increment or decrement in the performance metric (Goodput).

	with respect to 1-4 mW				with respect to 10 nodes				
# of Nodes	0 mW to(1-4 mW)	0 mW to(2-8 mW)	0 mW to(4-10 mW)		0 mW to(1-4 mW)	0 mW to(2-8 mW)	0 mW to(4-10 mW)		Ave. Effect
10	**0.00%**	**113.91%**	**178.19%**		**0.00%**	**0.00%**	**0.00%**		**0.00%**
15	**0.00%**	**103.11%**	**182.01%**		**-33.72%**	**-37.07%**	**-32.81%**		**-34.50%**
20	**0.00%**	**107.56%**	**172.61%**		**-48.94%**	**-50.46%**	**-49.97%**		**-49.97%**
30	**0.00%**	**84.99%**	**154.90%**		**-62.37%**	**-67.45%**	**-65.52%**		**-65.68%**
Ave. Effect		**105.56%**	**174.63%**						

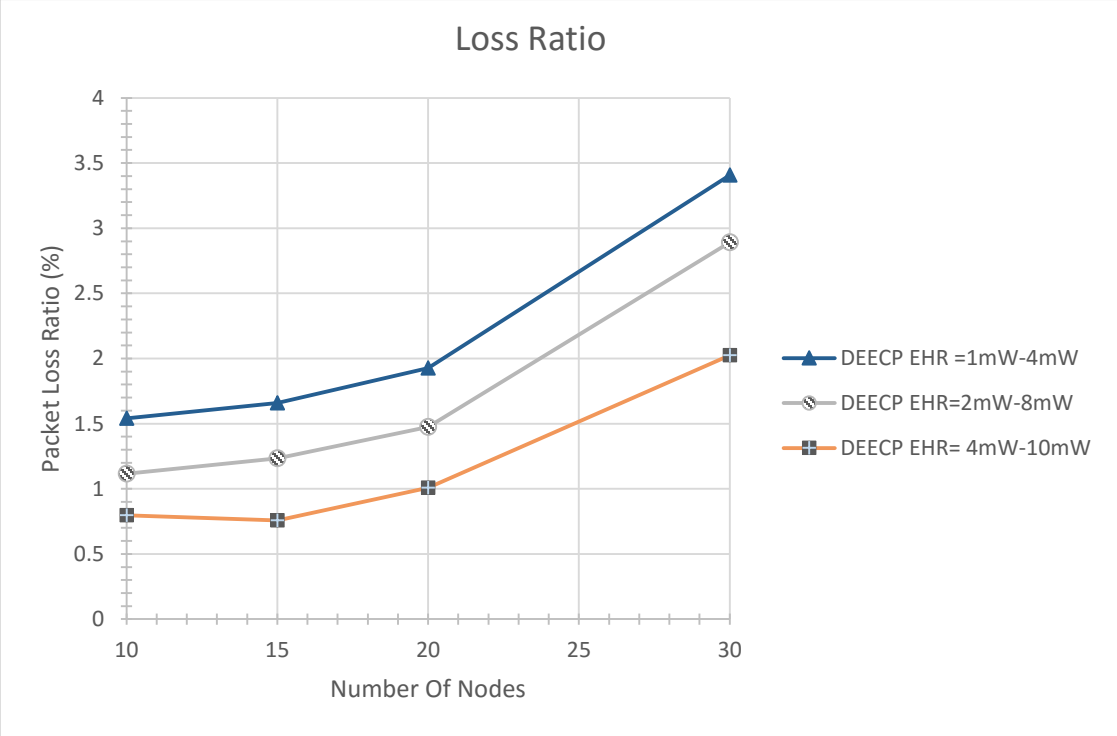

Figure 5.17: Loss Ratio at EHR [1-4], [2-8], and [4-10] mW. The routing protocol is DEECP. Application data rate = 80 kbps.

Figure 5.17 shows the average packet loss ratio of the flows versus the number of nodes. Packet loss ratio increases as the number of nodes increases. As expected, the configuration with highest energy harvesting rate achieves the lower packet loss ratio and vice versa. Table 5.21 shows the two factors full factorial analysis for varying configuration of energy harvesting rate and varying number of nodes effect. In average, Table 5.22 shows that at higher configuration energy harvesting rate the packet loss ratio decease by 46% with respect to lower configuration energy harvesting rate. Also the packet loss ratio increases by 140% in comparison to packet loss ratio at 10 nodes.

Table 5.21: Packet Loss Ratio of DEECP protocol. The table shows the effect of changing energy harvesting rate and number of data sources on Packet Loss Ratio.

	Harvesting Rate					
# of Nodes	0 mW to(1-4 mW)	0 mW to(2-8 mW)	0 mW to(4-10 mW)	Row Sum	Averege	Row Effect
10	1.5412	1.116816	0.79745	**3.455467**	**1.151822**	**-0.50136**
15	1.6593	1.234762	0.757931	**3.651996**	**1.217332**	**-0.43585**
20	1.92722	1.473743	1.00742	**4.408378**	**1.469459**	**-0.18372**
30	3.40624	2.892091	2.023966	**8.322296**	**2.774099**	**1.120921**
col. Sum	**8.53396**	**6.717412**	**4.586768**			
col. Ave.	**3.41358**	**2.686965**	**1.834707**		**1.653178**	
col. Effect	**1.76041**	**1.033787**	**0.181529**			

Table 5.22: Computed percentage of effects for DEECP protocol on the Loss Ratio with respect to lower energy harvesting rate and with respect to lower number of nodes, respectively. (+) and (-) signs indicate increment or decrement in the performance metric (Packet Loss Ratio)

	with respect to 1-4 mW				with respect to 10 nodes				
# of Nodes	0 mW to(1-4 mW)	0 mW to(2-8 mW)	0 mW to(4-10 mW)		0 mW to(1-4 mW)	0 mW to(2-8 mW)	0 mW to(4-10 mW)		Ave. Effect
10	**0.00%**	**-27.54%**	**-48.26%**		**0.00%**	**0.00%**	**0.00%**		**0.00%**
15	**0.00%**	**-25.59%**	**-54.32%**		**7.66%**	**10.56%**	**-4.96%**		**5.69%**
20	**0.00%**	**-23.53%**	**-47.73%**		**25.05%**	**31.96%**	**26.33%**		**27.58%**
30	**0.00%**	**-15.09%**	**-40.58%**		**121.01%**	**158.96%**	**153.80%**		**140.84%**
Ave. Effect		**-21.29%**	**-46.25%**						

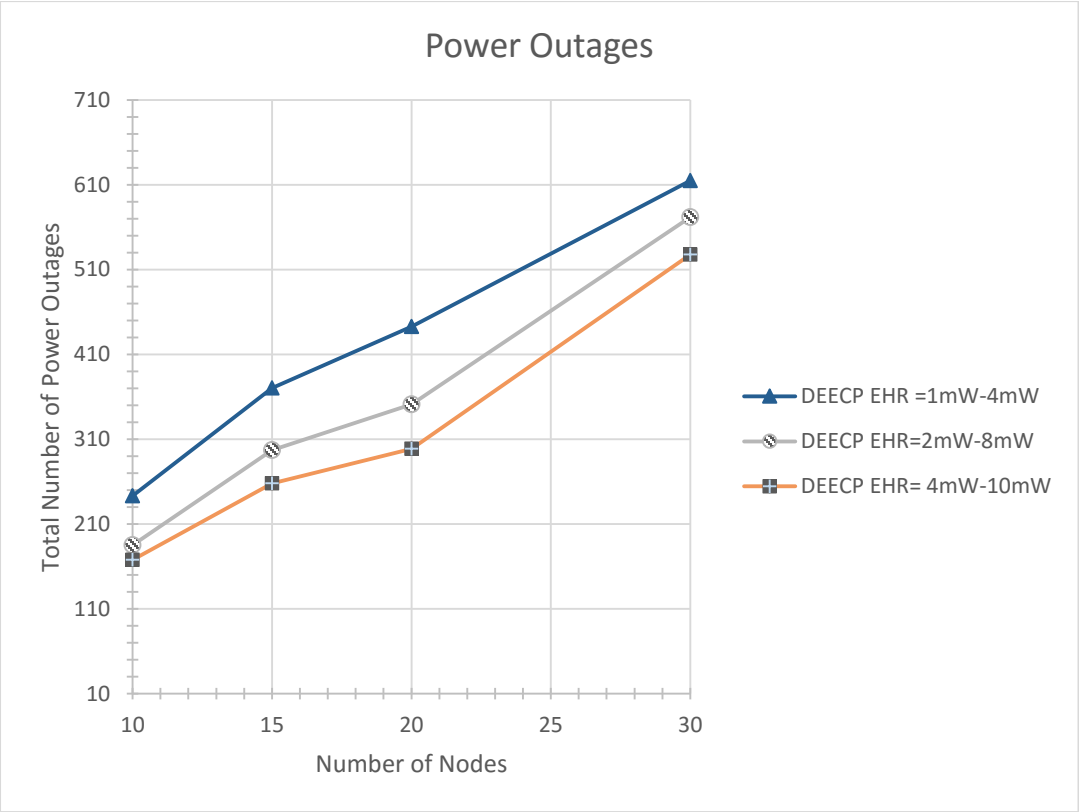

Figure 5.18: Power outages at EHR [1-4], [2-8], and [4-10] mW. The routing protocol is DEECP. Application data rate = 80 kbps.

Figure 5.18 shows the total power outages versus number of nodes. The lowest configuration of energy harvesting rate achieves highest level of power outages. This is because there are many weak nodes that cause the power outages to happen more frequently. The high level of power outages explains why the performance of the network with low harvesting rate is relatively poor in comparison to higher harvesting rate configurations. Table 5.23 shows the different configuration of energy harvesting rate and varying number of nodes effect. Table 5.24 shows that at higher configuration of energy harvesting rate the power outages less by 25% with respect to lowest configuration of energy harvesting rate.

Table 5.25 summarizes the effects of the different energy harvesting rates on the performance with reference to lowest configuration of energy harvesting rate.

Table 5.23: Power outages of DEECP protocol. The table shows the effect of changing energy harvesting rate and number of data sources on power outages.

	Harvesting Rate					
# of Nodes	0 mW to(1-4 mW)	0 mW to(2-8 mW)	0 mW to(4-10 mW)	row Sum	avarege	row efect
10	243.095	185	167.6923	**595.7875**	**198.5958**	**-162.061**
15	370.385	297.2093	258	**925.5939**	**308.5313**	**-52.1257**
20	442.791	350.9091	298.5714	**1092.271**	**364.0904**	**3.43342**
30	614.667	571.8372	527.7273	**1714.231**	**571.4104**	**210.7534**
col. Sum	**1670.94**	**1404.956**	**1251.991**			
col. Ave.	**417.734**	**351.2389**	**312.9978**		**360.657**	
col. Efect	**57.0773**	**-9.41809**	**-47.6592**			

Table 5.24: Computed percentage of effects for DEECP protocol on the power outages with respect to lower energy harvesting rate and with respect to lower number of nodes, respectively. (+) and (-) signs indicate increment or decrement in the performance metric (power outages)

	with respect to 1-4 mW				with respect to 10 nodes				
# of Nodes	0 mW to(1-4 mW)	0 mW to(2-8 mW)	0 mW to(4-10 mW)		0 mW to(1-4 mW)	0 mW to(2-8 mW)	0 mW to(4-10 mW)		Ave. Effect
10	**0.00%**	**-23.90%**	**-31.02%**		**0.00%**	**0.00%**	**0.00%**		**0.00%**
15	**0.00%**	**-19.76%**	**-30.34%**		**52.36%**	**60.65%**	**53.85%**		**55.36%**
20	**0.00%**	**-20.75%**	**-32.57%**		**82.15%**	**89.68%**	**78.05%**		**83.33%**
30	**0.00%**	**-6.97%**	**-14.14%**		**152.85%**	**209.10%**	**214.70%**		**187.73%**
col. Sum									
Ave. Effect		**-15.92%**	**-25.07%**						

Table 5.25: Computation of effects of EHR on the performance with respect to lowest EHR. (+) and (-) signs indicate increment or decrement in the corresponding performance metric, respectively.

Performance metric	**EHR**	
	0 mW to (2-8 mW)	**0 mW to (4-10 mW)**
End to end delay	79.91%	95.90%
Packet loss ratio	-21.29%	-46.25%
Goodput	105.56%	174.63%
Power outage	-17.82%	-27.44%

5.1.5 Study the Effect of Grid Topology.

In this scenario, a simulation experiment is conducted where the variable is the number of nodes arranged in a grid topology. The goal of the scenario is to compare the performance of DEECP and AODV in terms of end-end delay, goodput, and packet loss ratio when varying the number of nodes, application data rate with grid topology. The performance metrics were discussed in section 5.1. The simulation parameters are shown in Table 5.26 the other parameter as in Table 5.7. Figure 5.19 shows the grid placement of the 9, 25, and 30 nodes. The triangle shape represents sink node which located at the edge of the placement area.

Table 5.26: Simulation Parameters.

Parameter	**Value**
Test Area	According the number of nodes, distance between two sequenced nodes 70 m horizontally and vertically.
Number of nodes	3x3, 5x5, and 6x5.
Placement	Grid.
Initial Energy	0.02 J
Number of sources	Number of nodes -1
Simulation time	900 sec

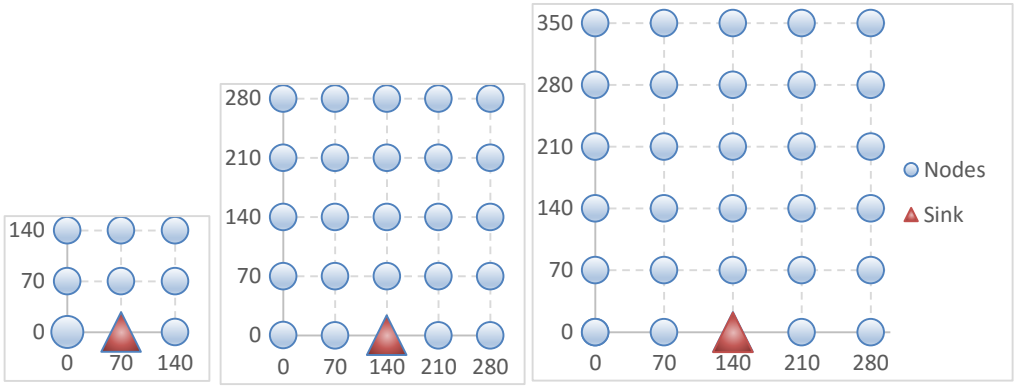

Figure 5.19: Grid topology for 3x3 nodes, 5x5 nodes, and 6x5 nodes.

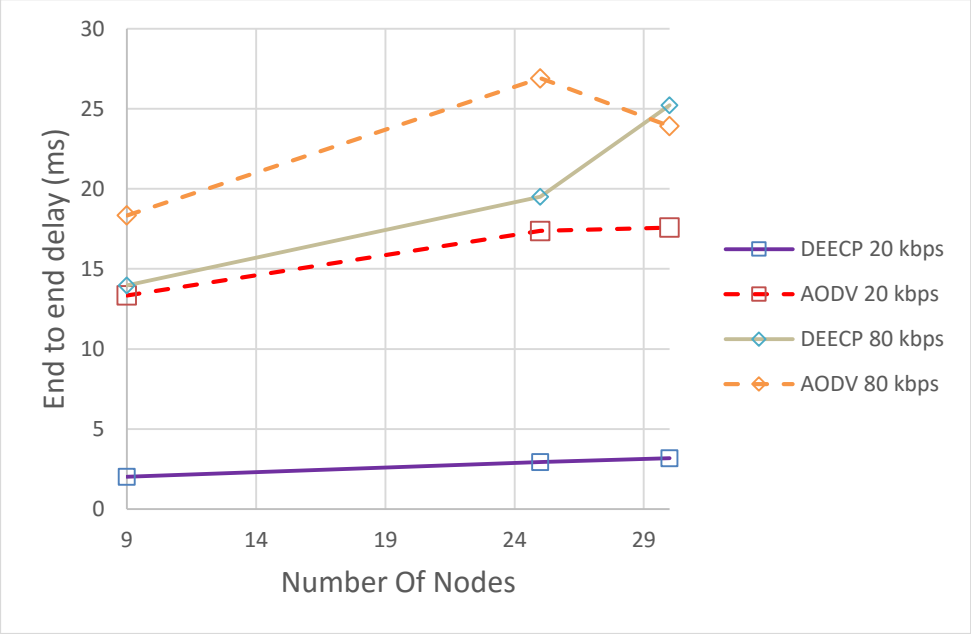

Figure 5.20: End-to-End Delay at data rate 20 kbps and 80 kbps. Number of nodes are 9, 25, and 30. UDP, Grid topology.

Figure 5.20 shows the average packet end-to-end delay of the flows versus the number of nodes for different application data rates where the nodes deployed in grid topology. The higher number of nodes increases the end to end delay. Increasing the application data rate causes higher buffering delay. The end to end delay increases as the number of nodes

increase, because utilization of the channel will be increased if the number of nodes increases or application data rate increases (each node act as a traffic source). Additionally, the packet end to end delay increases as the application data rate increases for both routing protocols AODV and DEECP. We can clearly observe from this figure that the AODV protocol has higher packet end to end delay, due to the reasons mentioned in discussion of section 5.1.1 in addition to the power outages in AODV and the on-off thresholds implemented in DEECP protocol, on-off thresholds enable all the DEECP nodes that located in a flow to support it a same time periods. Hence, the packet end to end delay and packet loss will be decreased, goodput and received bytes will be increased. In addition to soft hand over. While, the AODV do not consider the remaining energy on the not on its decision, the AODV node just turns on and off according to its energy level. Table 5.27 shows the two factors full factorial analysis for DEECP protocol and AODV protocol which can be interpreted as in section 5.3.1. The variable is Application data rate and the number of nodes. Table 5.32 shows the percentage of difference between AODV and DEECP with respect of AODV protocol. In average, the DEECP achieves less packet end to end delay than AODV protocol by 83.2% at 20 kbps. However, as the application data rate increases, the difference decreases, which is at 80 kbps reaches to 15.1%. In average of number of nodes and application rate, the DEECP achieved 43% less packet end to end delay than AODV with grid topology.

Table 5.27: End to End Delay for AODV and DEECP protocols. The table shows the effect of changing prtocol versus number of data sources on end to end delay (ms) (grid toplogy).

	# of Nodes	DEECP	AODV	Row Sum	Row Mean	Row Effect
20 kbps	9	2.019287	13.349	15.36829	7.684143	-1.72232
	25	2.943492	17.37203	20.31553	10.15776	0.751304
	30	3.175605	17.57933	20.75494	10.37747	0.971011
	Column Sum	8.138384	48.30037			
	Column Mean	2.712795	16.10012			
	Column Effect	-6.69366	6.693664		9.406458	
80 kbps	# of Nodes	DEECP	AODV	Row Sum	Row Mean	Row Effect
	9	13.97433	18.33989	32.31422	16.15711	-5.15211
	25	19.50188	26.89839	46.40027	23.20013	1.890913
	30	25.22302	23.91781	49.14084	24.57042	3.261198
	Column Sum	58.69923	69.15609			
	Column Mean	19.56641	23.05203			
	Column Effect	-1.74281	1.74281		21.30922	

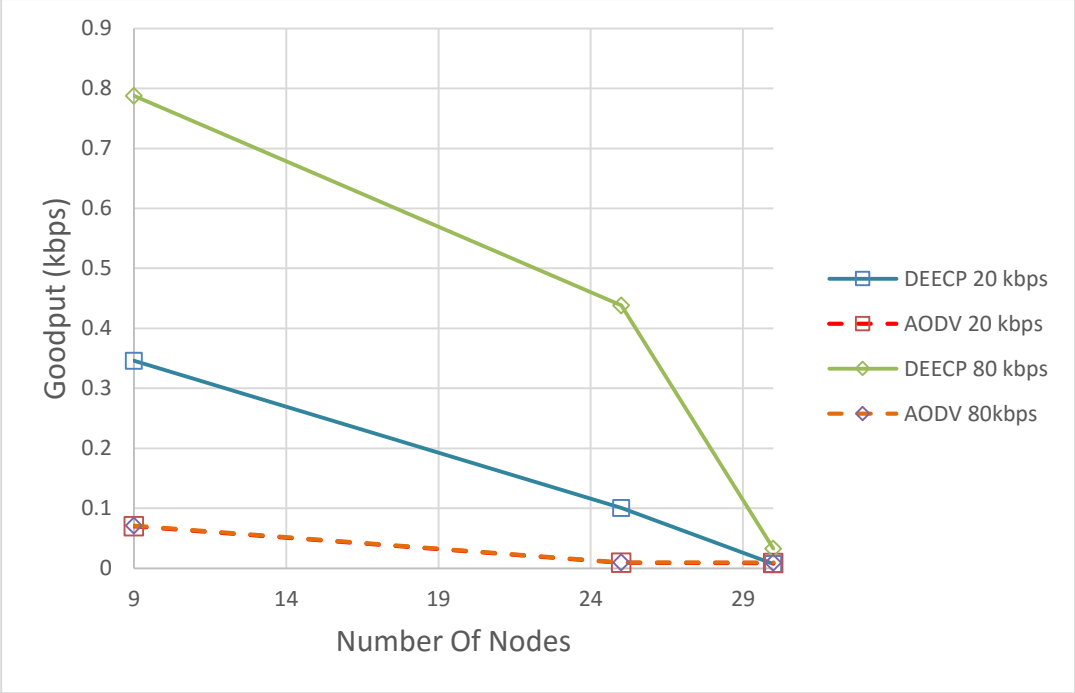

Figure 5.21: Goodput of DEECP and AODV protocols at 20 kbps and 80 kbps. UDP, The number of nodes (data sources) varying (9, 25, and 30).

Figure 5.21 shows the average goodput of the flows versus the number of nodes for different application data rates with grid topology. The goodput for AODV and DEECP decreases as the number of nodes increases. In Addition, it is expected that the goodput increases as the

application data rate increases for both AODV and DEECP protocol. We can observe that DEECP protocol outperformance AODV protocol in term of goodput except at 80 kbps, AODV achieves slightly more than DEECP protocol in terms of goodput by 17%. However on average, DEECP protocol achieves higher goodput than AODV protocol by 416% and 1292% at 20 kbps and 80 kbps. Table 5.28 shows the effect on goodput for varying application data rate and varying number of nodes for DEECP protocol and AODV protocol. Table 5.32 shows the computed percentage of effect for DEECP with respect to AODV. On average of varying the number of nodes and varying the application data rate, DEECP achieves higher goodput than AODV by 860%. At high number of nodes, the difference in goodput for AODV at 80 kbps is more than with respect AODV at 20kbps by101%. While the goodput for DEECP at 80 kbps is more than DEECP at 20 kbps by 357%. These value can calculated directly from Table 5.25. The reasons for goodput drops was discussed in previous sections and in section 4.6.

Table 5.28: Goodput of AODV and DEECP protocol. The table shows the effect of changing the protocol and number of data sources on Goodput (kbps).

	# of Nodes	DEECP	AODV	Row Sum	Row Mean	Row Effect
20 kbps	9	0.345998	0.070065	**0.416063**	**0.208032**	**0.11779**
	25	0.100453	0.009177	**0.109629**	**0.054815**	**-0.03543**
	30	0.007128	0.008628	**0.015756**	**0.007878**	**-0.08236**
	Column Sum	**0.453579**	**0.08787**			
	Column Mean	**0.151193**	**0.02929**			
	Column Effect	**0.060952**	**-0.06095**		**0.090241**	
80 kbps	# of Nodes	DEECP	AODV	Row Sum	Row Mean	Row Effect
	9	0.787963	0.071237	**0.8592**	**0.4296**	**0.204715**
	25	0.438238	0.009699	**0.447938**	**0.223969**	**-0.00092**
	30	0.032682	0.009492	**0.042174**	**0.021087**	**-0.2038**
	Column Sum	**1.258883**	**0.090429**			
	Column Mean	**0.419628**	**0.030143**			
	Column Effect	**0.194742**	**-0.19474**		**0.224885**	

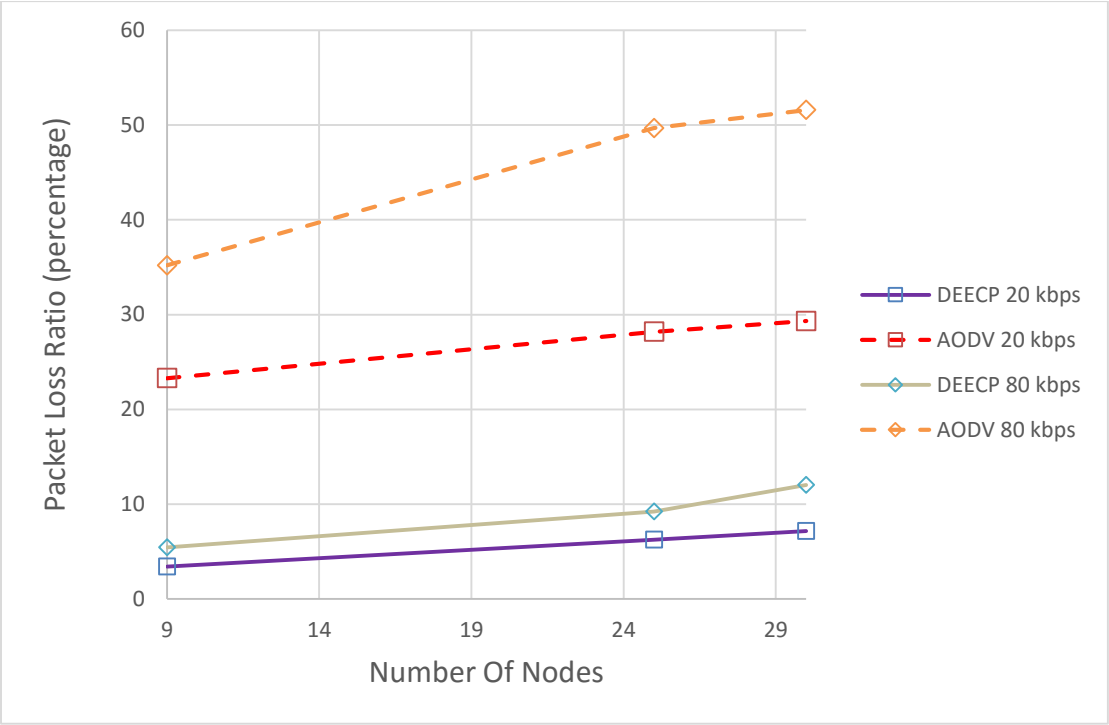

Figure 5.22: Packet Loss Ratio for DEECP and AODV at 20 kbps.UDP protocol.the number of node varying 9, 25, and 30 nodes including the sink node.

Figure 5.22 shows the average packet loss ratio of the flows versus the number of nodes. As expected, when the number of nodes increases the packet loss ratio increases. Also, the packet loss rate increases as the application data rate increases. It is clear from the figure that DEECP protocol has lower packet loss ratio than AODV. Table 5.29 shows the effect on packet loss ratio for varying the number of nodes for DEECP and AODV protocols. In average of varying the number of nodes, this table shows that the packet loss ratio increases as the application data rate increases. Table 5.32 shows the computed percentage of effect on packet loss ratio for DEECP with respect to AODV. The DEECP protocol achieves less packet loss ratio than AODV by nearly 79.2% at lowest application data rate, and at highest application data rate DEECP protocol achieves less loss ratio by 80.5%. However, in a total average of varying number of nodes and varying the application rate, the DEECP protocol achieves less packet loss ratio than AODV protocol by 80%. Table 5.32 shows the

percentage of difference for all the performance metric used in this scenario for DEECP and AODV protocols.

Table 5.29: Loss ratio of AODV protocol. The table shows the effect of changing application data rate and number of data sources on loss ratio (percentage).

	# of Nodes	DEECP	AODV	Row Sum	Row Mean	Row Effect
20 kbps	9	3.391095	23.29129	26.68239	13.34119	-2.92714
	25	6.25403	28.18458	34.43861	17.21931	0.950968
	30	7.170093	29.31894	36.48903	18.24451	1.976176
	Column Sum	16.81522	80.79481			
	Column Mean	5.605072	26.9316			
	Column Effect	-10.6633	10.66327		16.26834	
80 kbps	# of Nodes	DEECP	AODV	Row Sum	Row Mean	Row Effect
	9	5.421596	35.18478	40.60638	20.30319	-6.88019
	25	9.203547	49.68155	58.8851	29.44255	2.259174
	30	12.02356	51.58522	63.60878	31.80439	4.621015
	Column Sum	26.64871	136.4515			
	Column Mean	8.882903	45.48385			
	Column Effect	-18.3005	18.30047		27.18338	

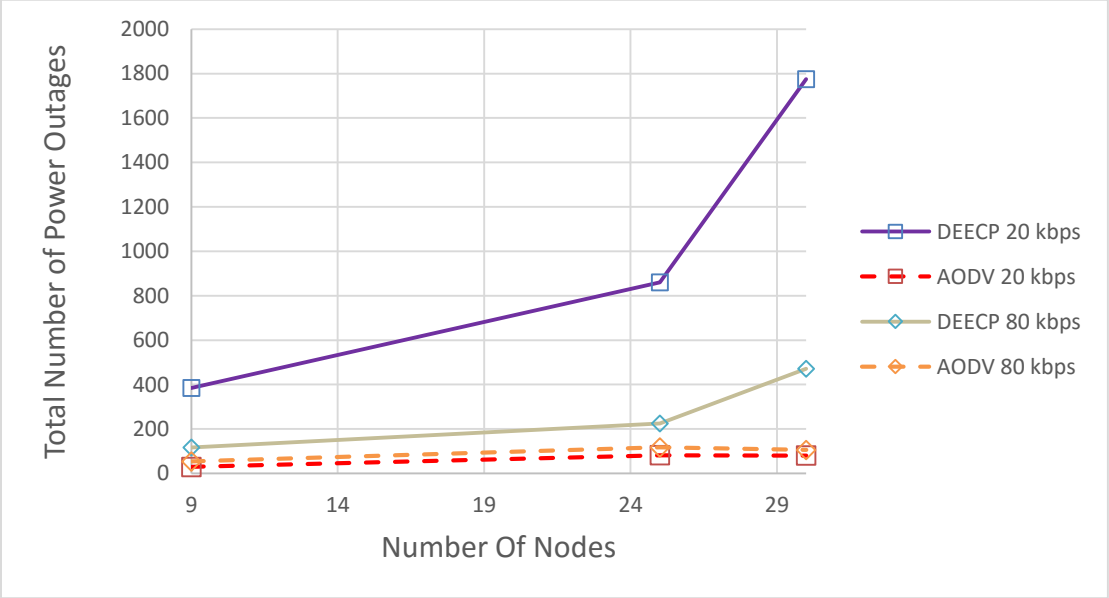

Figure 5.23: Total number of power outages for AODV and DEECP protocol at 20 kbps. UDP protocol. number of nodes 9, 25, and 30 .

Figure 5.23 shows the power outage for AODV and DEECP versus the number of nodes. In general, the DEECP protocol has higher power outages than AODV protocol, this happens

because the traffic is converged to collecting point (parent node). As it is expected, the power outage increases as the configured application data rate increases for AODV protocols. Conversely, the power outages of DEECP protocol decreases as the Application data rate increases. As a result of using on-off thresholds that is related to application data rate. On other hand, the power outages decrease as the number of nodes increases, because there is more paths available for DEECP and AODV Protocols. But for DEECP protocol after 25 nodes the total number of power outages increases. Table 5.30 shows the effected total power outage for varying application data rate and varying number of nodes for DEECP and AODV protocol, respectively. Table 5.32 shows the computed percentage of effect of total power outages for DEECP with respect to AODV. In average of number of nodes and application rate, the DEECP has higher power outage than AODV by 719%.

Table 5.30: Total power outages for AODV and DEECP at 20 kbps. The table shows the two factor full factorial effect of changing the protocol and number of data sources on power outages.

	# of Nodes	DEECP	AODV	Row Sum	Row Mean	Row Effect
20 kbps	9	42.73333	3.25	45.98333	22.99167	-1.26313
	25	34.42105	3.285714	37.70677	18.85338	-5.40142
	30	59.16129	2.677419	61.83871	30.91935	6.664553
	Column Sum	136.3157	9.213134			
	Column Mean	45.43856	3.071045			
	Column Effect	21.18376	-21.1838		24.2548	
80 kbps	# of Nodes	DEECP	AODV	Row Sum	Row Mean	Row Effect
	9	13.03448	5.947368	18.98185	9.490926	0.839649
	25	9	4.7	13.7	6.85	-1.80128
	30	15.70968	3.516129	19.22581	9.612903	0.961627
	Column Sum	37.74416	14.1635			
	Column Mean	12.58139	4.721166			
	Column Effect	3.93011	-3.93011		8.651276	

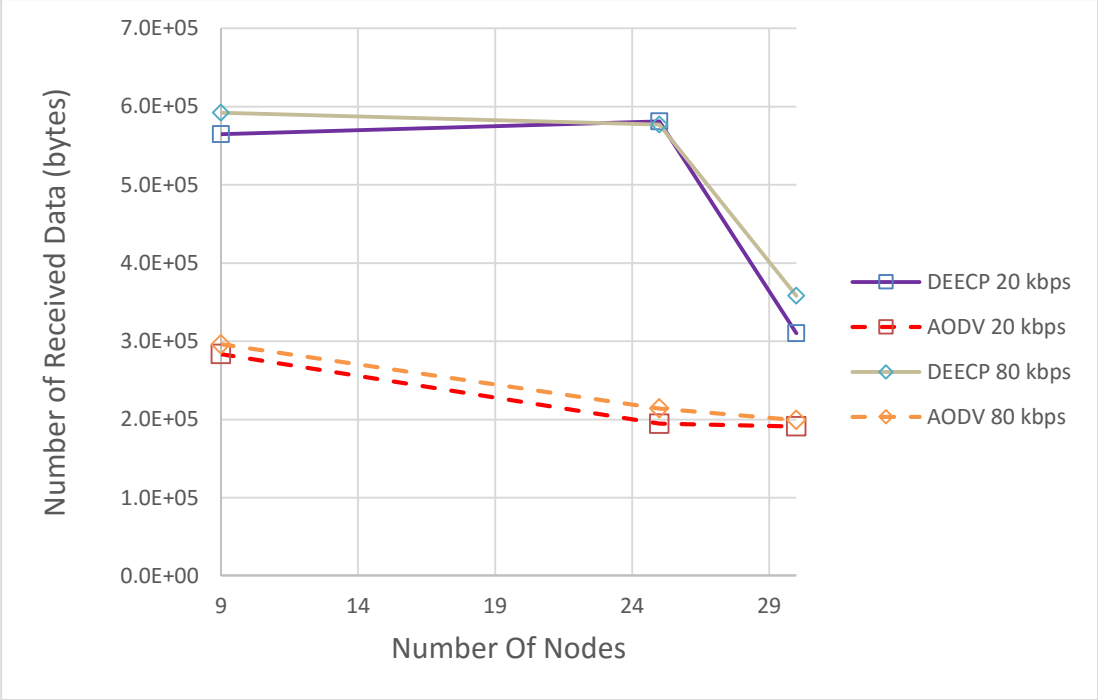

Figure 5.24: Total number received bytes for AODV and DEECP protocol at 20 kbps. UDP protocol. number of nodes 9, 25, and 49 .

Table 5.31 shows total number of received bytes for AODV protocol and DEECP protocol versus the number of nodes (data sources). As expected, the total received data increases as the application data rate increases for AODV protocol and DEECP protocol. In addition, the total number of received bytes decreases as the number of nodes increases for AODV protocol. This behavior can be explained as a result of packet loss increases as the number of nodes increases. In same manner, the total received bytes increase when the number of nodes increases until 25 nodes for DEEP protocol. After the number of nodes reached 25 nodes the total received bytes start decreasing. In general, the DEECP protocol has higher received bytes than AODV protocol. Table 5.12 shows the two factors full factorial analysis for three different application data rates. This table can be interpreted as previous sections. Table 5.32 shows the computed percentage of different between DEECP protocol and AODV protocol. In average, the DEECP has higher received bytes than AODV by 117% and 115% at 20kbps and 80 kbps respectively.

Table 5.31: Total number of received baytes for AODV and DEECP at 20 kbps. The table shows the two factor full factorial effect of changing the protocol and number of data sources on received data(bytes).

	# of Nodes	DEECP	AODV	Row Sum	Row Mean	Row Effect
20 kbps	9	564693.1	283716.2	848409.3	424204.6	69965.39
	25	580921.7	194567.8	775489.5	387744.7	33505.5
	30	310268.5	191268.2	501536.7	250768.4	-103471
	Column Sum	1455883	669552.2			
	Column Mean	485294.4	223184.1			
	Column Effect	131055.2	-131055		354239.2	
80 kbps	# of Nodes	DEECP	AODV	Row Sum	Row Mean	Row Effect
	9	591921.9	296172.4	888094.3	444047.1	71224.96
	25	576948.6	214112	791060.6	395530.3	22708.12
	30	358322.2	199456	557778.2	278889.1	-93933.1
	Column Sum	1527193	709740.4			
	Column Mean	509064.2	236580.1			
	Column Effect	136242	-136242		372822.2	

Table 5.32: Computed average percentage of effects for DEECP and AODV protocol on the performance with respect to application date rate = 30 kbps, respectively. (+) and (-) signs indicate increment or decrement in the performance metric.

	# of Nodes	End to End delay	Goodput	Loss	Power outages	Received data (Bytes)
20 kbps	9	-84.9%	393.8%	-85.4%	1215%	99%
	25	-83.1%	994.6%	-77.8%	948%	199%
	30	-81.9%	-17.4%	-75.5%	2110%	62%
	Average Effect	-83.2%	416.2%	-79.2%	1380%	117%
80kbps	# of Nodes	End to End delay	Goodput	Loss	Power outages	Received data (Bytes)
	9	-23.8%	1006.1%	-84.6%	119%	100%
	25	-27.5%	4418.2%	-81.5%	91%	169%
	30	5.5%	244.3%	-76.7%	347%	80%
	Average Effect	-15.1%	1292.1%	-80.5%	166%	115%

5.1.6 Comparison (Random Topology vs Grid topology).

In this scenario, a simulation experiment is held where the variables are the application data rate and topology (random and grid). The goal of this scenario is to show which topology is more suitable for DEECP protocol in terms of end-end delay, goodput, and packet loss ratio. The performance metrics were discussed in section 5.1. The simulation parameters are shown in Table 5.33 the other parameter as in Table 5.7. Figure 5.25 shows the grid placement of the 30 nodes. The triangle shape represents sink node which located at the edge of the area.

Table 5.33: Simulation Parameter

Parameter	Value
Number of nodes	30 nodes
Placement	Random placement and 5x6 grid placement (with step of 70 m)
Application data rate	20 kbps, 65 kbps, and 80 kbps.
Simulation Time	900 seconds
Initial Energy	0.02 J
Number of sources	Number of nodes -1

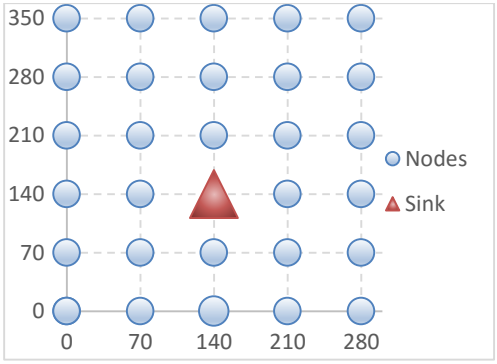

Figure 5.25: Grid topology for 5x6 nodes.

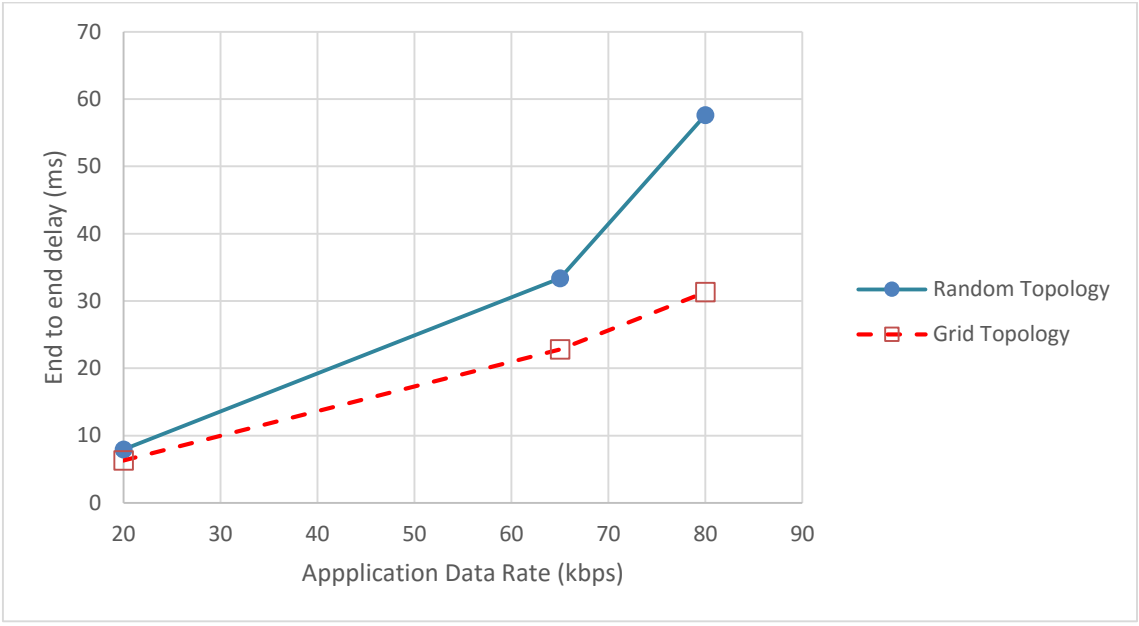

Figure 5.26: End-to-End Delay at data rate 20 kbps, 65 kbps, and 80 kbps. Number of nodes are 30 with random placement and 30 with grid placement.

Figure 5.26 shows the average packet end-to-end delay of the flows versus the application data rate. The packet end to end delay of random topology is higher than the packet end to end delay at grid topology. The figure shows that the packet end to end delay increases as the application data rate increases. Table 5.34 shows the two factors full factorial analysis of the packet end to end delay for random and grid topology. In average of application data rate, the grid topology has packet end to end delay less than random topology by 38.9% as shown in Table 5.39.

Table 5.34: Computation of effects of the topolygy on end-end delay.

App. Rate	Random Topology	Grid Topology	Row Sum	Row Mean	Row Effect
20	7.925196	6.319481	14.24468	7.122339	-19.4503
65	33.40286	22.8062	56.20906	28.10453	1.531882
80	57.6501	31.33206	88.98215	44.49108	17.91843
Column Sum	98.97815	60.45774			
Column Mean	32.99272	20.15258			
Column Effect	6.420069	-6.42007		26.57265	

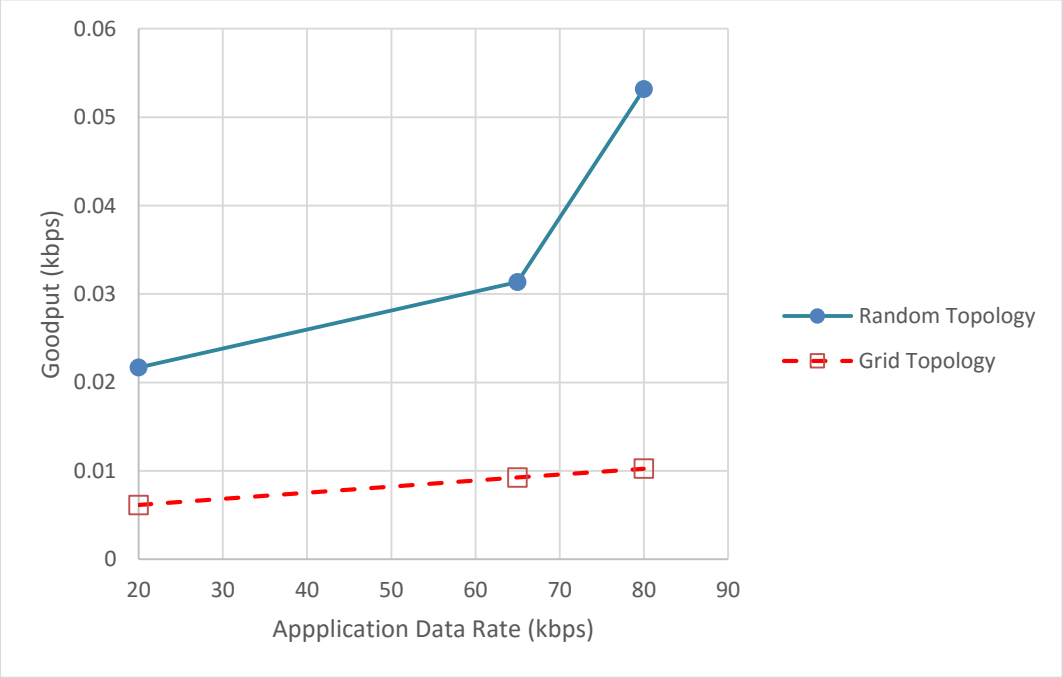

Figure 5.27:Avarage goodput at data rate 20 kbps, 65 kbps, and 80 kbps. Number of nodes are 30 with random placement and 30 with grid placement.

Figure 5.27 shows the average goodput of the flows versus the application data rates with grid topology and random topology. The goodput increases as the application data rate increases. The random topology outperformed grid topology for all configured application data rate except at 65 kbps. However, Table 5.39 shows that the random topology has higher average goodput than grid topology by 75%. Table 5.35 shows the two factors full factorial analysis. The random topology outperforms grid topology by nearly 0.0268 kbps in average of application data rate and topology.

Table 5.35: Computation of effects of the topology on goodput.

App. Rate	Random Topology	Grid Topology	Row Sum	Row Mean	Row Effect
20	0.021673	0.006131	**0.027804**	**0.013902**	**-0.00807**
65	0.031363	0.009241	**0.040603**	**0.020302**	**-0.00167**
80	0.053167	0.010251	**0.063418**	**0.031709**	**0.009738**
Column Sum	**0.106203**	**0.025622**			
Column Mean	**0.035401**	**0.008541**			
Column Effect	**0.01343**	**-0.01343**		**0.021971**	

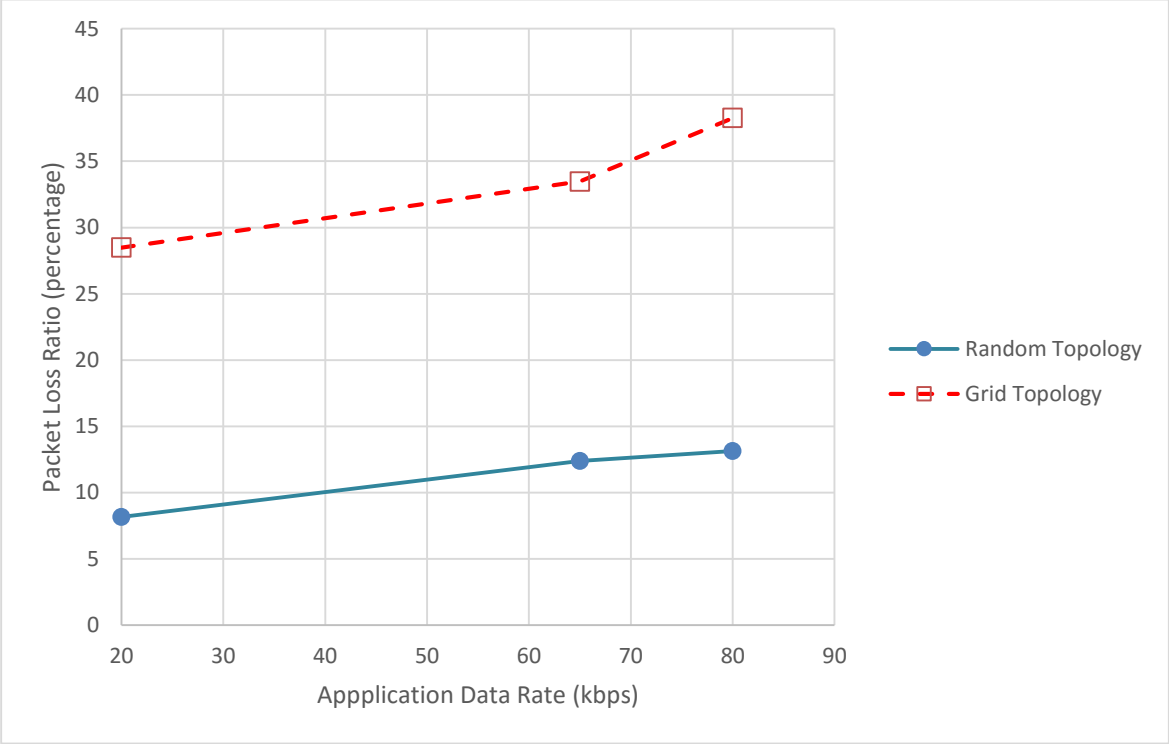

Figure 5.28: Percentage of average loss ratio at data rate 30 kbps, 65 kbps, and 80 kbps. Number of nodes are 30 with random placement and 30 with grid placement.

Figure 5.28 shows the average packet loss ratio of the flows versus the application data rate. The packet loss ratio increases as the application data rate increases. The random topology has higher packet loss ratio. Table 5.36 shows the full factorial analysis of random and grid topology. In average of application data rate, the random topology has packet loss ratio lower than grid topology by nearly 197% as shown in Table 5.39.

Table 5.36: Computation of effects of the topology on packet loss ratio

App. Rate	Random Topology	Grid Topology	Row Sum	Row Mean	Row Effect
20	8.156885	28.4901	36.64698	18.32349	-3.99479
65	12.39113	33.47306	45.8642	22.9321	0.613817
80	13.13435	38.26416	51.39851	25.69925	3.380974
Column Sum	33.68237	100.2273			
Column Mean	11.22746	33.40911			
Column Effect	-11.0908	11.09083		22.31828	

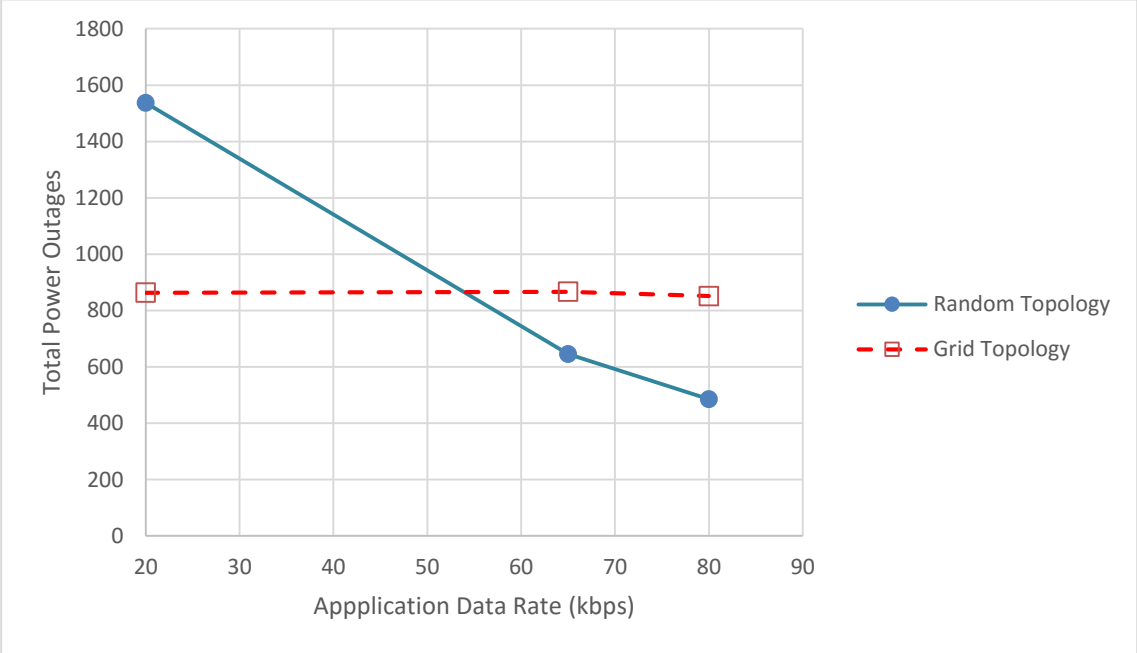

Figure 5.29: Average power outages at data rate 20 kbps, 65 kbps, and 80 kbps. Number of nodes are 30 with random placement and 30 with grid placement.

Figure 5.29 shows average number of power outages versus application data rate. The average power outages decrease as the application data rate increases. This behavior because the on-off power level threshold on DEECP protocol is related to application data rate. Table 5.37 shows the full factorial analysis of grid and random topologies. Table 5.39 shows that the random topology achieves higher power outage than grid topology by 3.3% in average of application data rates.

Table 5.37: Computation of effects of the topology on power outages.

App. Rate	Random Topology	Grid Topology	Row Sum	Row Mean	Row Effect
20	1537.031	863.5313	2400.563	1200.281	325.3513
65	645.5769	866.5456	1512.123	756.0613	-118.869
80	485.7273	851.1679	1336.895	668.4476	-206.482
Column Sum	2668.335	2581.245			
Column Mean	889.4451	860.4149			
Column Effect	14.51511	-14.5151		874.93	

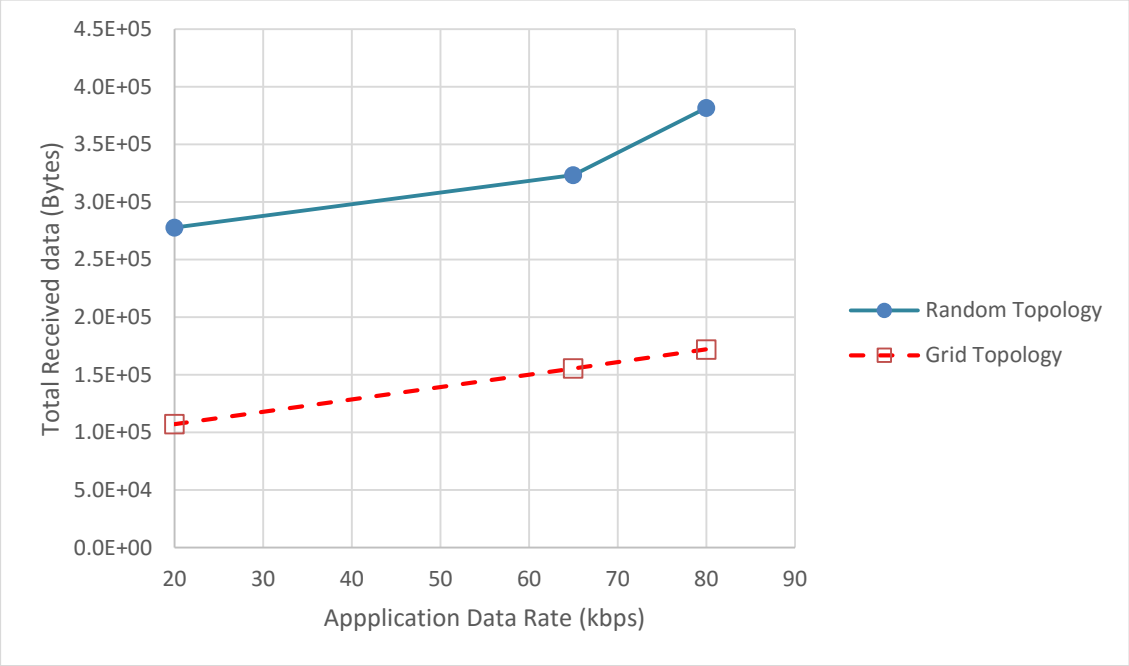

Figure 5.30: Total received data in bytes. Data rate 20 kbps, 65 kbps, and 80 kbps. 30 nodes arranged in grid topology and random topology.

Figure 5.30 shows the received bytes at the sink node versus application data rate. The DEECP with grid topology has higher received bytes than random topology for lower configured application data rate. But for higher configuration application data rate the random topology has higher received bytes. However, Table 5.39 shows that with grid topology DEECP has lower received byte than DEECP with random topology by 56%. From Figure 5.12 we can observe that the consumed energy nearly the same for all data rate.

Table 5.38: Computation of effects of the topology on received data (bytes).

App. Rate	Random Topology	Grid Topology	Row Sum	Row Mean	Row Effect
20	277946.4	107295.4	**385241.8**	**192620.9**	**-43712.4**
65	323426	155553	**478979**	**239489.5**	**3156.196**
80	381656.2	172122.8	**553779**	**276889.5**	**40556.19**
Column Sum	**983028.5**	**434971.2**			
Column Mean	**327676.2**	**144990.4**			
Column Effect	**91342.89**	**-91342.9**		**236333.3**	

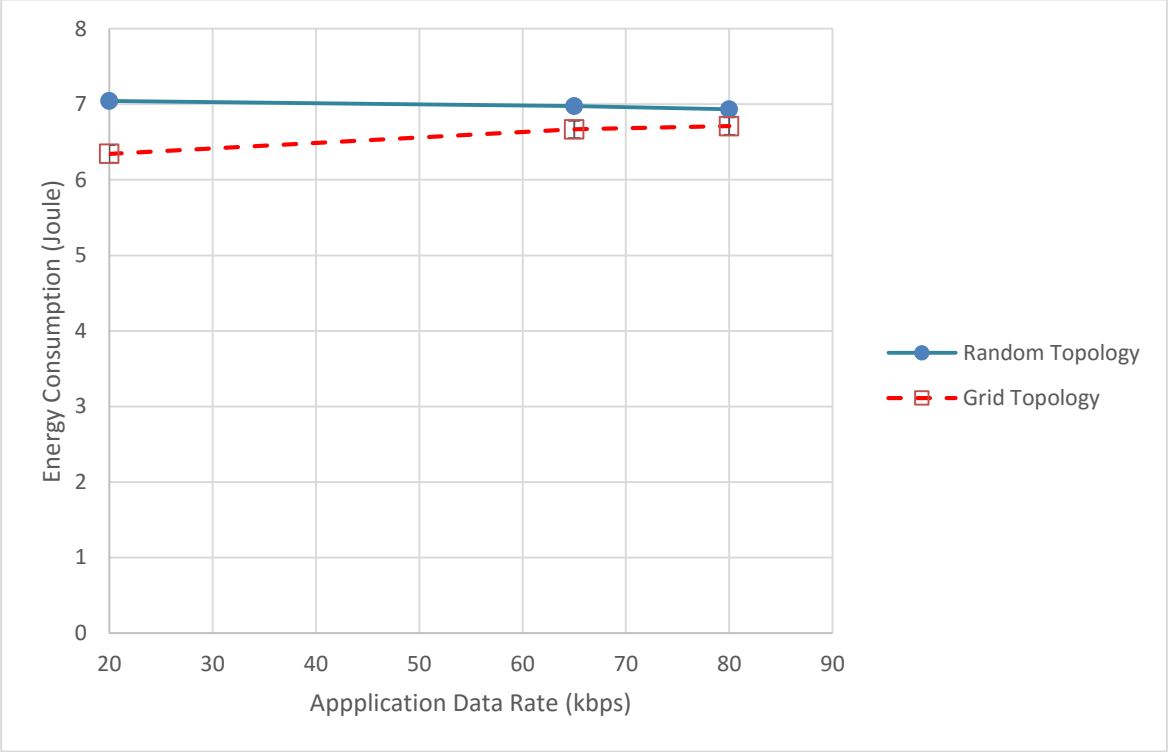

Figure 5.31: Total Energy Consumption (Joule). Data rate 20 kbps, 65 kbps, and 80 kbps. 30 nodes arranged in grid topology and random topology.

In summary, the DEECP with grid topology has less packet end to end delay and high packet loss ratio than DEECP with random topology by 38% and 197%, respectively. In addition, the DEECP with random node placement has higher goodput than DEECP with grid node placement by 75%. Also, the DEECP with grid node placement has less received data percent by 56%. This can be explained when the placement is random, the probability to have some region with higher network density for random placement is lower than grid

topology. When the network density increases the contention increases. Hence, the buffered time for the packets increases, which increases the end to end delay. In addition, increases the nodes density will increase the packet loss ratio. Also when the application data rate increase total received data increases as seen in Figure 5.30.

Table 5.39: Computed percentage of effects for grid topology on the performance with respect to random topology. (+) and (-) signs indicate increment or decrement in the performance metric , respectively.

App. Rate	end to end delay	Goodput	loss Ratio	Power Outages	Received bytes	Energy Consumption
20 kbps	-20.3%	-71.7%	249.3%	-43.8%	-61%	-10%
65 kbps	-31.7%	-70.5%	170.1%	34.2%	-52%	-4%
80 kbps	-45.7%	-80.7%	191.3%	75.2%	-55%	-3%
					-56%	-6%
Mean effect	-38.9%	-75.9%	197.6%	-3.3%	-56%	-6%

5.1.7 Studying the Effect of On-Off Relative Thresholds vs On-Off Fix Thresholds on DEECP Protocol.

In this scenario, a simulation experiment is held to evaluate the effect of Relative thresholds and fix thresholds in term of goodput, end-to-end delay, packet loss ratio, and power outages. The relative turn on threshold was defined in section 3.6. The fix threshold: define as when the turn on threshold and turn off Threshold set to certain level of node energy; for example set OFF energy equal to 0.002 joule and ON energy to 0.02 joule. The goal of this scenario is to study the effect of the relative threshold and fix threshold. Table 5.40 shows the simulation parameters. The rest of parameters are listed in Table 5.7.

Table 5.40: Simulation parameters.

Parameter	Value
Number of nodes	10, 15, 20, and 30 nodes
Placement	Random
Simulation Time	900 seconds
Initial Energy	0.02 J
Threshold	Fix threshold (minTh=0.002 joule. maxTh= 0.02.), Relative on-off Threshold see section 3.6
Application data rate	30 kbps.
Routing protocol	DEECP-Fth and DEECP-Rth

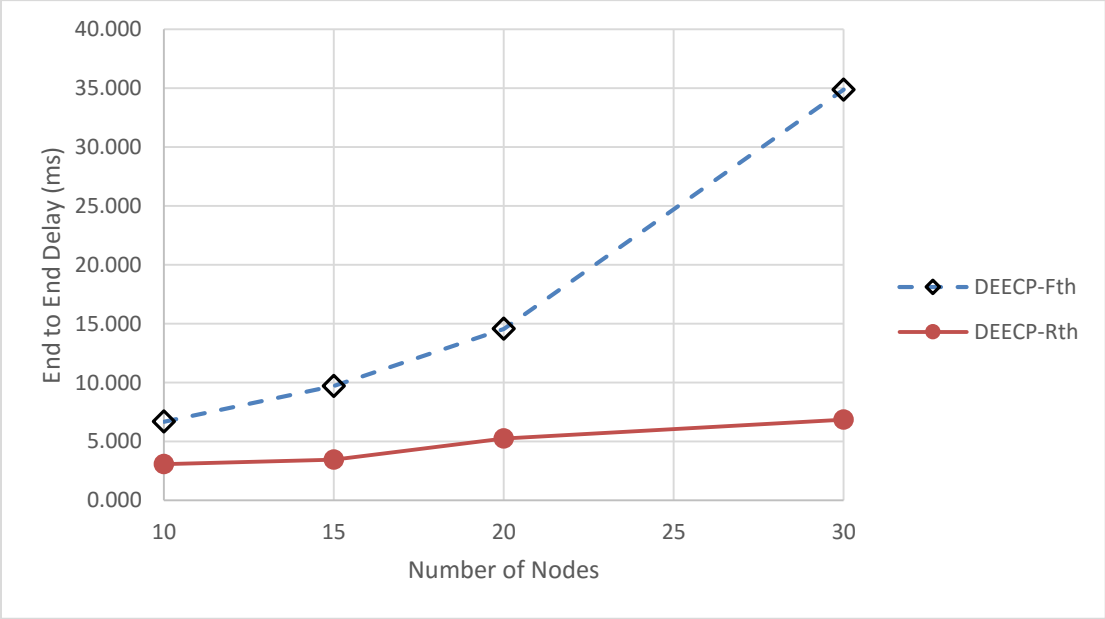

Figure 5.32: End to End Delay. Fth stands for Fix threshold and Rth stands for relative thresholds. Application data rate = 30 kbps.

Figure 5.32 shows the average packet end to end delay versus the varying number of nodes with fix threshold and relative threshold. When the number of nodes increases the packet end to end delay increases. The DEECP-Fth has higher packet end to end delay than DEECP-Rth, because when parent node goes to ON state with relative on-off threshold it fully support all of its children at a full application data rate. While the parent nodes with fix on-off threshold not considered the children energy demands. Table 5.41 shows the full

factorial analysis of DEECP-Fth and DEECP-Rth. In average of number of nodes, the DEECP-Rth achieves less packet end to end delay by 253% as shown in Table 5.45.

Table 5.41: Computation of effects of the DEECP-Fth and DEECP-Rth on end-end delay.

Protocol	DEECP				
# of Nodes	DEECP-Fth	DEECP-Rth	Row Sum	Row Mean	Row Effect
10	6.687	3.076	9.763	4.881	-5.680
15	9.716	3.454	13.171	6.585	-3.976
20	14.565	5.256	19.820	9.910	-0.651
30	34.883	6.856	41.739	20.869	10.308
Column Sum	65.851	18.641			
Column Mean	16.463	4.660		10.562	
Column Effect	5.901	-5.901			

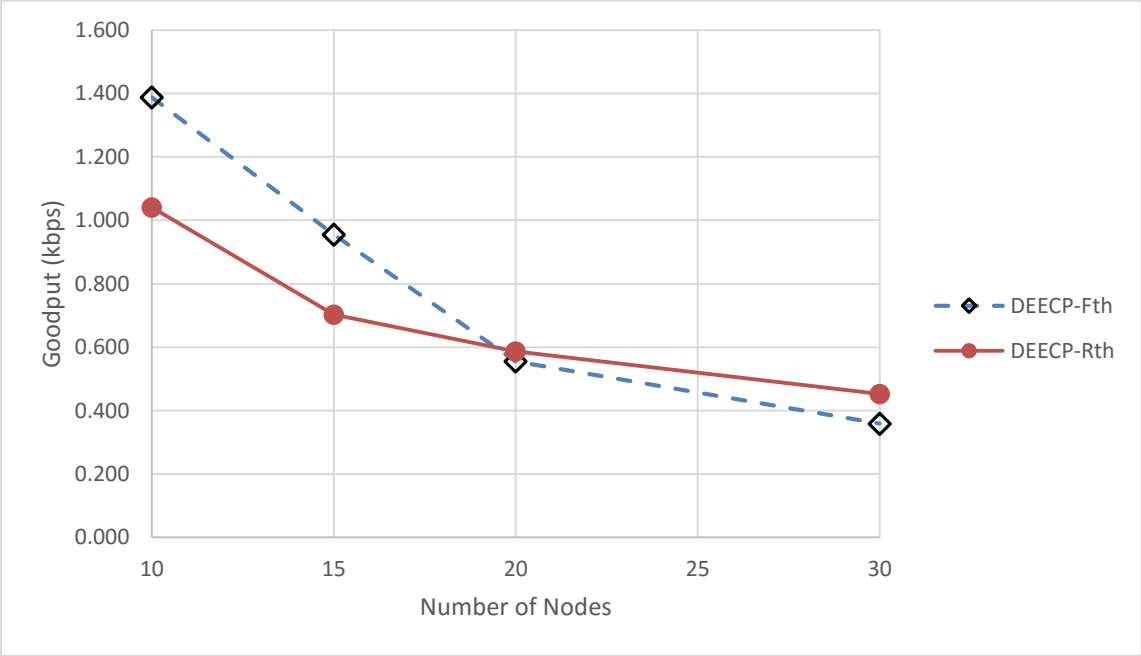

Figure 5.33: Average goodput. Fth stands for Fix threshold and Rth stands for relative thresholds. Application data rate = 30 kbps.

Figure 5.33 shows the average goodput of the flows versus the varying number of nodes with DEECP-Fth and DEECP-Rth. The goodput decreases as the number of nodes increases. At lower number of nodes the DEECP-Fth outperforms DEECP-Rth. But at 20 and 30 nodes the DEECP-Rth outperforms DEECP-Fth by 5.4% and 20.7%, respectively. This can be explained in this way; the parent nodes with fix on-off thresholds levels at low

number of nodes can support its children energy demands to fulfill application rate more than relative on-off thresholds. But, when the number of nodes increases (at 20 nodes) the parent nodes with relative on off thresholds continue to fully support its children demands by set the off threshold according to the number of its children. Table 5.42 shows a full factorial analysis of DEECP-Rth and DEECP-Fth, this table shows that with fix threshold DEECP has more goodput about 0.118 kbps than DEECP-Rth. Table 5.45 shows that in average of number of nodes the DEECP-Fth achieves higher goodput than DEECP-Rth by 17%.

Table 5.42: Computation of effects of the DEECP-Fth and DEECP-Rth on goodput.

# of Nodes	DEECP-Fth	DEECP-Rth	Row Sum	Row Mean	Row Effect
10	1.388	1.041	**2.429**	**1.215**	**0.459**
15	0.955	0.703	**1.659**	**0.829**	**0.074**
20	0.555	0.587	**1.142**	**0.571**	**-0.184**
30	0.359	0.453	**0.811**	**0.406**	**-0.349**
Column Sum	**3.258**	**2.784**			
Column Mean	**0.814**	**0.696**		**0.755**	
Column Effect	**0.059**	**-0.059**			

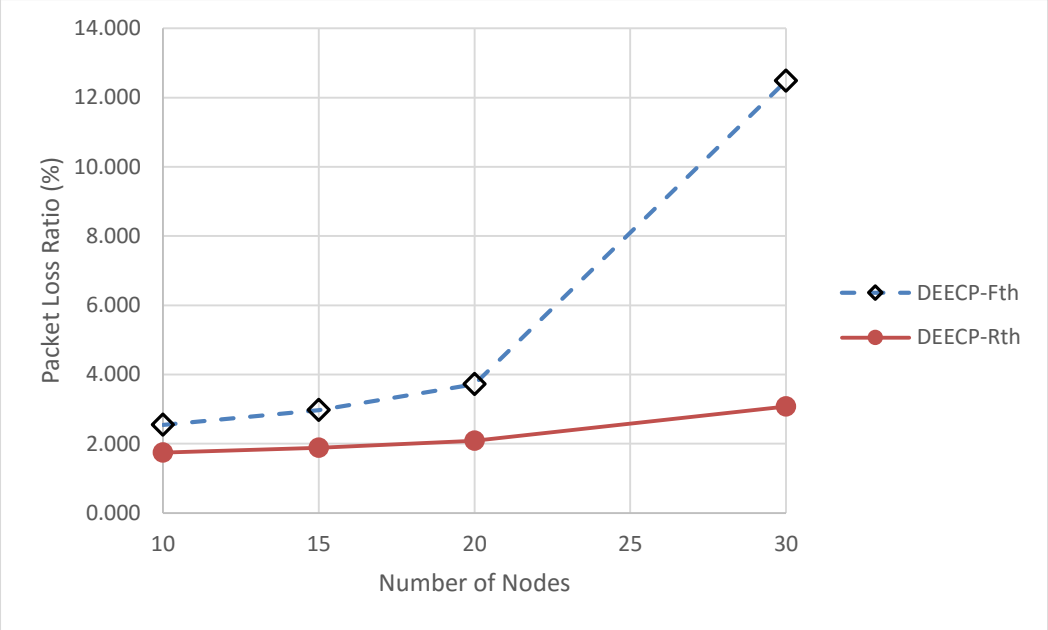

Figure 5.34: Average packet loss ratio. Fth stands for Fix threshold and Rth stands for relative thresholds. Application data rate = 30 kbps.

Figure 5.34 shows the average packet loss ratio. The packet loss ratio increases when the number of nodes increases for both situations. We can easily observe that DEECP-Fth has higher packets loss ratio than DEECP-Rth. Table 5.43 shows the full factorial analysis for DEECP-Fth and DEECP-Rth. At 30 nodes, the DEECP-Rth is less than DEECP-Fth by nearly 305%, and at lower number of nodes it has less loss ratio by nearly 46%. Table 5.45 shows that in average of number of nodes the DEECP-Rth has less packet loss ratio than DEECP-Fth by 147%.

Table 5.43: Computation of effects of the DEECP-Fth and DEECP-Rth on loss ratio

Protocol	DEECP				
# of Nodes	DEECP-Fth	DEECP-Rth	Row Sum	Row Mean	Row Effect
10	1.425	0.773	**2.198**	**1.099**	**-2.702**
15	2.411	1.697	**4.107**	**2.054**	**-1.747**
20	6.721	2.210	**8.931**	**4.465**	**0.665**
30	12.718	2.452	**15.170**	**7.585**	**3.784**
Column Sum	**23.274**	**7.131**			
Column Mean	**5.819**	**1.783**		**3.801**	
Column Effect	**2.018**	**-2.018**			

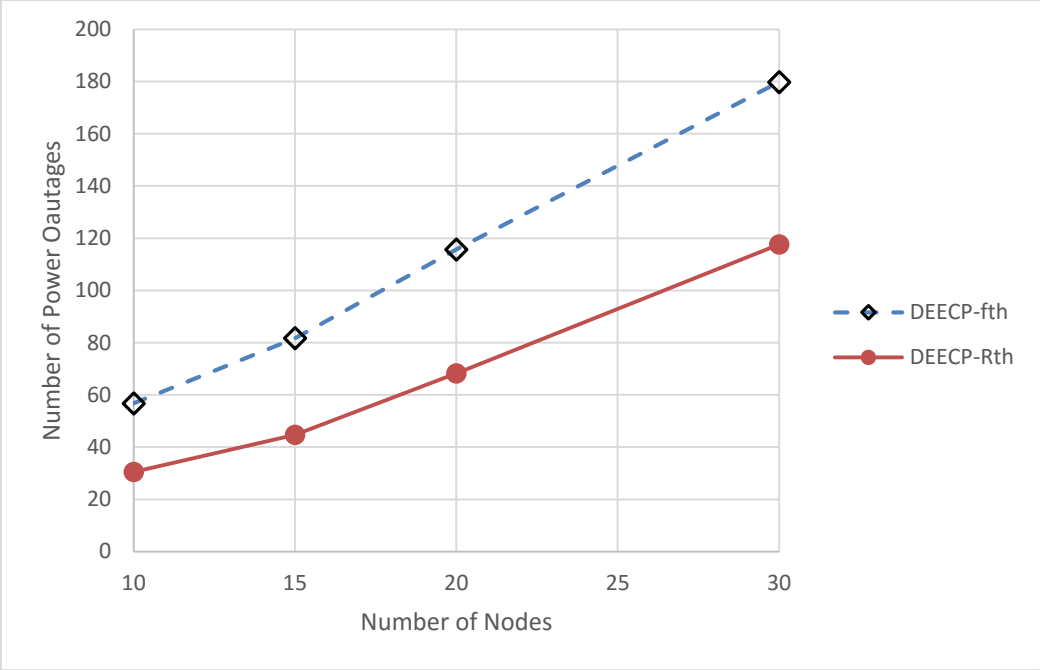

Figure 5.35: Average total number of power outages. Fth stands for Fix threshold and Rth stands for relative thresholds. Application data rate = 30 kbps.

Figure 5.35 shows the total number of power outage versus the varying number of nodes. In general, the power outage increases as the number of nodes increases. The DEECP-Rth has lower number of outages than DEECP-Fth. Table 5.44 shows a full factorial analysis for DEECP-Fth and DEECP-Rth in terms of total number of power outages. Table 5.45 shows that DEECP-Rth achieves less power outages than DEECP-Fth by 66% in average of number of nodes.

Table 5.44: Computation of effects of the DEECP-Fth and DEECP-Rth on total number of power outages.

# of Nodes	DEECP-Fth	DEECP-Rth	Row Sum	Row Mean	Row Effect
10	56.725	30.534	**87.259**	**43.629**	**-43.226**
15	81.662	44.644	**126.305**	**63.153**	**-23.703**
20	115.716	68.214	**183.931**	**91.965**	**5.110**
30	179.789	117.560	**297.349**	**148.674**	**61.819**
Column Sum	**433.891**	**260.952**			
Column Mean	**108.473**	**65.238**		**86.855**	
Column Effect	**21.617**	**-21.617**			

Table 5.45: Computed percentage of effects for DEECP-Fth on the performance with respect to DEECP-Rth. (+) and (-) signs indicate increment or decrement in the performance metric, respectively.

# of Nodes	End to End Delay	Goodput	Packet Loss Ratio	Power Outages
10	117.39%	33.33%	46.14%	85.77%
15	181.30%	35.88%	57.91%	82.92%
20	177.13%	-5.40%	77.90%	69.64%
30	408.82%	-20.72%	305.84%	52.93%
Column Mean Effect	253.26%	17.02%	147.07%	66.27%

In summary, the DEECP-Rth performs better than DEECP-Fth in terms of packet end to end delay. In addition, the packet end to end delay of DEECP-Fth increases exponentially while DEECP-Rth increases nearly linearly as the number of nodes increases. Also the DEECP-Fth goodput decreases rapidly than DEECP-Rth goodput as the number of nods increase. In terms of packet loss, the DEECP-Fth at high number of nodes increases in an exponentially trend, while DEECP-Rth increases in stable way when the number of nodes increases. Hence, we can conclude that the DEECP-Rth has more adaptability with number of nodes and also with application data rate, while DEECP-Fth more suitable for network with small number of nodes. The result of using relative threshold is increases the coverage area of the network, this done by allowing the parent nodes to sleep for a time that related to application data and the number of its children. Hence, more nodes are allowed to participate in the network, and more data will be collected from the network.

5.1.8 Study the Effect of Varying Transmission Power vs Fix Transmission Power on DEECP Protocol.

In this scenario, a simulation experiment is held to evalute two cases: first when the node has fix transsmission power. Second when the node has cabable of varying the transmission power. DEECP-VTx stands for DEECP protocol implemented in nodes with cababilty to varying its transmission power. DEECP-FTx stands for DEECP protocol

implemented in nodes with single transmission power. In this senario, we implemented Tmote sky sensor capabilty by implementing new Wifi radio energy mode in ns3, see section 2.5

Table 5.46: Simulation Parameter.

Parameter	Value
Number of nodes	10, 15, 20, and 30 nodes.
Placement	Random placement.
Simulation Time	900 seconds.
Initial Energy	0.02 J.
Application Data Rate	20 kbps.
Protocol	DEECP-VTx and DEECP-FTx.
Number of sources	Number of nodes -1.

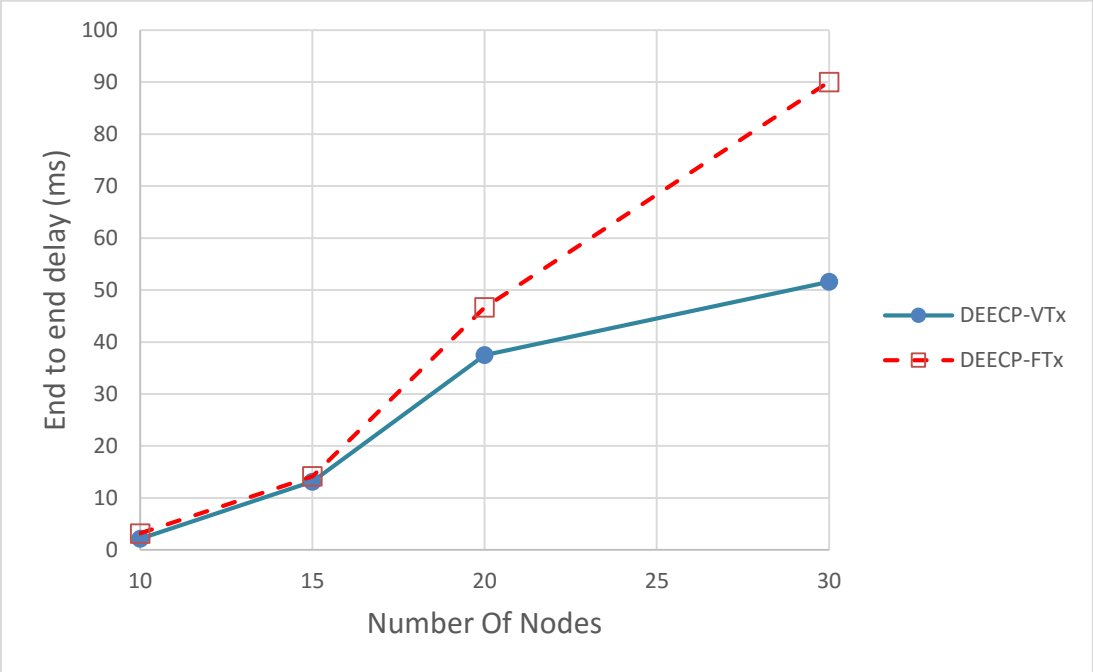

Figure 5.36: End to End Delay. Routing protocols DEECP-VTx and DEECP-FTx. Application data rate = 20 kbps.

Figure 5.36 shows the average packet end to end delay versus the varying number of nodes with DEECP-FTx and DEECP-VTx. When the number of nodes increases the packet end to end delay increases. The DEECP-VTx has less packet end to end delay than DEECP-FTx

when the number of nodes increases. Table 5.47 shows the full factorial analysis of DEECP-FTx and DEECP-VTx. Table 5.53 shows that DEECP-VTx in average of number of nodes has less end to end delay than DEECP-FTx by 32.2%. Where the DEECP-VTx has less packet end to end delay at 20 nodes by 31.6% and at 30 nodes by 42.7%.

Table 5.47: Computation of effects of the DEECP-FTx and DEECP-VTx on end-end delay.

# of Nodes	DEECP-FTx	DEECP-VTx	Row Sum	Row Mean	Row Effect
10	3.160923	2.160644	5.321567	2.660784	-29.6411
15	14.15533	13.14957	27.3049	13.65245	-18.6494
20	46.67369	37.48713	84.16082	42.08041	9.778563
30	90.02669	51.6008	141.6275	70.81375	38.5119
Column Sum	154.0166	104.3981			
Column Mean	38.50416	26.09954			
Column Effect	6.202313	-6.20231		32.30185	

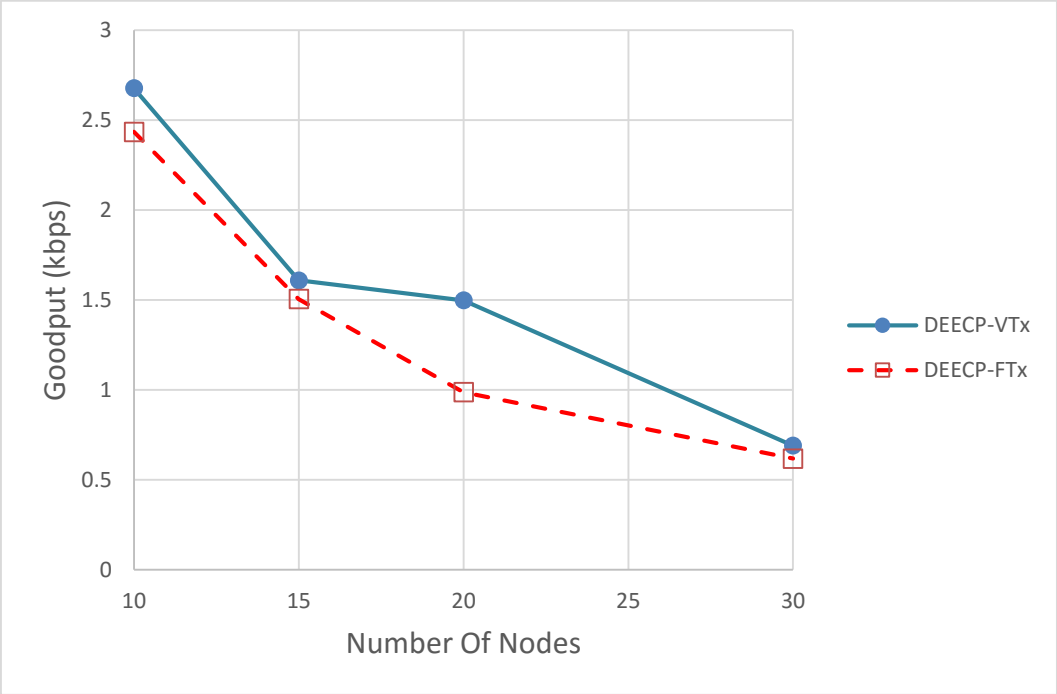

Figure 5.37: Goodput. Routing protocols DEECP-VTx and DEECP-FTx. Application data rate = 20 kbps, nodes varying 10, 15, 20, and 30 nodes.

Figure 5.37 shows the goodput of DEECP-VTx and DEECP-FTx versus the number of nodes. As expected, the goodput for both protocol decreases as the number of nodes increases. From the figure, we can observe that the two lines overlapped. The DEECP-VTx

has 10% and 11.5% goodput more than DEECP-FTx at 10 and 30 nodes, respectively. However in average of numbers of nodes, DEECP-VTx achieves better goodput than DEECP-FTx by 16.8% as shown in Table 5.53.

Table 5.48: Computation of effects of the DEECP-FTx and DEECP-VTx on goodput

# of Nodes	DEECP-FTx	DEECP-VTx	Row Sum	Row Mean	Row Effect
10	2.434434	2.677599	5.112034	2.556017	1.053373
15	1.505142	1.60954	3.114682	1.557341	0.054697
20	0.98735	1.498011	2.485361	1.242681	-0.25996
30	0.618886	0.69019	1.309076	0.654538	-0.84811
Column Sum	5.545812	6.475341			
Column Mean	1.386453	1.618835			
Column Effect	-0.11619	0.116191		1.502644	

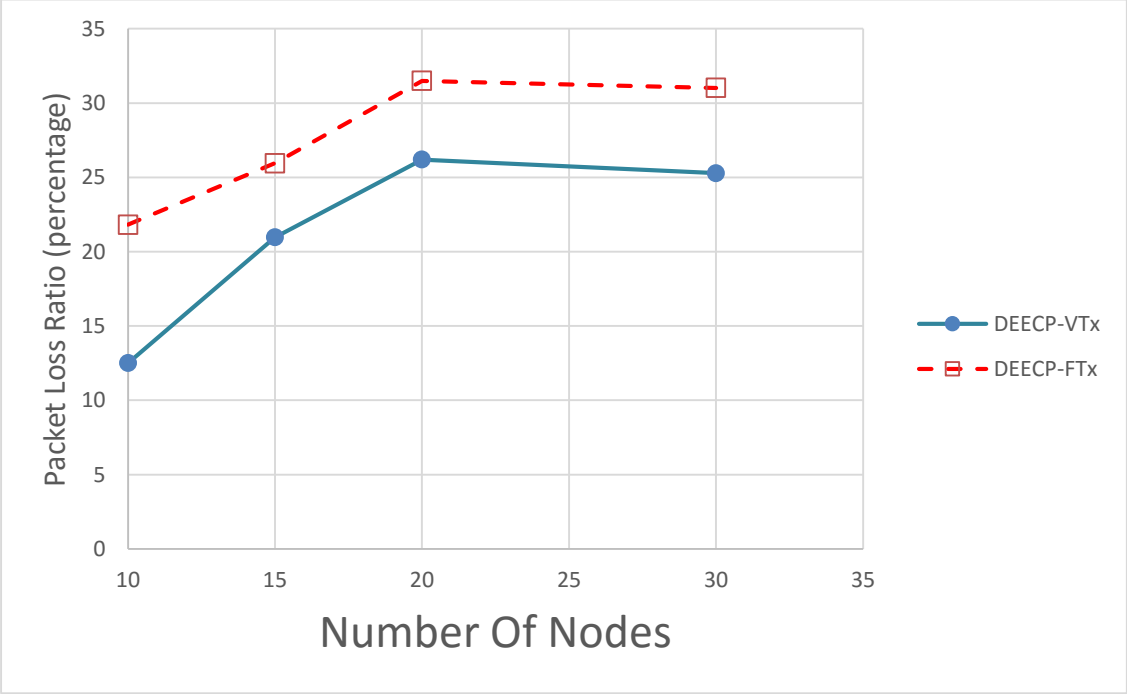

Figure 5.38: Packet loss Ratio. Routing protocols DEECP-VTx and DEECP-FTx. Application data rate = 20 kbps, nodes varying 10, 15, 20, and 30 nodes.

Figure 5.38 shows the average packet loss ratio of DEECP-FTx and DEECP-VTx versus the number of nodes. The packet loss ratio increases as the number of nodes increases. Table 5.49 shows the full factorial analysis of DEECP-FTx and DEECP-VTx. In

average of number of nodes, the DEECP-VTx has less packet loss ratio than DEECP-FTx by 23% as shown in Table 5.53.

Table 5.49: Computation of effects of the DEECP-FTx and DEECP-VTx on packet loss ratio

# of Nodes	DEECP-FTx	DEECP-VTx	Row Sum	Row Mean	Row Effect
10	21.81106	12.49833	34.30939	17.15469	-7.24453
15	25.94597	20.96843	46.91441	23.4572	-0.94202
20	31.48747	26.19107	57.67855	28.83927	4.440048
30	31.01332	25.27814	56.29146	28.14573	3.746504
Column Sum	110.2578	84.93598			
Column Mean	27.56446	21.234			
Column Effect	3.16523	-3.16523		24.39923	

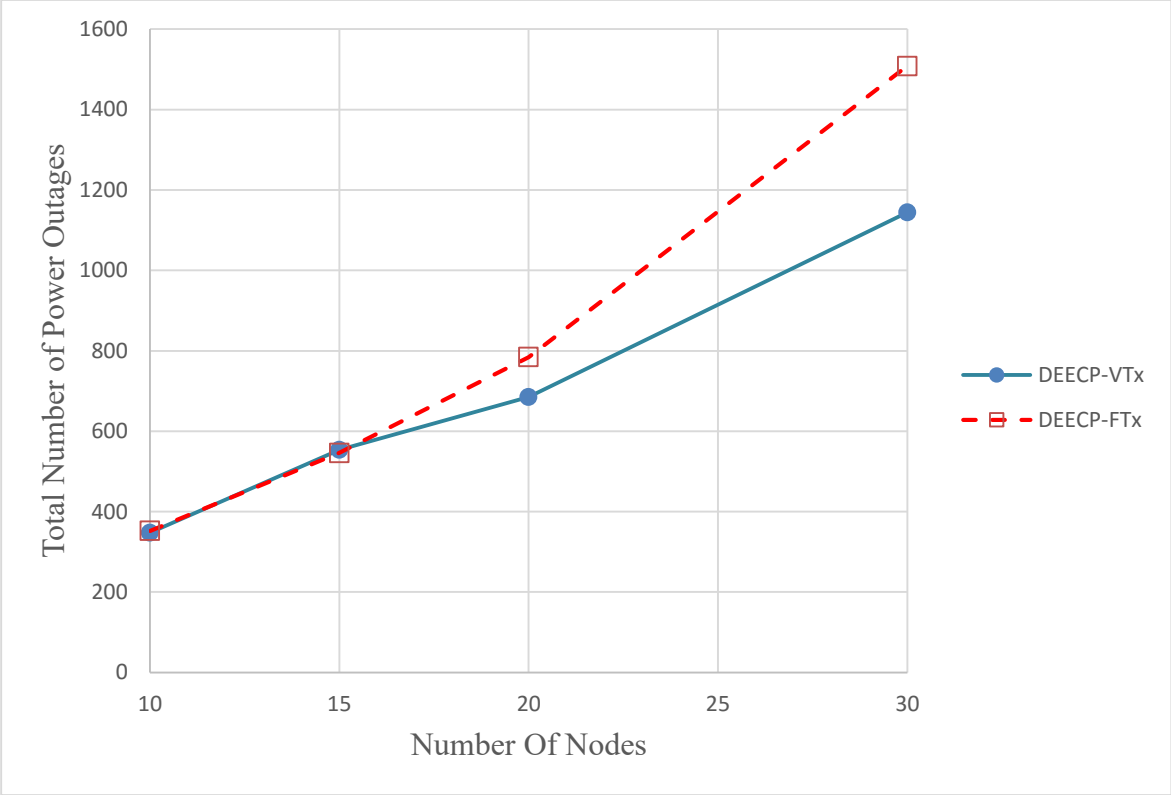

Figure 5.39: Total Number of Power Outages. Routing protocols DEECP-VTx and DEECP-FTx. Application data rate = 20 kbps, nodes varying 10, 15, 20, and 30 nodes.

Figure 5.39 shows the total power outages of DEECP-VTx and DEECP-FTx protocols versus the number of nodes. The power outage increases as the number of nodes increases for both protocols. For low number of nodes, the power outages of DEECP-VTx and DEECP-FTx nearly the same. But when the number of nodes becomes high, DEECP-VTx

has less power outages than DEECP-FTx significantly. Table 5.50 shows a full factorial analysis for both protocols. Table 5.53 shows that DEECP-VTx has power outages than DEECP-FTx by 16.9% in average of umber of nodes.

Table 5.50: Computation of effects of the DEECP-FTx and DEECP-VTx on total number of power outages

# of Nodes	DEECP-FTx	DEECP-VTx	Row Sum	Row Mean	Row Effect
10	352	347.3333	699.3333	349.6667	-390.354
15	546	553.9286	1099.929	549.9643	-190.056
20	784.2857	684.6154	1468.901	734.4505	-5.56983
30	1508	1144	2652	1326	585.9796
Column Sum	3190.286	2729.877			
Column Mean	797.5714	682.4693			
Column Effect	57.55105	-57.5511		740.0204	

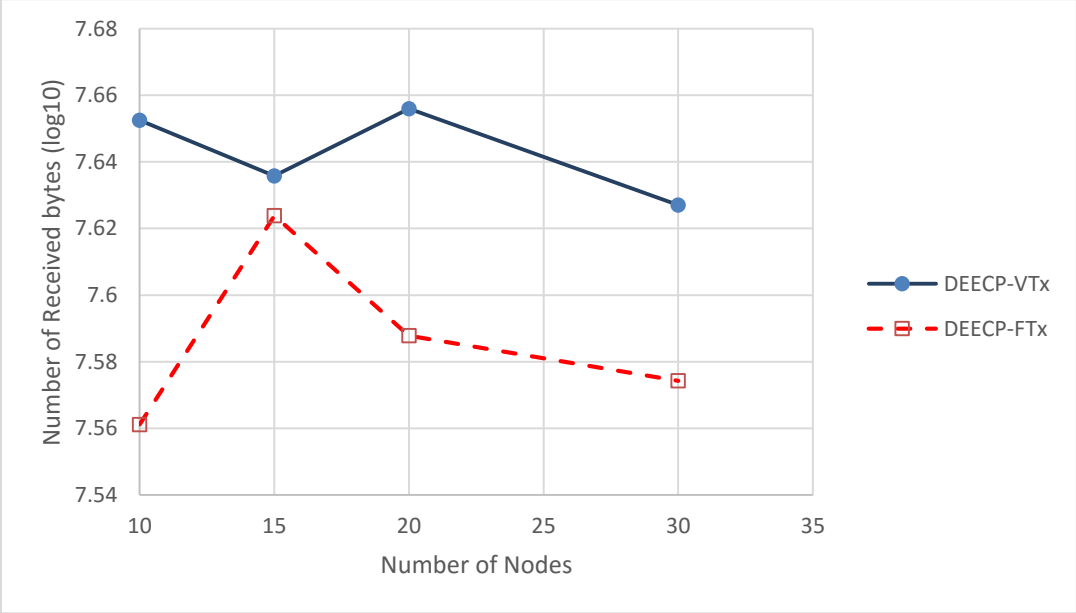

Figure 5.40: Total received bytes to the sink by DEECP-VTx and DEECP-FTx protocol. UDP, 20 kbps, Tmote sky sensor specifications.

Figure 5.40 shows the total received bytes to the sink node. The DEECP-VTx protocol has higher received data than DEECP-FTx protocol by 14% in average of nodes number. Even so, the DEECP-VTx consumed less energy than DEECP-FTx by 3% in average of number of nodes. Figure 5.41 shows the consumption energy of DEECP-FTx and DEECP-VTx

versus the number of nodes. The DEECP-VTx consumed less energy than DEECP-FTx by nearly 1.076 Joules as shown in Table 5.52.

Table 5.51: Computation of effects of the DEECP-FTx and DEECP-VTx on total receive bytes.

# of Nodes	DEECP-FTx	DEECP-VTx	Row Sum	Row Mean	Row Effect
10	36405202	44922862	81328064	40664032	-648409
15	42060704	43227697	85288402	42644201	1331760
20	38708014	45287111	83995125	41997563	685122.1
30	37520641	42367292	79887933	39943967	-1368474
Column Sum	1.55E+08	1.76E+08			
Column Mean	38673640	43951241			
Column Effect	-2638800	2638800		41312440	

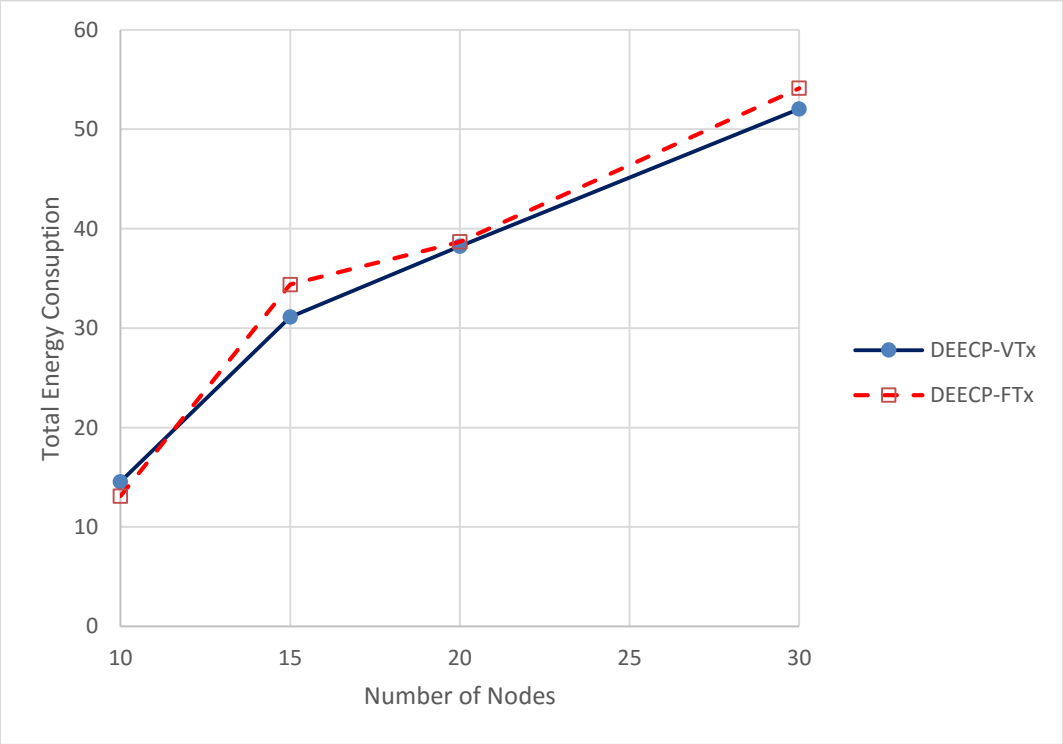

Figure 5.41: Total energy consumption. Routing protocols DEECP-VTx and DEECP-FTx protocols. Application data rate = 20 kbps, nodes varying 10, 15, 20, and 30 nodes.

Figure 5.41 shows the total energy consumption for versus the number of nodes for DEECP-VTx and DEECP-FTx. Table 5.52 shows the two factors full factorial analysis for energy consumption. Table 5.53 shows that DEECP-VTx has less energy consumption than DEECP-FTx by 3% in average of number of nodes.

Table 5.52: Total energy consumption by DEECP-VTx and DEECP-FTx protocols. UDP, 20 kbps, Tmote sky sensor specifications.

# of Nodes	DEECP-FTx	DEECP-VTx	Row Sum	Row Mean	Row Effect
10	13.11547	14.56243	27.6779	13.83895	-20.6963
15	34.38098	31.13203	65.51301	32.7565	-1.77874
20	38.67912	38.25018	76.9293	38.46465	3.929407
30	54.1177	52.04403	106.1617	53.08086	18.54562
Column Sum	140.2933	135.9887			
Column Mean	35.07332	33.99717			
Column Effect	0.538074	-0.53807		34.53524	

In summary, the DEECP-VTx achieves enhanced packet end to end delay and higher goodput. Also total received bytes are higher and lower energy consumption. The effect of DEECP-VTx become clearer in terms of performance metrics when the number of nodes becomes higher. Hence, the probability to have more nodes closer to its neighbors is high. So, the nodes can benefit from varying transmission range. Varying transmission range decreases the contention area around the node. In addition, it leads to less interference with its neighbors nodes.

Table 5.53: Computed percentage of effects for DEECP-VTx on the performance with respect to DEECP-FTx. (+) and (-) signs indicate increment or decrement in the performance metric, respectively.

# of Nodes	End to End delay	Goodput	Packet loss Ratio	Power Outages	Received Bytes	Consumed Energy
10	-31.6%	10.0%	-42.7%	1.3%	23%	11%
15	-7.1%	6.9%	-19.2%	-1.4%	3%	-9%
20	-19.7%	51.7%	-16.8%	14.6%	17%	-1%
30	-42.7%	11.5%	-18.5%	31.8%	13%	-4%
Percentage of Average Effect	-32.2%	16.8%	-23.0%	16.9%	14%	-3%

5.1.9 Study the Difference between Harvesting Energy and Battery Energy with DEECP and AODV

This scenario evaluates the effect of using energy harvesting with respect to battery energy. For the battery energy case, the nodes will get an energy budget and it will be divided equally among all the nodes. For the energy harvesting case, the harvester will stop harvesting when the sum initial energy and the sum harvested energy become equal to the energy budget. In consequence, the sum of the energy for all number of nodes will be the same for simulation time.

Table 5.54: Simulation parmeter

Parameter	Value
Number of nodes	10, 15, 20, and 30 nodes.
Placement	Random placement.
Simulation Time	900 seconds.
Initial Energy	0.02 J for harvesting case and 1.8/ number of nodes for battery case
Application Data Rate	20 kbps.
Protocol	DEECP-HE, DEECP-BE, AODV-HE, AODV-BE
Replications	60
Number of sources	Number of nodes -1.

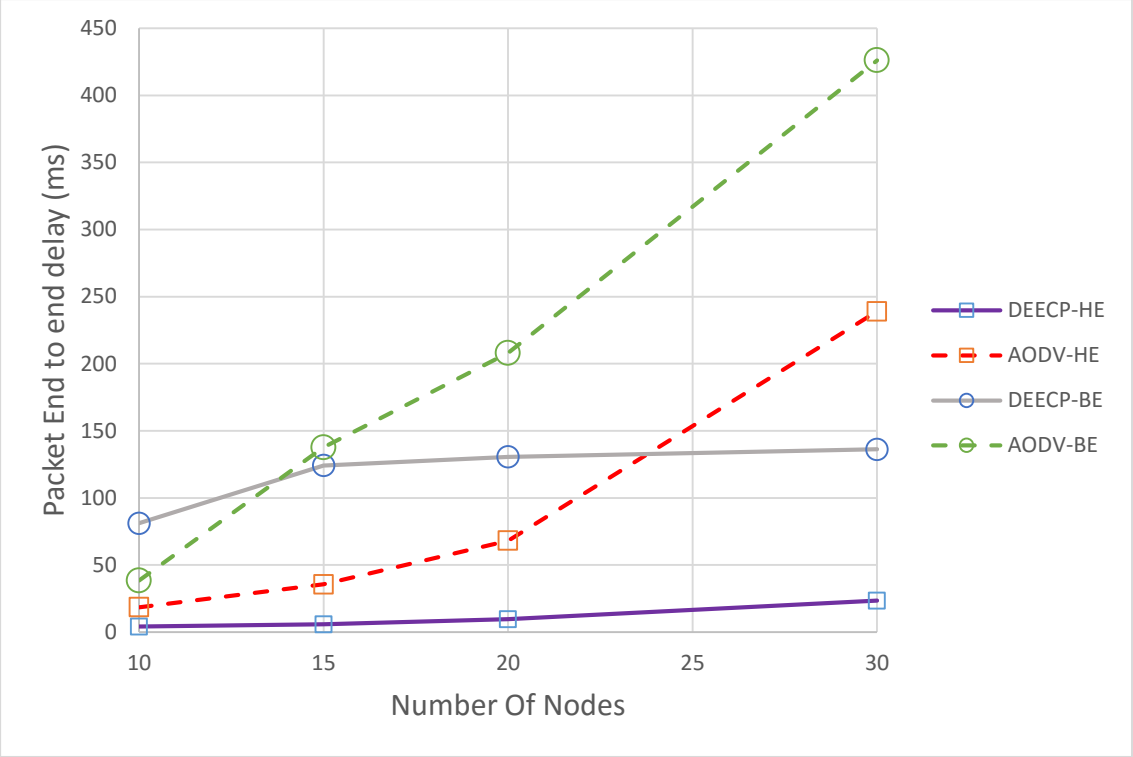

Figure 5.42: Packet end-to-end delay at data rate 20 kbps, for AODV protocol and DEECP protocol with harvesting and battery energy sources. Number of nodes are varying from 10 to 30.

Figure 5.42 shows the average packet end to end delay of the flows versus the number of nodes for harvesting energy source and battery energy source. The higher number of nodes increases the packet end to end delay. For both protocols, the nodes with battery energy have more end to end delay. The DEECP protocol has less packet end to end delay in average of all energy sources. Table 5.55 shows the full factorial analysis for DEECP and AODV protocols with battery and harvesting energy sources. Table 5.58 shows that DEECP has less packet end to end than AODV by 88.1% and 41% with harvesting and battery energy respectively. From Table 5.59, the DEECP-HE has less packet end to end delay than DEECP-BE by 91%. AODV-HE has less packet end to end delay than AODV-BE by 55%.

Table 5.55: End to End Delay of DEECP protocol and AODV protocol. The table shows the effect of varying number of nodes and varying the routing protocols with harvesting and battery energy, on pakets end to end delay

	# of Nodes	DEECP	AODV	Row Sum	Row Mean	Row Effect
Harvesting Energy	10	4.117781	18.50269	22.62047	11.31023	-39.1956
	15	5.765058	35.51821	41.28327	20.64163	-29.8642
	20	9.53383	68.16812	77.70195	38.85097	-11.6549
	30	23.39243	239.0486	262.441	131.2205	80.71466
	Column Sum	42.8091	361.2376			
	Column Mean	10.70227	90.3094			
	Column Effect	-39.8036	39.80356		50.50584	
Battery Energy	# of Nodes	DEECP	AODV	Row Sum	Row Mean	Row Effect
	10	81.06455	38.45043	119.515	59.75749	-100.516
	15	124.1175	137.6091	261.7266	130.8633	-29.4106
	20	130.6474	208.0093	338.6567	169.3283	9.054362
	30	136.1959	426.0976	562.2935	281.1467	120.8728
	Column Sum	472.0253	810.1664			
	Column Mean	118.0063	202.5416			
	Column Effect	-42.2676	42.26764		160.274	

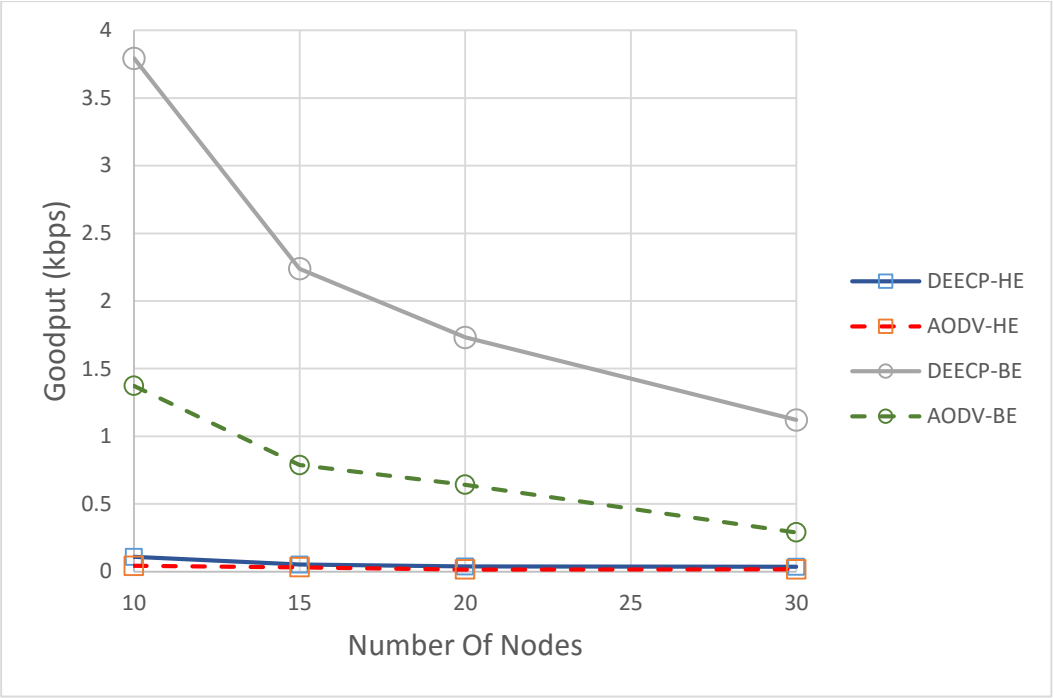

Figure 5.43: Goodput of DEECP and AODV protocols at 20kbps and with harvesting and battery energy sources . The number of nodes (data sources) changed from 10 nodes to 30 nodes.

Figure 5.43 shows the average goodput of the flows versus the number of nodes for battery and harvesting energy sources. The goodput for AODV and DEECP decreases as the number of nodes increases. In addition, the goodput with battery energy source is higher than the goodput with harvesting energy source. Table 5.56 shows the effect for varying application data rate and varying number of nodes on the goodput for DEECP and AODV protocols with harvesting and battery energy sources respectively. Table 5.58 shows that DEECP has higher goodput than AODV by 117% and 286% with harvesting energy and battery energy sources, Table 5.59 shows that DEECP with harvesting has less goodput than DEECP with battery source by 97%, and AODV with harvesting has less goodput than AODV with battery source by 97%.

Table 5.56: Goodput of DEECP protocol and AODV protocol. The table shows the effect of varying number of nodes and varying the routing protocols with harvesting and battery energy, on goodput

	# of Nodes	DEECP	AODV	Row Sum	Row Mean	Row Effect
Harvesting Energy	10	0.109457	0.043114	0.152571	0.076286	0.033422
	15	0.051918	0.032161	0.084079	0.042039	-0.00082
	20	0.038243	0.015769	0.054012	0.027006	-0.01586
	30	0.035365	0.016881	0.052246	0.026123	-0.01674
	Column Sum	0.234982	0.107925			
	Column Mean	0.058746	0.026981			
	Column Effect	0.015882	-0.01588		0.042863	
Battery Energy	# of Nodes	DEECP	AODV	Row Sum	Row Mean	Row Effect
	10	3.792488	1.372799	5.165286	2.582643	1.085571
	15	2.238611	0.787391	3.026002	1.513001	0.015929
	20	1.731215	0.642779	2.373993	1.186997	-0.31008
	30	1.121432	0.289862	1.411294	0.705647	-0.79142
	Column Sum	8.883746	3.09283			
	Column Mean	2.220936	0.773207			
	Column Effect	0.723864	-0.72386		1.497072	

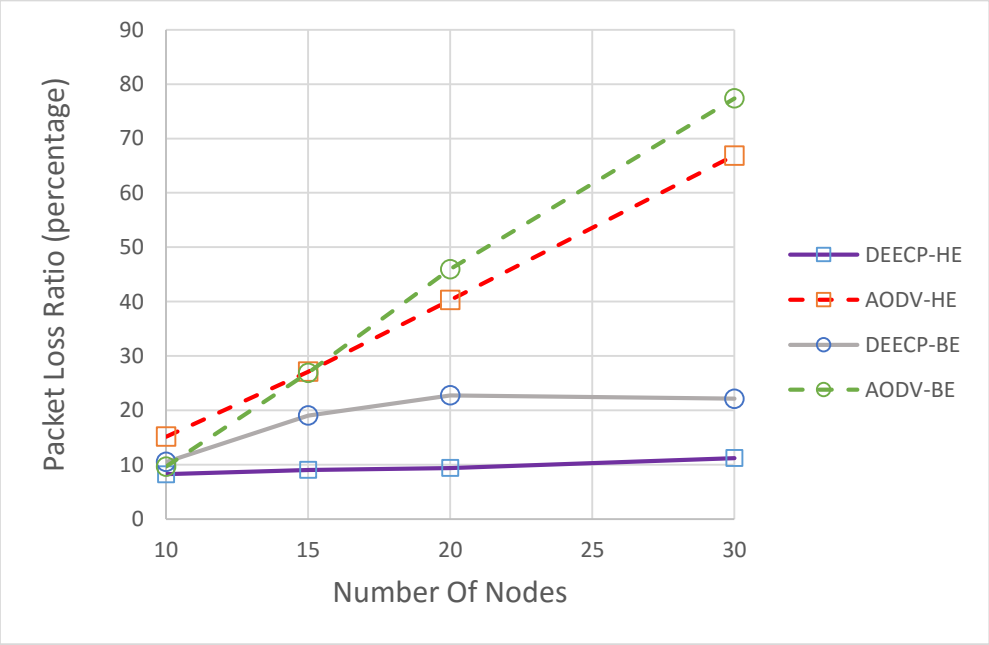

Figure 5.44: Packet Loss Ratio for DEECP-HE, DEECP-BE, AODV-HE and AODV-BE at 20kbps.the number of node varying from 10 to 30 nodes including the sink node.

Figure 5.44 shows the average packet loss ratio of the flows versus the number of nodes. Packet loss ratio increases as the number of nodes increases. As expected, the protocols with harvesting energy have less packet loss ratio for both protocols. The DEECP has less packet

loss ratio than AODV with harvesting energy and battery energy source. In addition, when the number of nodes (number of data sources) increases the packet loss also increases. Table 5.57 shows the effected packet loss ratio for varying application data rate and varying number of nodes for DEECP and AODV protocols at 20 kbps with harvesting energy and battery energy respectively. Table 5.58 shows the computed percentage of packet loss ratio for DEECP with respect to AODV, the DEECP has less packet loss ratio than AODV by 74% and 53% with harvesting energy and battery energy respectively. Table 5.59 shows that DEECP with harvesting energy source has less packet loss than DEECP with battery by 49%, and AODV with harvesting energy has less packet loss than AODV with battery energy source by 7%.

Table 5.57: Packet Loss Ratio of DEECP protocol and AODV protocol. The table shows the effect of varying number of nodes and varying the routing protocols with harvesting and battery energy, on packet loss ratio

	# of Nodes	DEECP	AODV	Row Sum	Row Mean	Row Effect
Harvesting Energy	10	8.262289	15.19191	23.4542	11.7271	-11.7036
	15	9.053564	27.12215	36.17571	18.08786	-5.34288
	20	9.404243	40.31578	49.72002	24.86001	1.429272
	30	11.22374	66.87223	78.09597	39.04798	15.61725
	Column Sum	37.94383	149.5021			
	Column Mean	9.485958	37.37552			
	Column Effect	-13.9448	13.94478		23.43074	
Battery Energy	# of Nodes	DEECP	AODV	Row Sum	Row Mean	Row Effect
	10	10.52201	9.674433	20.19645	10.09822	-19.2074
	15	19.06017	26.90943	45.9696	22.9848	-6.32087
	20	22.77908	45.97868	68.75777	34.37888	5.073211
	30	22.15844	77.36313	99.52157	49.76078	20.45511
	Column Sum	74.5197	159.9257			
	Column Mean	18.62993	39.98142			
	Column Effect	-10.6757	10.67575		29.30567	

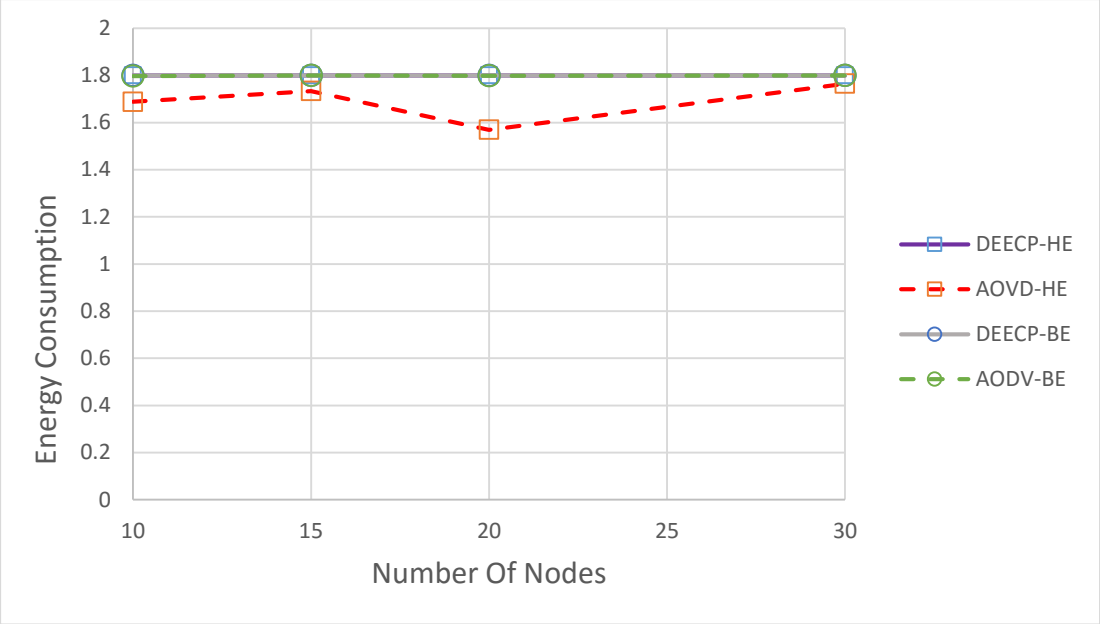

Figure 5.45: Total energy consumption (Joule) for DEECP and AODV protocols at 20 kbps with energy harvesting and battery energy rource.

Figure 5.45 shows the consumption energy versus the number of nodes. As this scenario has equal energy budget, the figure shows that the consumption is nearly equals except at AODV with energy harvesting, beacons some fare nodes still having some energy. Because it isolated when the nodes near the sink die.

Table 5.58: Computed average percentage of effects for DEECP protocol on the performance with respect to AODV protocol. for harvesting energy sorce and battery energy source, respectively. (+) and (-) signs indicate increment or decrement in the performance metric.

Energy Source	# of Nodes	End to End delay	Goodput	Packet Loss Ratio
Harvesting Energy	10	-77.7%	153.9%	-45.6%
	15	-83.8%	61.4%	-66.6%
	20	-86.0%	142.5%	-76.7%
	30	-90.2%	109.5%	-83.2%
	Average Effect	-88.1%	117.7%	-74.6%
	# of Nodes	End to End delay	Goodput	Loss
Battery Energy	10	110.8%	176.3%	8.8%
	15	-9.8%	184.3%	-29.2%
	20	-37.2%	169.3%	-50.5%
	30	-68.0%	286.9%	-71.4%
	Average Effect	-41.7%	187.2%	-53.4%

Table 5.59: Computed average percentage of effects for DEECP and AODV protocol with harvesting energy source respect to DEECP and AODV protocol with battery energy source on the performance. (+) and (-) signs indicate increment or decrement in the performance metric.

Performance metric	DEECP	AODV
Packet End to End Delay	-91%	-55%
goodput	-97%	-97%
Packet Loss Ratio	-49%	-7%
Total Rx bytes	18%	-1%

5.1.10 Study the Varying Application Data Rate with Harvesting Energy on DEECP and IEEE 802.11s

The aim of this scenario is to compare the performance of the IEEE 802.11s structure defined by the 802.11s draft with DEECP. Both protocols operated on nodes with harvesting energy. Table 5.60 shows the simulation parameter the rest parameter as in Table 5.7.

Table 5.60: Simulation parmeter

Parameter	Value
Number of nodes	10
Placement	Random placement.
Simulation Time	900 seconds.
Initial Energy	0.02 J
Application Data Rate	5 kbps, 10 kbps, 20 kbps, 50 kbps, and 80 kbps. On off application with 50% duty cycle
Protocol	DEECP, IEEE 802.11s with routing capabilities of MAC layer (proactive mode)
Channel type	OFDM Rate 6Mbps
Number of sources	Number of nodes -1.

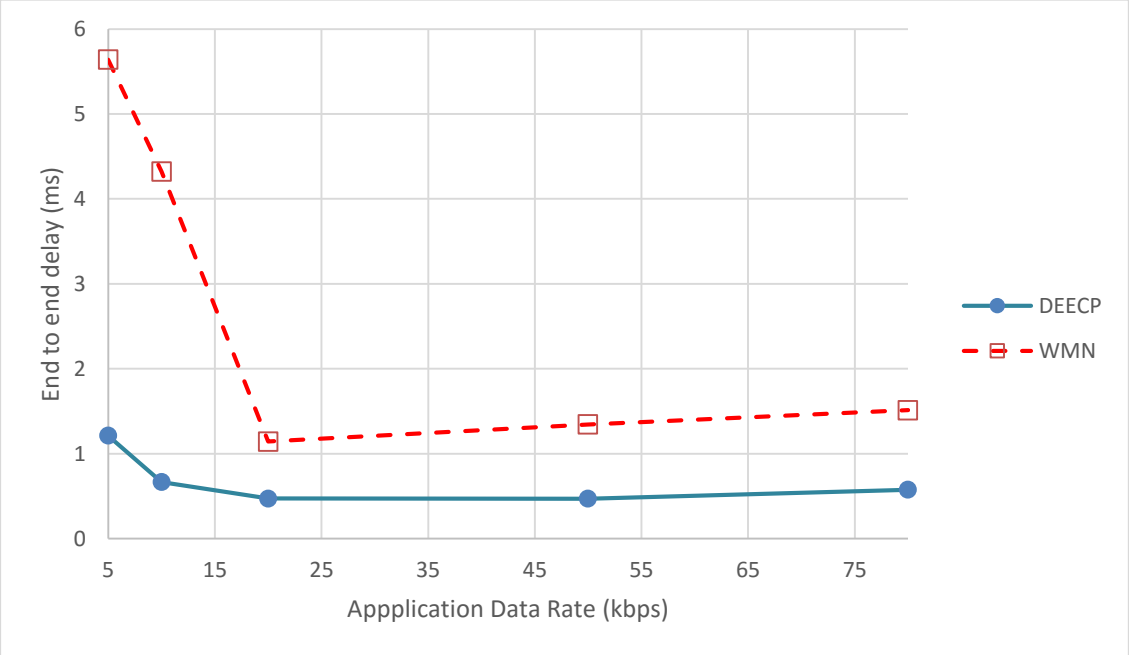

Figure 5.46: Packet end-to-end delay at 10 nodes, for IEEE 802.11s protocol and DEECP protocol with harvesting.

Figure 5.46 shows the average packet end-to-end delay of the flows versus the application data rate. The packet end to end delay of wireless mesh network with proactive mode is higher than the packet end to end delay for DEECP. The figure shows that the packet end to end delay decreases as the application data rate increases until the application rate reach 20 kbps, after that the delay increases as the end to end delay increases, because the packet loss ratio also increases. To understand the reason that make DEECP better than IEEE

802.11s at proactive mode you must understand the path selection criteria for both protocols, the path selection for IEEE 802.11s was discussed in section 1.2.5. IEEE 802.11s does not take in the account the energy level in routing metric and it has more overhead to establish a route to root node, when a node wake up it need to send and receive back a test frame, and to exchange 5 messages to join the tree and two messages for route discovery, this will increases packet end to end delay and increases packet loss ratio. Table 5.61 shows the two factors full factorial analysis of the packet end to end delay for DEECP and IEEE 802.11s. In average of application data rate, the DEECP has packet end to end delay lower than IEEE 802.11s by 75% as it shown in Table 5.65.

Table 5.61: Computation of effects of the topolygy on end-end delay.

App. Rate (Kbps)	DEECP	WMN	Row Sum	Row Mean	Row Effect
5	1.2131528	5.6387188	**6.851872**	**3.425936**	**1.690229**
10	0.6666912	4.3203851	**4.987076**	**2.493538**	**0.757832**
20	0.471641	1.1437357	**1.615377**	**0.807688**	**-0.92802**
50	0.4698472	1.3450146	**1.814862**	**0.907431**	**-0.82828**
80	0.576588	1.5112896	**2.087878**	**1.043939**	**-0.69177**
Column Sum	**3.3979202**	**13.959144**			
Column Mean	**0.679584**	**2.7918287**			
Column Effect	**-1.056122**	**1.0561224**		**1.735706**	

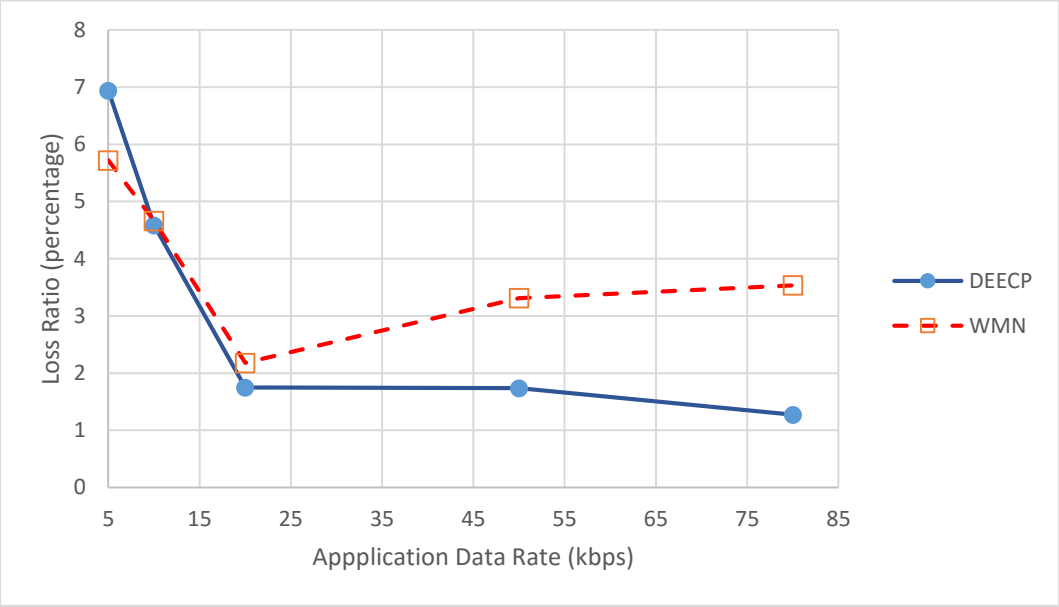

Figure 5.47: Percentage of average packet loss ratio at data rate 5 kbps, 10 kbps, 20 kbps, and 50 kbps. Number of nodes is 10 with DEECP and IEEE 802.11s protocols.

Figure 5.47 shows the average packet loss ratio of the flows versus the application data rate. The packet loss ratio decreases as the application data rate increases, until the throughput reaches to high utilization point. The peak utilization point for IEEE 802.11s is at 20 kbps then its packet loss ratio increased [54] . DEECP has higher packet loss ratio at lower application data rate, but it has lower packet loss ratio than IEEE 802.11s at higher data rate, due to using relative on-off thresholds Table 5.62 shows the full factorial analysis of DEECP and WMN protocols. In average, the DEECP has packet loss ratio lower than IEEE 802.11s by nearly 16% as shown in Table 5.65.

Table 5.62: Computation of effects of the topology on packet loss ratio

App. Rate (Kbps)	DEECP	WMN	Row Sum	Row Mean	Row Effect
5	6.9382764	5.7206151	12.65889	6.329446	2.761016
10	4.5833042	4.6610792	9.244383	4.622192	1.053762
20	1.7483729	2.1793082	3.927681	1.963841	-1.60459
50	1.7373582	3.3108509	5.048209	2.524105	-1.04433
80	1.2710807	3.5340497	4.80513	2.402565	-1.16586
Column Sum	16.278392	19.405903			
Column Mean	3.2556785	3.8811806			
Column Effect	-0.312751	0.3127511		3.56843	

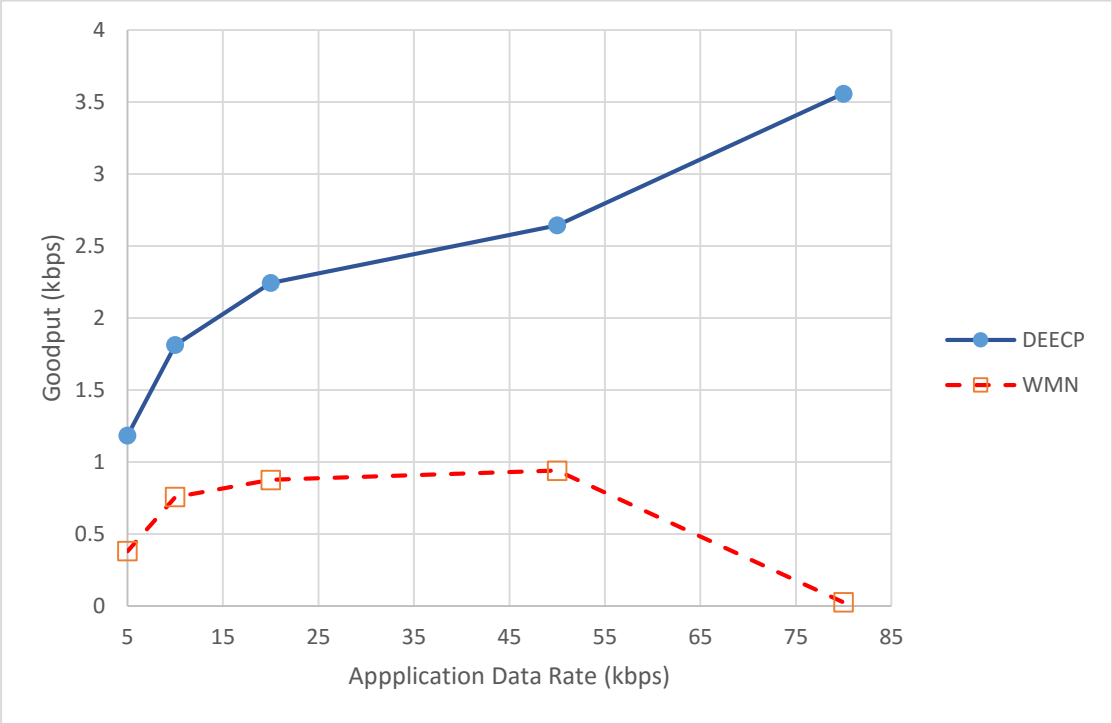

Figure 5.48: Avarage goodput at data rate 5 kbps, 10 kbps, and 20 kbps. Number of nodes is 10 with DEECP and IEEE 802.11s.

Figure 5.48 shows the average goodput of the flows versus the application data rates for DEECP and IEEE 802.11s. The goodput increases as the application data rate increases, until it reaches a peak utilization point, after that point the goodput decreases as application data rate increases. DEECP has not reach to that point at 80 kbps yet. The DEECP outperformed IEEE 802.11s for all configured application data rate. Table 5.65 shows that the DEECP has higher average goodput than IEEE 802.11s by 284.8%. Table 5.63 shows

the two factors full factorial analysis. The DEECP outperforms IEEE 802.11s by nearly 1.69 kbps in average of application data rate and protocols.

Table 5.63: Computation of effects of the topology on Average Goodput

App. Rate (Kbps)	DEECP	WMN	Row Sum	Row Mean	Row Effect
5	1.1843743	0.3803601	1.564734	0.782367	-0.65962
10	1.8122857	0.75682069	2.569106	1.284553	-0.15743
20	2.2437765	0.87505294	3.118829	1.559415	0.11743
50	2.6432126	0.93974053	3.582953	1.791477	0.349492
80	3.5587843	0.02543846	3.584223	1.792111	0.350127
Column Sum	11.442433	2.97741272			
Column Mean	2.2884867	0.59548254			
Column Effect	0.8465021	-0.8465021		1.441985	

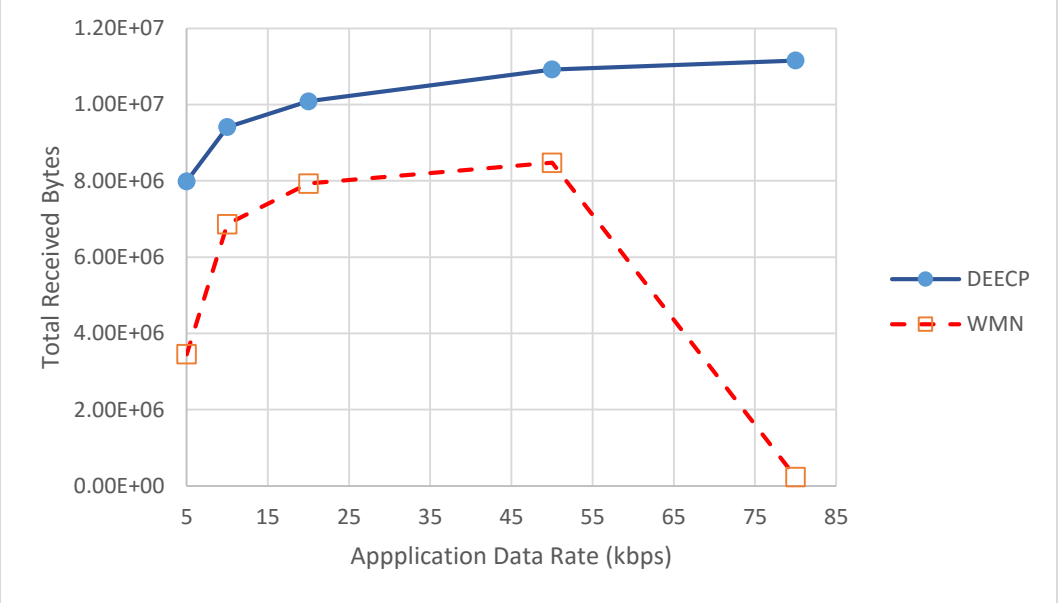

Figure 5.49: Total received bytes. Data rate 5 kbps, 10 kbps, and 20 kbps. 10 nodes, DEECP and IEEE 802.11s protocols.

Figure 5.49 shows the total received bytes at the sink node versus application data rate. The DEECP has higher total received bytes than WMN for all configured application data rate. The WMN has lower total received bytes at 80 kbps due to higher packet loss ratio. Table 5.64 shows the full factorial analysis of the packet end to end delay for DEECP and IEEE 802.11s. Table 5.65 shows that the DEECP has higher received byte than IEEE 802.11s by 83%.

Table 5.64: Computation of effects of the topology on total received bytes

App. Rate (Kbps)	DEECP	WMN	Row Sum	Row Mean	Row Effect
5	7987045.8	3450994.3	**11438040**	**5719020**	**-1932192.8**
10	9411646.2	6864242.8	**16275889**	**8137945**	**486731.68**
20	10085244	7930261	**18015505**	**9007752**	**1356539.5**
50	10921259	8474493.1	**19395752**	**9697876**	**2046663.2**
80	11156079	230862.93	**11386942**	**5693471**	**-1957741.6**
Column Sum	**49561274**	**26950854**			
Column Mean	**9912254.8**	**5390170.8**			
Column Effect	**2261042**	**-2261042**		**7651213**	

Table 5.65: Computed percentage of effects for DEECP with respect IEEE 802.11s. (+) and (-) signs indicate increment or decrement in the performance metric , respectively.

App. Rate	end to end delay	Goodput	loss Ratio	Rx Bytes
5 kbps	**-78.5%**	**211.4%**	**21.3%**	**131.4%**
10 kbps	**-84.6%**	**139.5%**	**-1.7%**	**37.1%**
20 kbps	**-58.8%**	**156.4%**	**-19.8%**	**27.2%**
50 kbps	**-65.1%**	**181.3%**	**-47.5%**	**28.9%**
80 kbps	**-61.8%**	**13889.8%**	**-64.0%**	**4732.3%**
Mean effect	**-75.7%**	**284.3%**	**-16.1%**	**83.9%**

CHAPTER 6

CONCLUSION AND FUTURE WORK

This chapter summarizes the thesis work and its contribution. This research has tackled important problems in energy-harvesting based WSNs [55] . These problems included minimizing the end to end delay and maximizing the throughput.

6.1 Conclusion

This thesis proposed DEECP algorithm to collect the data from nodes based on its energy, energy harvesting rate, and RSSI. This algorithm increases the flow goodput about 1148%, decreases the packet loss ratio about 80%, and decreases the packet end to end delay about 65% in comparison with AODV protocol. The DEECP with relative On threshold has more adaptability with network than DEECP with fix On threshold. In addition, the DEECP increase the flow goodput about 284%, decreases the packet loss ratio about 16%, and decreases the packet end to end delay about 75% in comparison with IEEE 802.11s protocol in proactive mode where in this mode the IEEE 802.11s built a tree to collect the data to sink node.

6.2 Future Work

In DEECP routing protocol operates in layer three. The children node connected to parent considers transmission time based on its energy and other parameter used by DEECP. To offer more optimal routing protocol the DEECP must expand to work in the MAC layer, which is called cross layers protocols. Hence, the DEECP can grant the time slot to children

nodes with PR. It is expected to achieve higher throughput and less delay. In addition, this will more efficiently manage harvested energy. As a result, the operation time of the wireless sensor network will extend. In addition, for more satisfaction a comparison with xCTP [56] can be conducted.

REFERENCES

[1] D. Puccinelli and M. Haenggi "Wireless Sensor Networks: Applications and Challenges of Ubiquitous Sensing" IEEE CIRCUITS AND SYSTEMS MAGAZINE,2005.pp. 9-29.

[2] J. Li, C. Blake, D. S. De Couto, H. I. Lee, and R. Morris, "Capacity of ad hoc wireless networks," in *Proceedings of the 7th annual international conference on Mobile computing and networking*, 2001, pp. 61-69.

[3] C. de Morais Cordeiro and D. P. Agrawal, "Mobile ad hoc networking," *Center for Distributed and Mobile Computing, ECECS, University of Cincinnati,* 2002.

[4] C. Mbarushimana and A. Shahrabi, "Comparative study of reactive and proactive routing protocols performance in mobile ad hoc networks," in *Advanced Information Networking and Applications Workshops, 2007, AINAW'07. 21st International Conference on*, 2007, pp. 679-684.

[5] I.D. Chakeres, E. M. Belding-Royer, "AODV Routing Protocol Implementation Design" 24th International Conference on Distributed Computing Systems Workshops, IEEE 2004.

[6] X. Wang and A. O. Lim, "IEEE 802.11s wireless mesh networks: Framework and challenges," *Ad Hoc Networks*, 2007

[7] A. Mohsin1 , K. Abu Bakar , A. Adekiigbe, K. Zrar "A Survey of Energy-Aware Routing and MAC Layer Protocols in MANETS: Trends and Challenges "Microthink Institute, Network Protocols and Algorithms, 2012, Vol. 4, No. 2

[8] I. Cisco, Internet protocol architecture for the Smart Grid. 2010. Available: http://www.cisco.com/web/strategy/docs/energy/CISCO_IP_INTEROP_STDS_PPR_TO_NIST_WP.pdf.

[9] T. Voight, H. Ritter, and J. Schiller, "Utilizing solar power in wireless sensor networks," inProc. 28th Annu. IEEE Int. Conf. LCN, Oct. 2003, pp. 416–422.

[10] Yin Wu, Wenbo Liu," Routing protocol based on genetic algorithm for energy harvesting-wireless sensor networks" *IET Wireless Sensor Systems*, doi: 10.1049/iet-wss.2012.0117, 2013.

[11] M. Xiao, X. Zhang, and Y. D. Shenzhen," An Effective Routing Protocol for Energy Harvesting Wireless Sensor Networks" 2013 IEEE Wireless Communications and Networking Conference (WCNC), pp. 2080-2084.

[12] Heinzelman W,Chandrakasan A. "Energy-efficient communication protocol for wireless micro sensor networks "Proceedings of the 33th Hawaii International Conference on System Sciences,2000.

[13] Y. Lu, D. Zhang, Y. Chen, X. Liu, P. Zong, "Improvement of LEACH in Wireless Sensor Networks Based on Balanced Energy Strategy". *IEEE 2012.*

[14] G. Martinez, S. Li, and C. Zhou," Wastage-Aware Routing in Energy-Harvesting Wireless Sensor Networks" IEEE SENSORS JOURNAL, VOL. 14, NO. 9, SEPTEMBER 2014. pp. 2967-2974.

[15] S. Peng and C. P. Low, “Energy neutral routing for energy harvesting wireless sensor networks,” in Proc. IEEE WCNC, Apr. 2013,pp. 2063–2067

[16] Z. A. Eu and H. P. Tan, “Adaptive opportunistic routing protocol for energy harvesting wireless sensor networks,” *in Proc. IEEE ICC, Jun. 2012, pp. 318–322*

[17] Rong Cui; Zhaowei Qu; Sixing Yin, "Energy-efficient routing protocol for energy harvesting wireless sensor network," in *Communication Technology (ICCT), 2013 15th IEEE International Conference on* , vol., no., pp.500-504, 17-19 Nov. 2013doi: 10.1109/ICCT.2013.6820427

[18] A. Kansal, J. Hsu, M. Srivastava, and V. Raghunathan, “Harvesting aware power management for sensor networks,” in Proc. 43rd IEEE/ACM, Jul 2006, pp. 651–656.

[19] M. K. Jakobsen, J. Madsen, and M. Hansen, “DEHAR: A distributed energy harvesting aware routing algorithm for ad-hoc multi-hop wireless sensor networks,” in Proc. IEEE Int. Symp. World Wireless Mobile Multimedia Netw. Jun. 2010, pp. 1–9.

[20] L. Lin, N. Shroff, and R. Srikant, “Asymptotically optimal energy-aware routing for multihop wireless networks with renewable energy sources,” ACM/IEEE Trans. Network, vol. 15, no. 5, pp. 1021-1034, October 2007

[21] Wendi Rabiner Heinzelman, Anantha Chandrakasan, and Hari Balakrishnan, “Energy-efficient communication protocols for wireless microsensor networks,” in Proceedings of the Hawaii International Conference on Systems Sciences, Jan. 2000 .

[22] L. Nguyen, X. Defago, R. Beuran, Y. Shinoda,” An Energy Efficient Routing Scheme for Mobile Wireless Sensor Networks”, 978-1-4244-2489-4/08, 2008 IEEE

[23] Hesham Abusaimeh, Shuang-hua Yang.” Dynamic Cluster Head for Lifetime Efficiency in WSN “, International Journal of Automation and Computing06 (1), Feb 2009, pp 48–54, 2009, springer.

[24] Sangho Yi, Junyoung Heo, Yookun Cho, Jiman Hong.” PEACH: Power-efficient and adaptive clustering hierarchy protocol for wireless sensor networks”, Computer Communications 30 (2007) 2842-2852, ELSEVIER.

[25] Zhi Ang Eu, Hwee-Pink Tan, Winston K. G. Seah, ” -Routing and Relay Node Placement in Wireless Sensor Networks Powered by -Ambient -Energy -Harvesting “,978-1-4244-2948-6/09, 2009 IEEE.

[26] I. Mathews, G. Kelly, P. J. King, and R. Frizzell, "GaAs solar cells for Indoor Light Harvesting," in *Photovoltaic Specialist Conference (PVSC), 2014 IEEE 40th*, 2014, pp. 0510-0513.

[27] X. Lu, S. H. Yang “Thermal Energy Harvesting for WSNs” IEEE 2010 pp. 3046-3052

[28] Y. K. Tan and S. K. Panda, "Energy harvesting from hybrid indoor ambient light and thermal energy sources for enhanced performance of wireless sensor nodes," *IEEE Transactions on Industrial Electronics,* vol. 58, No. 9, pp. 4424-4435, 2011.

[29] R. Doost, K. R. Chowdhury, and M. Di Felice, "Routing and link layer protocol design for sensor networks with wireless energy transfer," in IEEE Globecom 2010.

[30] B. Jiang, K. Cao, L. Chen, H. Chen, H. Zhang, and Q. Wang, "Low-power design of a self-powered piezoelectric energy harvesting system," in *Control Conference (CCC), 2014 33rd Chinese*, 2014, pp. 6937-6940.

[31] F. I. Simjee and P. H. Chou, "Efficient Charging of Supercapacitors for Extended Lifetime of Wireless Sensor Nodes," IEEE Trans on Power Electronics, vol. 23, no. 3, pp. 1526–1536, May 2008.

[32] R. C. Shah and J. M. Rabaey. "Energy Aware Routing for Low Energy Ad Hoc Sensor Networks ", IEEE wireless Communications and Networking Conference. (WCNC(, Mar 17-21, 2002, Orlando, FL.

[33] J. Maraševi, C. Stein, G.Zussman, "Max-min Fair Rate Allocation and Routing in Energy Harvesting Networks: Algorithmic Analysis" ACM 978-1-4503-2620-9/14/08, August 11–14, 2014.

[34] S. Singh and Meenaxi. "Comparative analysis of QoS parameters in wireless sensor network using ant colony optimization", International Conference on Control, Communication and Computer Technology, 2013.

[35] T. S. Rappaport. Wireless Communications: Principles and Practice. Prentice Hall, 1996.

[36] ProFLEX01 TRANSCEIVER MODULE DATASHEET, Integrated Transceiver Modules for ZigBee / 802.15.4 (2.4 GHz)

[37] http://en.wikipedia.org/wiki/ZigBee.

[38] NS3 AODV code: https://www.nsnam.org/docs/release/3.16/doxygen/classns3_1_1aodv_1_1_routing_table.html

[39] Ns3 documents site: https://www.nsnam.org/

[40] Mirko Stoffers, George Riley "Comparing the ns–3 Propagation Models "*U. S. National Science, 2012*

[41] E. Damosso and L. M. Correia, "Digital Mobile Radio Towards Future Generation Systems*" COST Action 231*. European Commission, Brussels, Belgium, 1999.

[42] H. T. Friis, "A Note on a Simple Transmission Formula," *Proceedings of the Institue of Radio Engineers*, vol. 34, no. 5, pp. 254–256, 1946

[43] V. Erceg, L. Greenstein, S. Tjandra, S. Parkoff, A. Gupta, B. Kulic, A. Julius, and R. Bianchi, "An Empirically Based Path Loss Model for Wireless Channels in Suburban Environments," *IEEE Journal on Selected Areas in Communications*, vol. 17, no. 7, pp. 1205–1211, 1999.

[44] T. S. Rappaport, *Wireless Communications, Principles and Practice*. Prentice Hall, 1996.

[45] Y. R. Zheng and C. Xiao, "Simulation Models with Correct Statistical Properties for Rayleigh Fading Channels," *IEEE Transactions on Communications*, vol. 51, no. 6, pp. 920–928, 2003.

[46] M. Nakagami, "The m-Distribution, A General Formula of Intensity Distribution of Rapid Fading," *Statistical Methods in Radio Wave Propagation*, pp. 3–36, 1960.

[47] Y. Guo, F. Kong, D.Zhu "Sensor Placement for Lifetime Maximization in Monitoring Oil Pipelines" ACM, 2010.

[48] CC2420 chipset Datasheet: http://www.ti.com/product/CC2420/technicaldocuments.

[49] MICAz Datasheet: http://www.memsic.com/userfiles/files/Datasheets/WSN/micaz_datasheet-t.pdf.

[50] NS3 documents, at site: https://www.nsnam.org/docs/models/html/flow-monitor.html.

[51] P. Oppenheimer, "Top-Down Network Design. A system analysis approach network design," Ed: Cisco Press, 2010.

[52] R. Jain, *The art of computer systems performance analysis*: John Wiley & Sons, 2008

[53] F. Reátegui, M. A.Imran, and R. Tafazolli, "The Cognitive Interference Channel with a Causal Relay in Very Strong Interference," IEEE communication letters, VOL. 19, NO. 4, APRIL 2015.

[54] N. Bisnik and A. A. Abouzeid "Queuing Delay and Achievable Throughput in Random Access Wireless Ad Hoc Networks" IEEE 2006.

[55] W. K. Seah, Z. A. Eu, and H.-P. Tan, "Wireless sensor networks powered by ambient energy harvesting (WSN-HEAP)-Survey and challenges," Wireless VITAE'09, IEEE 2009.

[56] B. P. Santos ,M. A. M. Vieira, and L.F. Vieira, "eXtend Collection Tree Protocol "Wireless Communications and Networking Conference (WCNC), IEEE, 2015.

Vitae

Name : Tariq Mahmoud Ahmad Abu Amria

Nationality : Palestinian

Date of Birth : November 10 1982

Email1 : tariq20110175@yahoo.com

Email2 : tariq20110175@Gmail.com

Address : Bethlehem-Palestine

Academic Background:

- MSc in Computer Networks, KFUPM, 2015
- Bachelor degree in Computer Engineering, Al Quds University, 2007

Publications:

- Accepted conference paper: **T. Abu Amria and U. Baroudi, "Data Collection Energy Efficient Routing Protocol for Energy Harvested Based Wireless Sensor Network", in ICCSI 2016.**

Professional experience:

- System and Network Engineer, Private sector, Ramallah, from 2008 to January 2010.
- System and Network Engineer, Public sector, Ramallah, from January 2010 to January 2013.

Certifications:

- Red Hat Certified System Administrator.
- EC-Council Ethical Hacking and Countermeasures.
- EC-Council Disaster Recovery and Virtualization Technology.
- CCNA: Cisco Certified Network Associate Routing & Switching.
- MCSA: Microsoft Certified Systems Administrator.
- MCSE: Microsoft Certified Systems Engineer.